CONTENTS

CHAPTER 1

OVERVIEW OF THE PHYSICS CASE FOR CEPC-SPPC

1.1 CEPC: the precision frontier

The discovery of a Higgs boson in 2012 by the ATLAS and CMS collaborations [1, 2] at the Large Hadron Collider (LHC) has opened a new era in particle physics. Subsequent measurements of the properties of this new particle have indicated compatibility with the predictions of the Standard Model (SM) [**? ? ? ? ?**] [need updates]. While the SM has been remarkably successful in describing experimental phenomena, it is important to recognize that the SM is not a complete theory. In particular, the SM does not *predict* the parameters in the Higgs potential, such as the Higgs mass. The vast difference between the Planck scale and the weak scale remains a major mystery. In addition, there is not a complete understanding of the nature of electroweak phase transition. The discovery of a spin zero Higgs boson, the first elementary particle of its kind, has only sharpened these questions. It is clear that any attempt of addressing these questions will involve new physics beyond the SM. Therefore, the Higgs boson discovery marks the beginning of a new era of theoretical and experimental explorations.

A physics program of precision measurement of Higgs properties will be a critical component of any roadmap for high energy physics in the coming decades. Potential new physics beyond the SM could lead to observable deviations in the Higgs boson couplings from the SM expectations. Typically, such deviations can be parametrized as

$$\delta = c\frac{v^2}{M_{\rm NP}^2}, \tag{1.1}$$

where v and $M_{\rm NP}$ are the vacuum expectation value of the Higgs field and the typical mass scale of new physics, respectively. The size of the proportionality constant c depends on model, but it should not be much larger than $\mathcal{O}(1)$. The current and upcoming LHC runs

will measure the Higgs couplings to about 5% Ref [**?**]. At the same time, LHC will directly search for new physics from a few hundreds of GeV to at least a TeV. Eq. (1.1) implies that probing new physics significantly beyond the LHC reach would require the measurement of the Higgs boson couplings with sub percent level accuracy. Achieving such a level of precision will need new facilities, a lepton collider operating as a Higgs factory is an obvious candidate.

We briefly summarized the projections for the precision of the CEPC measurements below. The details of the analysis which lead to these projections are presented in Section [refer to the physics potential section].

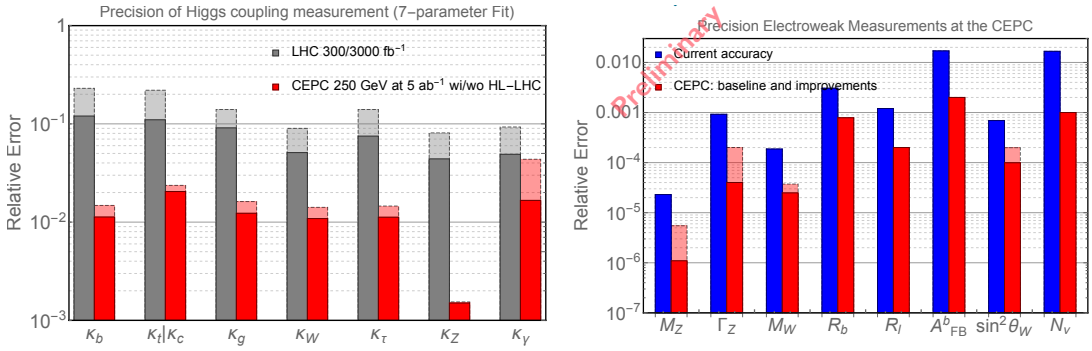

Figure 1.1: Left: Higgs coupling extraction in the κ-framework. Right: Projection for the precision of the Z-pole measurements.

The CEPC will operate at a center-of-mass energy of $\sqrt{s} \sim 240$ GeV. The capability of CEPC in measuring Higgs couplings and electroweak observables, shown in the left panel of Fig. 1.1. The main mode of Higgs production is through $e^+e^- \to ZH$ process. At the CEPC, in contrast to the LHC, Higgs boson candidate events can be identified through a technique known as the recoil mass method without tagging its decay products. Therefore, Higgs boson production can be disentangled from its decay in a model independent way. Moreover, the cleaner environment at a lepton collider allows much better exclusive measurement of Higgs boson decay channels. All of these give the CEPC impressive reach in probing Higgs boson properties. For example, with an integrated luminosity of 5 ab^{-1}, over one million Higgs bosons will be produced. With this sample, the CEPC will be able to measure the Higgs boson coupling to the Z boson with an accuracy of 0.25% [update], about a factor of 10 better than the reach of the High Luminosity upgrade of the LHC (HL-LHC). Such a precise measurement gives the CEPC unprecedented reach into interesting new physics scenarios which are very difficult to probe at the LHC. The CEPC also has strong capability in detecting Higgs boson invisible decay. For example, with 5 ab^{-1}, it can improve the accuracy of the measurement of invisible decay branching ratio to 0.14% [update]. In addition, it is expected to have good sensitivities to exotic decay channels which are swamped by backgrounds at the LHC. It is also important to stress that an e^+e^- Higgs factory can perform *model independent* measurement of the Higgs boson width. This unique feature in turn allows for the determination of the Higgs boson couplings without assumptions about Higgs decay channels.

The CEPC is also designed to run at the Z-pole (producing close to 10^{12} Zs) and near the W^+W^- threshold (with about 10^7 W pairs). Hence, it will have a robust program on electroweak precision measurement. The projected precision for a set of such observables

is shown in on the right panel of Fig. 1.1. In comparison with the current precision, CEPC can improve by about one order of magnitude.

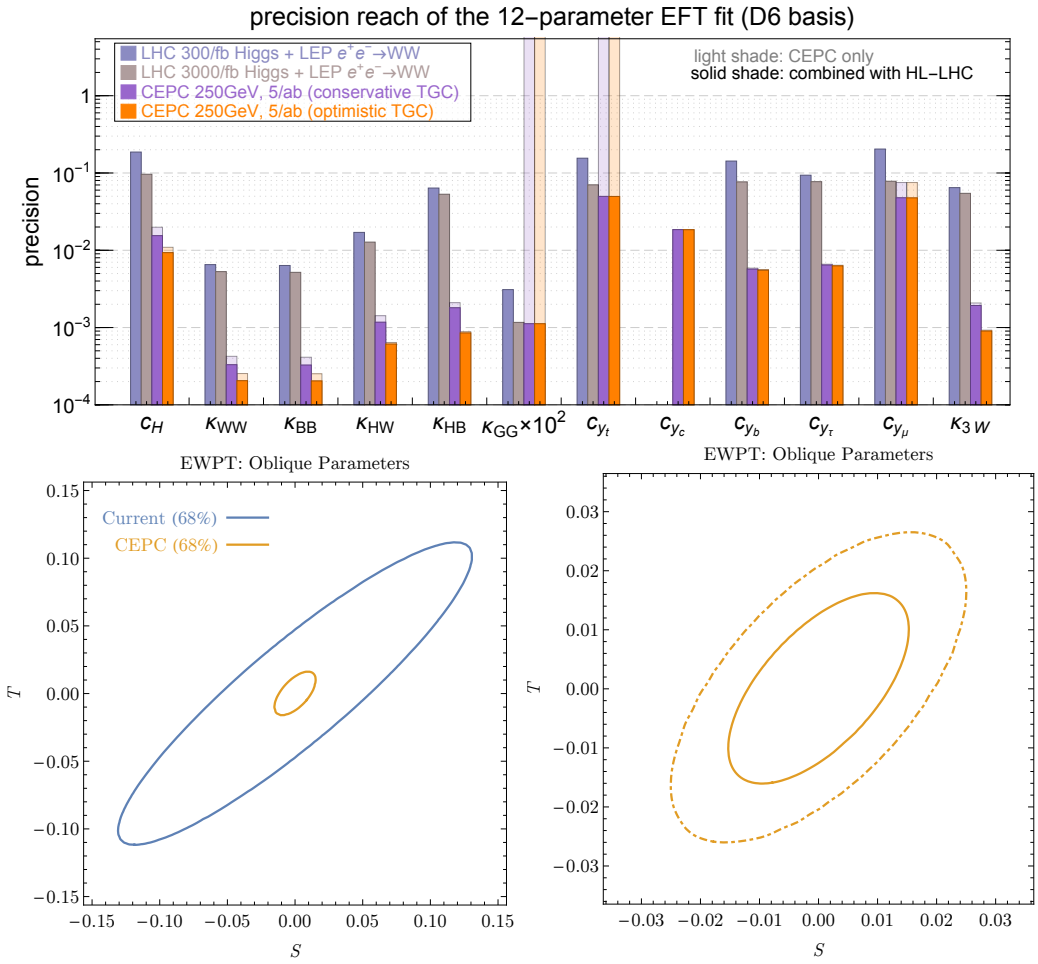

Figure 1.2: Upper panel: The reach of the Higgs measurement on the size of effective field theory operators, normalized as $c_i(\mathcal{O}_i/v^2)$. Lower panel: On the left, the CEPC limit on the oblique parameters in comparison with the current precision. On the right, 68% (dash-dot) and 95% (solid) contours from CEPC measurement.

Another convenient of representing the physics reach of the Higgs coupling measurements is the limits they can place on the EFT operators, shown in Fig. 1.2. The standard way of representing the reach of electroweak precision measurements is the limits on the so called oblique parameters, shown in the upper panel of Fig. 1.2. The significant improvement from the LHC measurement is apparent. It is also customary to present the reach of electroweak precision in terms of the constraint on the so called oblique parameters. This is shown in the lower panel of Fig. 1.2. The improvement is expected to be about a factor of 10.

In the rest of this section, we will discuss the potential of using these precision measurements to address important open questions of the Standard Model and explore new physics.

1.2 Higgs and electroweak symmetry breaking

1.2.1 Naturalness

The appearance of large numerical hierarchies in fundamental theories has long been a source of discomfort, articulated in the modern era by Dirac [3] and subsequently refined in the context of quantum field theory by Wilson [4], Susskind [5], 't Hooft [6], and others. In the context of quantum field theory, dimensionless parameters of a quantum field theory are naturally expected to be $\mathcal{O}(1)$, while the dimensionful parameters are naturally the size of the fundamental scale at which the theory is defined. An exception arises when a symmetry is manifested in the limit that a parameter of the theory is taken to zero. In this case, it is "technically natural" for some parameters to remain smaller than others, in the sense that they are protected from large quantum corrections, though even in this case one is left to find an explanation for the dynamical origin of the small parameter. This notion of naturalness has been reinforced by the widespread successes of effective field theory and diverse realizations in both particle physics and condensed matter physics.

Famously, all of the observed parameters of the Standard Model satisfy the naturalness criterion in some form, with the exception of the Higgs mass parameter and the strong CP angle. The naturalness of these parameters remains an open question, and in each case a natural explanation entails a significant extension of the Standard Model. Of these, the naturalness of the weak scale is perhaps the most pressing, as it is drawn into sharp relief by the discovery of an apparently elementary Higgs boson at the LHC. Evidence for a natural explanation for the value of the weak scale has yet to appear, with null results across a suite of experimental searches imperiling many preferred candidate. But the LHC is not capable of decisively deciding the naturalness of the weak scale, providing strong motivation for colliders that complement LHC sensitivity to natural new physics.

The oft-cited quadratically divergent radiative corrections to the Higgs mass parameter,

$$\delta m_h^2 \sim \frac{3y_t^2}{8\pi^2}\Lambda^2\,, \tag{1.2}$$

are not the naturalness problem in and of themselves, but rather an indication of the problem. Such divergences indicate that the Higgs mass parameter is precisely that – a parameter – and incalculable in the Standard Model. But the robust expectation is that the Higgs mass and other parameters of the Standard Model are fully calculable in a fundamental theory. In this case, the quadratically divergent contributions to the Higgs mass parameter in the Standard Model are replaced by finite contributions dictated by the fundamental theory. The Higgs mass in terms of underlying parameters will take the form

$$m_h^2 = a\Lambda_h^2 + b\frac{3\lambda_t^2}{8\pi^2}\Lambda_h^2 + \ldots \tag{1.3}$$

where $a, b, \ldots$ are dimensionless constants and Λ_h is an underlying mass scale of the fundamental theory. If the Higgs mass is *natural*, the parameters a and b will be $\mathcal{O}(1)$, up to possible manifestations of technical naturalness associated with symmetries in the underlying theory. In this case, one expects $m_h \sim \Lambda_h$, corresponding to the appearance of new physics near the weak scale. Alternately, $m_h << \Lambda_h$ points either to *fine-tuning* among fundamental parameters, or to a correlation between ultraviolet and infrared aspects of the theory with no known counterpart in effective field theory.

The most promising strategy for rendering the weak scale natural in a more fundamental theory is to extend the Standard Model to include additional symmetries that render the Higgs mass parameter technically natural. In four dimensions, the available symmetries are supersymmetry and global symmetry. In the former case, the fields of the Standard Model are extended into complete supersymmetric multiplets, and supersymmetry is softly broken to accommodate the non-degeneracy of Standard Model fields and their partners [7–9]. The Higgs is related to a fermionic partners, thereby rendering the Higgs mass technically natural by the same chiral symmetries that protect the fermion masses. In the latter case, the Higgs is a pseudo-Nambu-Goldstone boson (pNGB) of a spontaneously broken global symmetry, with a mass parameter protected by the corresponding shift symmetries. The scale of global symmetry breaking in such theories must itself be rendered natural, leading to e.g. composite Higgs models [10] and little Higgs models [11] (for an excellent recent review, see [12]).

In both cases, these symmetries predict an abundance of new physics near the weak scale. Although this new physics may be searched for efficiently at the LHC, such searches typically leverage ancillary properties of the new physics unrelated to the naturalness of the weak scale. For example, searches for the scalar top partners predicted by supersymmetry typically leverage QCD quantum numbers of the stop and decay modes unrelated to the stop-Higgs coupling. The sensitivity of LHC searches to inessential features of the new physics makes them imperfect probes of electroweak naturalness.

In this respect, a Higgs factory provides the ideal context for probing natural new physics via precision Higgs couplings. The same couplings and diagrams that control the size of the Higgs mass in a natural theory generate radiative corrections to its couplings. As such, precision tests of Higgs properties directly probe natural physics in a way that is complementary to, and less subject to caveats than, direct searches at the LHC.

Signatures of natural new physics in precision Higgs measurements take a variety of forms. In most symmetry solutions, there are Higgs coupling deviations due to tree-level mixing with additional Higgs-like states. However, these tree-level deviations need not be the leading effect. Radiative corrections are also significant, due to both the size of Higgs couplings and the proximity of new particles to the weak scale. In theories where new physics associated with naturalness carries Standard Model quantum numbers, such as conventional supersymmetric and composite models, the most distinctive radiative corrections modify loop-induced Higgs couplings to gluons and photons. In addition, all symmetry solutions – whether or not they involve new states charged under the Standard Model – radiatively modify Higgs couplings through effective wavefunction renormalization of the physical Higgs scalar, an effect that may be observed in loop-level corrections to tree-level Higgs couplings.

Although our discussion of naturalness has focused on symmetries, they are not the only mechanism for explaining the value of the weak scale. The most notable alternative is to lower the cutoff in Eq. (1.3), the avenue realized by technicolor [5, 13] and large [14, 15] or warped [16, 17] extra dimensions. However, these solutions typically do not predict a significant mass gap between the Higgs and additional degrees of freedom, making them more susceptible to LHC null results. More recent proposals, such as relaxation of the weak scale [18], can potentially lead to $m_h << \Lambda_h$ without fine-tuning, and remain interesting targets for exploration. Nonetheless, these alternatives still involve new particles coupling to the Higgs, and may leave their imprint on Higgs couplings or exotic decays.

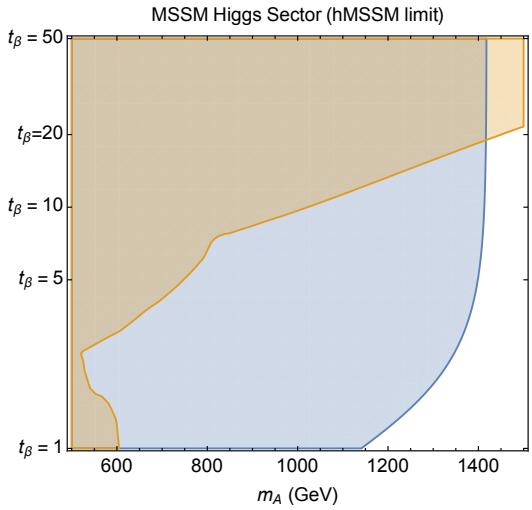

Figure 1.3: Potential coverage of the MSSM Higgs sector in the hMSSM limit [20] at the CEPC is shown in blue. Sensitivity is driven largely by modifications of the Higgs coupling to bottom quarks. Projected HL-LHC coverage of the MSSM Higgs sector in the same limit due to direct searches for heavy Higgs states is shown in orange [21].

1.2.1.1 Supersymmetry

Supersymmetric extensions of the Standard Model have the virtue of rendering the weak scale natural with an elementary Higgs scalar, consistent with properties observed thus far at the LHC. While searches for supersymmetric partner particles at the LHC have excluded large regions of the natural supersymmetric parameter space, significant blind spots remain that are best covered by precision Higgs coupling measurements.

Tree-level modifications to Higgs properties Supersymmetric extensions of the Standard Model necessitate more than one Higgs doublet. Mass mixing between the CP-even neutral Higgs scalars leads to tree-level deviations in Higgs properties. In the limit that the additional Higgs scalars are heavy and may be integrated out, this leads to dimension-six operators that shift Higgs couplings to fermions and dimension-eight operators that shift Higgs couplings to massive vectors. As a result, deviations are largest in Higgs couplings to fermions, particularly those in the down quark and lepton sectors. Percent-level CEPC sensitivity to modifications of the Higgs coupling to bottom quark enables indirect tests of the MSSM Higgs sector to the TeV scale, as illustrated in Fig. 1.3. More broadly, CEPC sensitivity to tree-level effects in extended Higgs sectors such as the MSSM is studied comprehensively in [19]. However, due to the decoupling properties of the MSSM Higgs sector, heavy Higgs states may remain above the TeV scale without increasing the fine-tuning of the weak scale. In this respect, tree-level modifications to Higgs properties arising in supersymmetric theories represent a discovery opportunity but not an irreducible constraint.

Loop-level modifications to Higgs properties The plethora of new partner particles predicted by supersymmetric extensions of the Standard Model leads to a wealth of loop-level contributions to Higgs couplings. These contributions are typically largest in the stop sector, due to the large coupling to the Higgs required by supersymmetry, but may be significant for any of the partners of third-generation fermions. The most distinctive

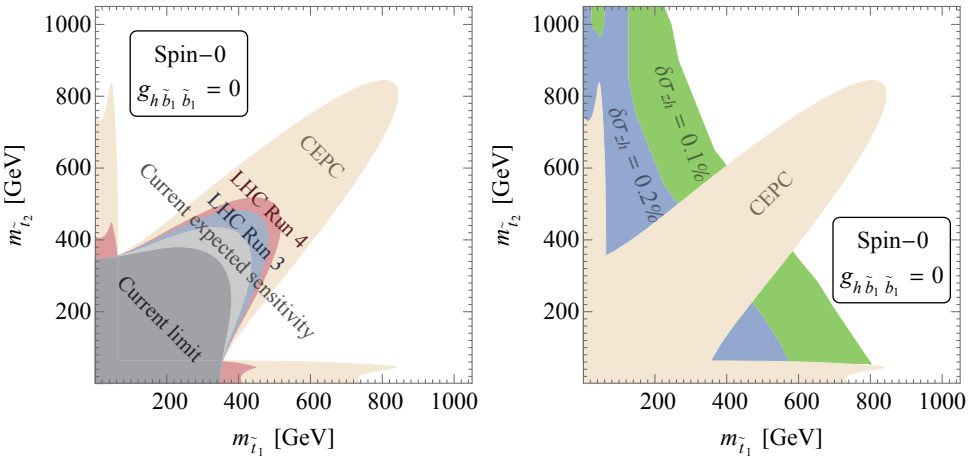

Figure 1.4: Left: LHC and CEPC precision Higgs constraints in the $m_{\tilde{t}_1} - m_{\tilde{t}_2}$ plane from Higgs couplings to gluons and photons. Right: Coverage of blind spots including precision measurement of the Zh cross section. Figures adapted from [25].

consequences are modifications to the loop-level Standard Model couplings of the Higgs to gluons and photons, though radiative corrections to tree-level couplings arise as well and may be used to cover blind spots arising in the loo-level couplings. The potential for CEPC to probe a suite of loop-level corrections to Higgs and electroweak observables in supersymmetric models is comprehensively studied in [22].

For simplicity, here we will focus on the loop-level consequences in the stop sector, corresponding to the scalar partners of both the right-handed and left-handed top quarks. In the limit that the stops are significantly heavier than the Higgs, the correction to gluons and photons is proportional to

$$\frac{1}{4}\left(\frac{m_t^2}{m_{\tilde{t}_1}^2} + \frac{m_t^2}{m_{\tilde{t}_2}} - \frac{m_t^2 X_t^2}{m_{\tilde{t}_1}^2 m_{\tilde{t}_2}^2}\right) \tag{1.4}$$

where $m_{\tilde{t}_1}, m_{\tilde{t}_2}$ are the stop mass eigenstates and $X_t = A_t - \mu \cot\beta$ is the off-diagonal mixing parameter in the stop mass matrix. The mixing parameter is bounded from above by the avoidance of tachyonic stops, and from below by precision measurements of the Higgs coupling to gluons and photons. A robust bound may be placed on the stop sector whenever the minimum value exceeds the maximum value [23]. The strongest constraints arise in the degenerate limit when $m_{\tilde{t}_1} = m_{\tilde{t}_2}$, in which case the CEPC is capable of probing stop masses close to the TeV scale; this is illustrated in the left panel of Fig. 1.4. However, the modification of Higgs couplings is highly sensitive to the mixing in the stop sector, and blind spots arise when the mixing leads to vanishing deviations in the Higgs coupling to gluons and photons [22, 24]. However, as illustrated in the right panel of Fig. 1.4, these blind spots may be covered by precision measurements of the Zh cross section, which is sensitive to loop-level corrections to the tree-level hZZ coupling that are generically nonzero in the gluon/photon blind spot [24].

1.2.1.2 Global symmetry

Global symmetry approaches to the weak scale cover a vast array of specific models and UV completions, but share the common features of an approximately elementary Standard

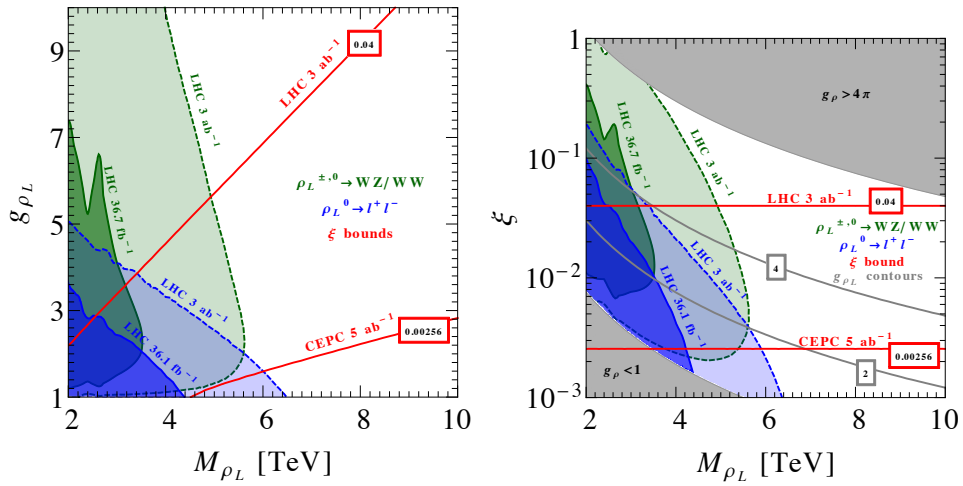

Figure 1.5: Potential coverage of composite-type global symmetry models in terms of resonance mass m_ρ and Higgs mixing parameter $\xi \equiv v^2/f^2$ via direct searches at the LHC (dark blue) and precision Higgs measurements (light blue).

Model-like Higgs mixing with heavier resonances and further influenced by the presence of light fermionic excitations.

Tree level In global symmetry solutions, the Higgs is a pNGB of a spontaneously broken global symmetry. This invariably implies tree-level corrections, which can be interpreted as arising from mixing between the Standard Model-like Higgs and heavy states associated with the spontaneously broken global symmetry. This mixing is typically proportional to v^2/f^2, where f is the decay constant associated with the broken global symmetry (see e.g. [26] for a comprehensive parameterization), although precise corrections may vary between Higgs couplings to fermions and gauge bosons depending on the model. As shown in Fig. 1.5, the precision attainable at the CEPC probes this mixing to better than one part in one hundred, translating to an energy reach of several TeV. In the simplest composite realizations of global symmetries, bounds on v^2/f^2 translate directly into lower bounds on the tuning of the electroweak scale, but this tuning may be avoided in Little Higgs models and related constructions. The complementarity between precision measurements of Higgs couplings and direct searches at future colliders in probing global symmetry approaches to the hierarchy problem is explored in detail in e.g. [27].

Loop level Global symmetry approaches to naturalness likewise feature a plethora of new states near the weak scale, albeit with the same statistics as their Standard Model counterparts. While corrections to Higgs couplings from loops of these new particles are typically sub-dominant compared to tree-level corrections, they provide a more immutable test of naturalness. As with supersymmetry, the largest corrections are typically due to the fermionic top partner sector, due to the large coupling of these partners to the Higgs and their proximity to the weak scale. As such partners typically carry Standard Model quantum numbers, the most striking corrections are to the loop-level couplings of the Higgs to gluons and photons.

For the sake of definiteness, consider a theory involving two top partners T_1, T_2 whose couplings are dictated by the global symmetry protecting the Higgs mass. In this case

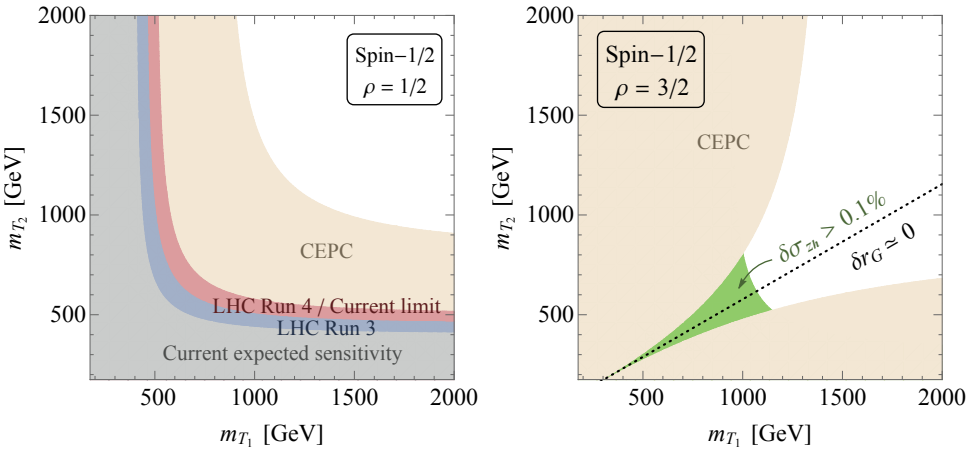

Figure 1.6: Left: LHC and CEPC precision Higgs constraints in the $m_{T_1} - m_{T_2}$ plane from Higgs couplings to gluons and photons assuming equal couplings. Right: Coverage of blind spots including precision measurement of the Zh cross section. Figures adapted from [25].

corrections to the Higgs coupling to gluons and photons are proportional to [25]

$$-\left(\rho\frac{m_t^2}{m_{T_1}^2}+(1-\rho)\frac{m_t^2}{m_{T_2}^2}\right) \tag{1.5}$$

where ρ parameterizes the fraction of the quadratic divergence cancellation coming from the T_1 field, which is directly reflected in the modification of Higgs couplings. In the case of equal couplings, the CEPC is capable of probing fermionic top partners above the TeV scale, as shown in the left panel of Fig. 1.6. Note that the existence of more than one fermionic top partner allows for the possibility of a blind spot to arise when $\rho > 1$, which may be constrained by radiative corrections to the Zh cross section (shown in the left panel of Fig. 1.6) in analogy with the stop blind spot in supersymmetry. A comprehensive exploration of the CEPC potential to constrain radiative corrections to Higgs couplings arising in global symmetry solutions to the hierarchy problem may be found in [25].

1.2.1.3 Neutral naturalness

While it is entirely possible that the naturalness of the weak scale is explained by conventional symmetries that have thus far evaded LHC detection, LHC null results may indicate that the weak scale is stabilized by less conventional symmetries that do not lead to partner particles carrying Standard Model quantum numbers. This form of "neutral naturalness" [28] can occur, for example, when only discrete symmetries are operative at the weak scale. To date both opposite-statistics and same-statistics examples of neutral naturalness have been constructed. The former case is exemplified by Folded Supersymmetry [29], which features new partner particles carrying electroweak quantum numbers but no irreducible tree-level corrections. The latter case is exemplified by the Twin Higgs [30], which features new partner particles entirely neutral under the Standard Model, as well as significant tree-level Higgs coupling deviations. Examples also exist of theories with entirely neutral scalar top partners [31] and electroweak-charged fermionic top partners [32], both of which share the tree-level modifications to Higgs couplings of the Twin Higgs.

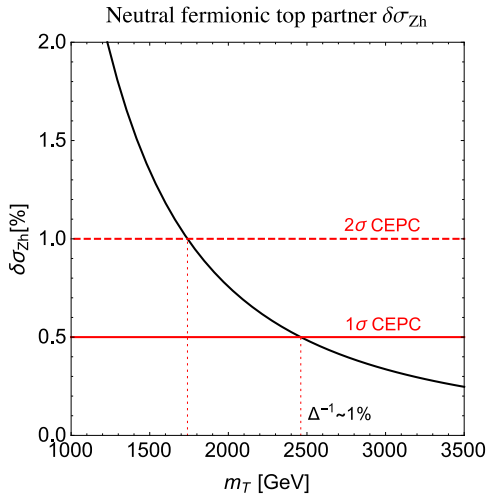

Figure 1.7: CEPC reach in the mass scale of neutral fermionic top partners due to tree-level mixing corrections to σ_{Zh}.

The primary phenomenological consequences of neutral naturalness are (1) a significant weakening of direct search limits due to the paucity of states charged under the Standard Model, and (2) the reduction of loop-level corrections to loop-level Higgs couplings. However, these models still lead to distinctive patterns of Higgs coupling deviations that may be first revealed at a Higgs factory.

Tree level Many theories of neutral naturalness, most notably the Twin Higgs [30], feature significant tree-level mixing between the Standard Model-like Higgs and an additional CP even scalar state. Much as with conventional global symmetries, this leads to $\mathcal{O}(v^2/f^2)$ deviations in Higgs couplings. In contrast to conventional global symmetries, however, these corrections are typically universal in the sense that they are the same for Higgs couplings to both vectors and scalars. Bounds on v^2/f^2 may be translated directly into bounds on the mass of the twin top partner, as shown in Fig. 1.7. In such cases, CEPC can probe multi-TeV scales and test the efficacy of neutral naturalness down to the percent level.

Loop level While all models of neutral naturalness feature loop-level corrections to Higgs properties, they are the leading effect in many opposite-statistics models such as folded supersymmetry. New partner particles in these models still carry electroweak quantum numbers, leading to loop-level deviations in the Higgs coupling to photons, as shown in Fig. 1.8. This allows the CEPC to place constraints on the mass scale of folded partner particles in the hundreds of GeV, probing tuning of the weak scale to the 20% level in these theories.

It is also possible that the weak scale is stabilized by scalar top partners entirely neutral under the Standard Model without accompanying tree-level Higgs coupling deviations. In this case, all of the distinctive direct search channels and corrections to loop-level Higgs couplings are absent. However, a precision measurement of the Zh cross section is still sensitive to the wavefunction renormalization of the physical Higgs scalar induced by loops of the scalar top partners [33]. In general, n_ϕ scalars ϕ_i coupling via the Higgs portal interaction $\sum_i \lambda_\phi |H|^2 |\phi_i|^2$ leads to a correction to the Zh cross section of the form

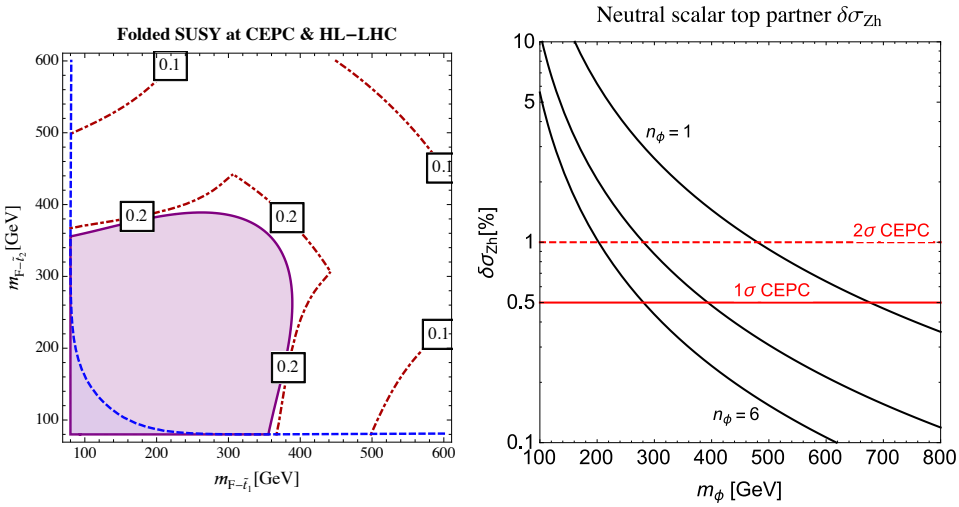

Figure 1.8: Left: CEPC reach for color-neutral folded stops in Folded SUSY from Higgs couplings to photons, from [22]. Right: CEPC reach in the mass scale of neutral scalar top partners due to loop-level corrections to σ_{Zh}, adapted from [33].

$$\delta\sigma_{Zh} = \frac{n_\phi |\lambda_\phi|^2}{8\pi^2} \frac{v^2}{m_h^2} \left[1 + \frac{1}{4\sqrt{\tau(\tau-1)}} \log\left(\frac{1 - 2\tau - 2\sqrt{\tau(\tau-1)}}{1 - 2\tau + 2\sqrt{\tau(\tau-1)}} \right) \right] \tag{1.6}$$

where $\tau = m_h^2/4m_\phi^2$. This leads to the sensitivity shown in Fig. 1.8, for which the CEPC is able to place constraints in the hundreds of GeV on a scenario that is otherwise largely untestable at colliders.

1.2.1.4 Other solutions

Symmetries are not the only mechanism for explaining the origin of the weak scale, though other solutions may not be manifestly natural in the same way. However, even non-symmetry explanations for the value of the weak scale (excepting anthropic ones) generically entail some degree of coupling between new degrees of freedom and the Higgs itself. This typically leads to deviations in Higgs couplings, new exotic decay modes of the Higgs, or a combination thereof.

A compelling example of non-symmetry solutions is the relaxion [18], in which the value of the weak scale is set by the evolution of an axion-like particle across its potential in the early universe. The relaxion necessarily couples to the Higgs boson in order for its evolution to influence the Higgs mass. This leads to a variety of signatures that may be tested via precision Higgs measurements depending on the specific model.

The most promising signature is that of the Higgs decaying into new invisible states. This signature arises in a range of different relaxion models. One such realization, illustrated in Fig. 1.9, generically possesses significant couplings between the Higgs and a pair of relaxion fields whose strength is dictated by the back-reaction of the Higgs on the evolution of the relaxion. Substantial limits on the parameter space of the relaxion may be set by indirect bounds on the non-SM width of the Higgs [34].

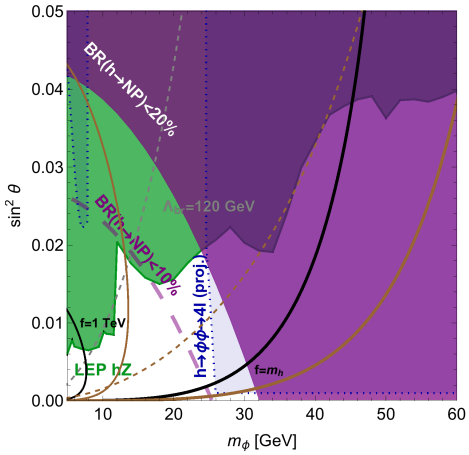

Figure 1.9: Constraints on the relaxion parameter space of [34] from non-SM decay of the Higgs into relaxion pairs.

1.2.2 Electroweak phase transition

The discovery of the Higgs boson marks the culmination of a decades-long research program to understand the source of electroweak symmetry breaking (EWSB). We have known since the mid-20^{th} century that this symmetry is not realized in nature and that the weak gauge bosons are massive. Now measurements at the Large Hadron Collider (LHC) have provided overwhelming evidence that EWSB results from the recently-discovered Higgs. With the Higgs boson discovery we have learned *why* the electroweak symmetry is broken in nature, but we still do not understand *how* it is broken dynamically — this is the question of the *electroweak phase transition*.

The nature of the electroweak phase transition (EWPT) is controlled by the properties and interactions of the Higgs boson. For instance the Higgs mass sets the temperature scale of the phase transition to be roughly $T \sim m_h \simeq 125\,\text{GeV}$. The more detailed and interesting features of the phase transition depend also upon the interactions of the Higgs boson with itself, with other Standard Model particles, and with possible new physics. The nature of these interactions will not be determined very precisely at the LHC, where we have only just begun to study the Higgs. Rather, if we want to understand the nature of the electroweak phase transition, we require precision measurements of Higgs physics at a dedicated Higgs factory experiment like the CEPC.

First order phase transition or continuous crossover?

Despite years of careful study at the LHC, we still have such a poor understanding of the Higgs that it is impossible to determine even the *order of the electroweak phase transition*. In general, these two scenarios are used to classify symmetry-breaking phase transitions:

- A *first order phase transition* proceeds through the nucleation of *bubbles* that grow, coalesce, and eventually fill the system.
- By contrast, a *continuous crossover* occurs smoothly throughout the system.

See also Fig. 1.10. If the phase transition is determined to be first order, there would be profound implications for early-universe cosmology and the origin of the matter-antimatter asymmetry. Moreover, determining the order of the EWPT is simply the first step in a

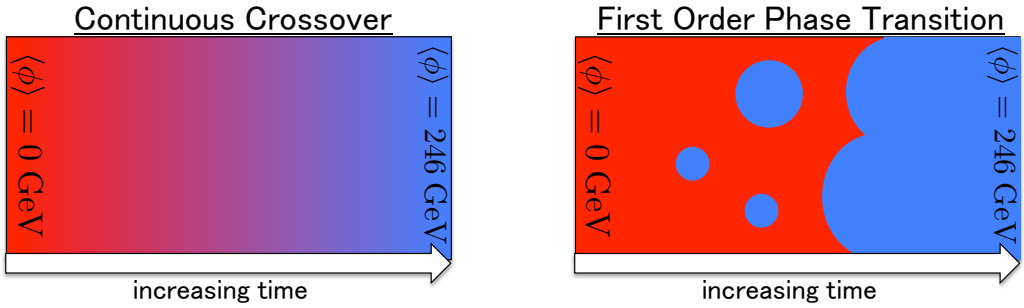

Figure 1.10: An illustration of a continuous crossover (left) and a first order phase transition (right).

much richer research program that deals with other aspects of the phase transition including its latent heat, bubble wall velocity, and plasma viscosity.

The Higgs potential

The order of the EWPT is intimately connected to the shape of the *Higgs potential energy function*. For each value of the Higgs field, ϕ, there is an associated potential energy density, $V(\phi)$. During the electroweak phase transition, the Higgs field passes from $\phi = 0$ where the electroweak symmetry is unbroken to $\phi = v \simeq 246$ GeV where the electroweak symmetry is broken and the weak gauge bosons are massive. Thus the order of the phase transition is largely determined by the shape of $V(\phi)$ in the region $0 < \phi < v$.

For instance, if the Higgs potential has a barrier separating $\phi = 0$ from $\phi = v$, then electroweak symmetry breaking is accomplished through a first order phase transition with the associated bubble nucleation that we discussed above. If there is no barrier in $V(\phi)$, the transition may be either first order or a crossover depending on the structure of the *thermal effective potential*, $V_{\text{eff}}(\phi, T)$.

Currently we know almost nothing about the shape of the Higgs potential. This situation is illustrated in Fig. 1.11 and the following discussion. When we make measurements of the Higgs boson in the laboratory, we only probe small fluctuations of the potential around $\phi = v$. By measuring the strength of the weak interactions, $G_F = (\sqrt{2}v^2)^{-1} \simeq 1 \times 10^{-5}$ GeV^{-2}, we learn that the Higgs potential has a local minimum at $v \simeq 246$ GeV. By measuring the Higgs boson's mass, we learn that the local curvature of the potential at its minimum is $(d^2V/d\phi^2)\big|_{\phi=v} = m_h^2 \simeq (125 \text{ GeV})^2$. This is the extent of what we know today about the Higgs potential. Even the third derivative, which is related the Higgs boson's cubic self-coupling, is completely undetermined!

Measurements of the Higgs boson thus far are consistent with the predictions of the Standard Model of particle physics. The Standard Model asserts that the Higgs potential has the form

$$V(\phi) = \frac{1}{2}\mu^2\phi^2 + \frac{1}{4}\lambda\phi^4 \,, \tag{1.7}$$

which only depends on the two parameters μ^2 and λ. Taking $\lambda > 0$ and $\mu^2 < 0$ induces a vacuum expectation value (VEV) for the Higgs field and triggers electroweak symmetry breaking. At the minimum of the potential $v = \sqrt{-\mu^2/\lambda}$ gives the Higgs field VEV and $m_h^2 = -2\mu^2$ gives the Higgs boson's mass. Thus, having measured both $v \simeq 246$ GeV and $m_h \simeq 125$ GeV in the laboratory, the Standard Model completely predicts the shape of the Higgs potential.

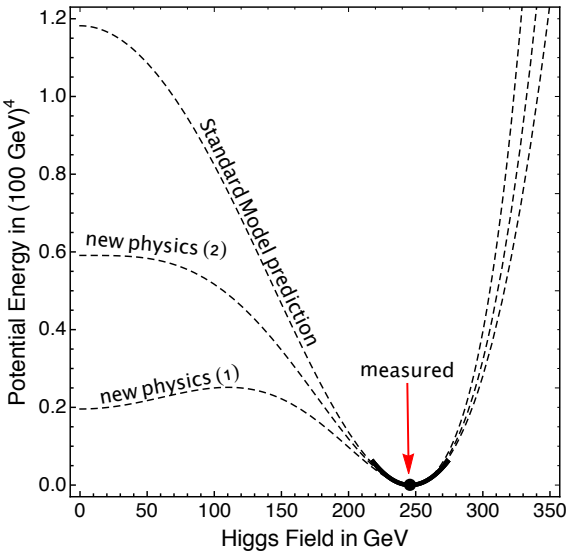

Figure 1.11: The Higgs potential energy function. All we know about the shape of the Higgs potential is the local curvature at its minimum. These observations are consistent with the Standard Model, but they are also consistent with models containing new physics that can dramatically change the nature of the electroweak phase transition.

However the presence of new physics can dramatically change the shape of the Higgs potential without disrupting the measurements of v and m_h. For example, a simple generalization of Eq. (1.7) is to include a sextic term and write the Higgs potential as [35–37]

$$V(\phi) = \frac{1}{2}\mu^2\phi^2 + \frac{1}{4}\lambda\phi^4 + \frac{1}{8\Lambda^2}\phi^6 \,. \tag{1.8}$$

A potential of this form arises if new, heavy particles are coupled to the Higgs boson, and then Λ is related to the mass scale of the new particles. This potential has enough structure to support two local minima with a barrier between, which we see in Fig. 1.11 for the curve labeled "new physics (1)." The nature of the electroweak phase transition in this model is expected to be very different from the Standard Model due to the barrier [38–40]. Alternatively the new physics can manifest through a non-analytic term in the Higgs potential, such as the one proposed by Coleman and Weinberg [41],

$$V(\phi) = \frac{1}{4}\lambda\phi^4 \, \log\frac{\phi^2}{\Lambda^2} \,. \tag{1.9}$$

Such a potential arises when new physics is coupled to the Higgs and leads to a strong running in the Higgs quartic self-coupling [42]. As shown by the curve labeled "new physics (2)" in Fig. 1.11, this potential is very flat near the origin allowing thermal corrections to induce a barrier and thus a first order phase transition.

Precision measurements of the Higgs boson's interactions with itself and other particles will probe the shape of the potential energy function and thereby provide much-needed experimental input to test the order of the electroweak phase transition.

Cosmological implications

Since we cannot reproduce the high-temperature conditions of the electroweak phase transition in the laboratory, the question of the EWPT has the most relevance for studies of

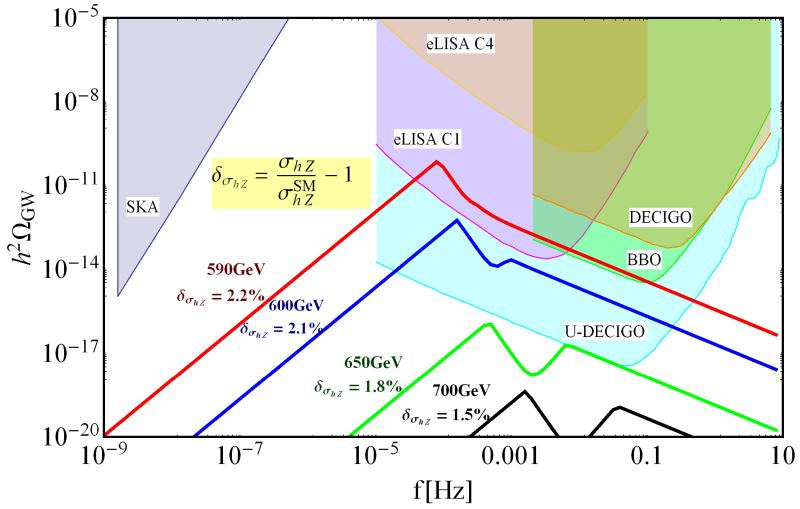

Figure 1.12: The spectrum of gravitational waves generated during a first order electroweak phase transition for the model described in Eq. (1.8). Colored curves show the predicted spectrum for different models as the scale of new physics, Λ, is varied. The figure is reproduced from Ref. [40].

the early universe. Most cosmologists expect that a thermal EWPT occurred soon after the Big Bang when the universe was filled with a very hot plasma. If the early universe EWPT was first order, it may have left behind interesting cosmological relics that could be accessible to observations today.

Gravitational Waves. During a first order electroweak phase transition, gravitational waves are produced from the collisions of bubbles, the decay of magnetohydrodynamic turbulence, and the damping of sound waves [43]. Today these gravitational waves would look like a stochastic and isotropic "noise" from all directions on the sky. As we see in Fig. 1.12 the predicted gravitational wave spectrum falls within reach of future space-based interferometer experiments, including LISA, DECIGO, BBO, Taiji, and TianQin. The detection of these gravitational waves would provide direct evidence that the cosmological EWPT was a first-order one, but a future collider like the CEPC is required to uncover the new physics that explains *why* the EWPT is first order.

Matter-Antimatter Asymmetry. A first order cosmological EWPT provides the right environment to explain the Universe's excess of matter over antimatter through the mechanism of *electroweak baryogenesis* [44]. This mechanism uses the fact that baryon number is violated in the Standard Model through reactions mediated by the electroweak sphaleron. Before the cosmological EWPT, the sphaleron efficiently converts matter into antimatter, but during the electroweak phase transition the sphaleron-mediated reactions are shut off. If this shutoff is sufficiently abrupt, then an excess of matter over antimatter can be generated. This requires that the electroweak phase transition is *strongly first order* in the sense that

$$\frac{v(T_{\rm pt})}{T_{\rm pt}} \gtrsim 1.0 \qquad \text{("strongly first order" electroweak phase transition)} \tag{1.10}$$

where $v(T_{\rm pt})$ is the value of the Higgs field inside of the bubbles during the phase transition at temperature $T_{\rm pt}$.

Electroweak baryogenesis is not viable in the Standard Model, because the electroweak phase transition is a continuous crossover, $v(T_{\rm pt}) = 0$, and thus the observed excess of matter over antimatter is an irrefutable motivation for physics beyond the Standard Model. In general the new physics can take many forms, but in the context of electroweak baryogenesis, it is clear that the new physics must couple to the Higgs boson so that the sphaleron-suppression condition in Eq. (1.10) is satisfied. Therefore this condition directly quantifies the required departure from Standard Model physics.

New physics and the electroweak phase transition

The Standard Model predicts that the EWPT is a continuous crossover, but we have seen in the discussion of Fig. 1.11 that even minimal extensions of the Standard Model can drastically change the predictions for electroweak symmetry breaking. Thus for any model with new physics coupled to the Higgs, it is necessary to ask: What is the nature of the electroweak phase transition?

In the years before the LHC started running, much of the work was focused on the *light stop scenario* of the Minimal Supersymmetric Standard Model (MSSM) [45, 46]. Early LHC data determined that this scenario is ruled out [47], because the light stops, which are colored and charged particles with spin-0, should have been easy to produce and detect at the LHC. However, if the new scalar particles were not charged or colored, the electroweak phase transition could still be first order while evading collider constraints; to leading order, the electroweak phase transition only cares about couplings with the Higgs, not quantum numbers [48]. Therefore in order to assess the unique power of the CEPC to test new physics that leads to a first order electroweak phase transition, it is useful to consider models with uncharged and uncolored particles, which are very difficult to probe at the LHC.

A viable model with a first order EWPT is found in even the most minimal extension of the Standard Model with a real, scalar singlet field S [49–51]. The relevant Lagrangian is written as

$$\begin{aligned}\mathscr{L} = &\left(D_\mu H\right)^\dagger \left(D^\mu H\right) + \frac{1}{2}\left(\partial_\mu S\right)\left(\partial^\mu S\right) - \mu_H^2 H^\dagger H - \lambda_H \left(H^\dagger H\right)^2 \\ &- \frac{\mu_S^2}{2} S^2 - \frac{a_S}{3} S^3 - \frac{\lambda_S}{4} S^4 - \lambda_{HS} H^\dagger H S^2 - 2 a_{HS} H^\dagger H S \end{aligned} \tag{1.11}$$

where $H(x)$ denotes the Higgs doublet field. The last two operators in Eq. (1.11) correspond to the so-called Higgs portal interactions. The Higgs field acquires a vacuum expectation value, $\langle H \rangle = (0\,,\, v/\sqrt{2})$ that breaks the electroweak symmetry. In general the singlet field may acquire a vacuum expectation value, $\langle S \rangle = v_S$, and it can mix with the Higgs boson, which is parametrized by an angle θ. The spectrum of this theory contains two scalars with masses $m_h \simeq 125$ GeV and m_S.

It is also interesting to consider the model that is obtained by imposing a $\mathbb{Z}_2$ symmetry on Eq. (1.11). This symmetry transformation, $S(x) \to -S(x)$, enforces $a_{HS} = a_S = 0$, and it is conventional to also assume that $v_S = 0$.

The singlet extension of the Standard Model allows for a first order electroweak phase transition in a variety of ways [48]. If the singlet particle is heavy, $m_S \gg m_h$, then it can be integrated out of the theory generating an effective potential for the Higgs field. In the regime where the a_S and λ_S terms are negligible and $\mu_S^2 \gg \lambda_{HS} v^2$, the Higgs potential

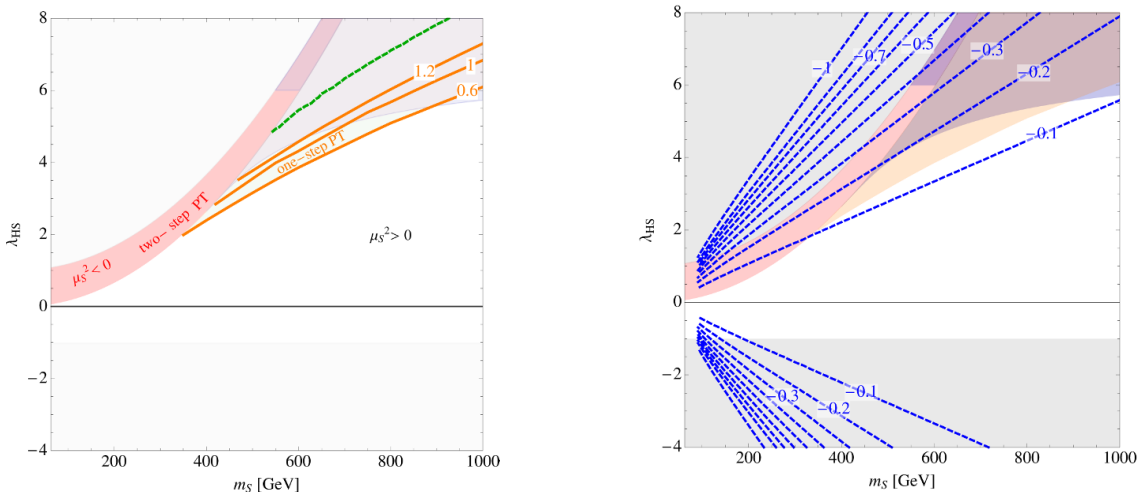

Figure 1.13: Parameter space of the real scalar singlet model with $\mathbb{Z}_2$ symmetry. *Left:* Regions of parameter space that lead to a first order electroweak phase transition that proceeds in one or two steps. The orange curves show the strength of the electroweak phase transition, $v(T_c)/T_c$, in the one-step region. *Right:* Blue curves show the fractional change to the Zh production cross section relative to the SM prediction in percent; these values are $2\,\delta g_{hZZ}$ using the notation in the text (1.13). The figures are taken from Ref. [53]

takes the form

$$V(\phi) = \frac{1}{2}\mu_H^2\phi^2 + \frac{1}{4}\left(\lambda_H - \frac{2a_{HS}^2}{\mu_S^2}\right)\phi^4 + \frac{\lambda_{HS}\,a_{HS}^2}{2m_S^4}\phi^6\,, \tag{1.12}$$

which has the same structure as the one that we encountered in Eq. (1.8). The two potentials are matched by taking $\Lambda^2 = m_S^4/(4\lambda_{HS}a_{HS}^2)$. For smaller Λ the shape of the Higgs potential begins to deviate more from the Standard Model prediction, and the phase transition becomes first order. This example illustrates the intuition that models with a first order electroweak phase transition require new, light particles with a large coupling to the Higgs boson. If the singlet particle is so light that we are not justified to integrate it out ($m_S \sim m_h$) the analysis above is inapplicable, but the phase transition can still be made first order due to the presence of large loop corrections to the Higgs potential [42], large thermal corrections, and/or a multi-step phase transition [52]. Some of these scenarios are illustrated in the left panel of Fig. 1.13 for the $\mathbb{Z}_2$-symmetric singlet extension.

In general the presence of new particles coupled to the Higgs boson modifies how strongly the Higgs couples to itself and to the other Standard Model particles. It is precisely the goal of Higgs factory experiments, like the CEPC, to measure these couplings with high precision. Therefore, if the electroweak phase transition is first order, we expect that the measurements of these couplings must deviate from their Standard Model predictions.

The coupling that will be measured most precisely at the CEPC and future lepton colliders is the Higgs-Z-Z coupling. We can parametrize deviations in this parameter away from the Standard Model prediction with the variable

$$\delta g_{hZZ} \equiv \frac{1}{2}\left(\frac{\sigma(e^+e^- \to hZ)}{\sigma_{\rm SM}(e^+e^- \to hZ)} - 1\right)\Bigg|_{s=(250\ \text{GeV})^2} = \frac{g_{hZZ}}{g_{hZZ,\rm SM}} - 1\Bigg|_{s=(250\ \text{GeV})^2}\,. \tag{1.13}$$

In the singlet extension model, the strength of the hZZ coupling is suppressed compared to the SM prediction. The leading-order suppression arises from the Higgs-singlet mixing, and the sub-leading effect arises from Higgs wavefunction renormalization [33] and the Higgs triple self-coupling [54]. Combining these effects, the fractional suppression is written as [53, 55]

$$\begin{aligned}\delta g_{hZZ} =&\big(\cos\theta - 1\big) - 2\frac{|a_{HS} + \lambda_{HS} v_S|^2}{16\pi^2} I_B(m_h^2; m_h^2, m_S^2) \\ &- \frac{|\lambda_{HS}|^2 v^2}{16\pi^2} I_B(m_h^2; m_S^2, m_S^2) + 0.006 \left(\frac{\lambda_3}{\lambda_{3,\text{SM}}} - 1\right)\end{aligned} \tag{1.14}$$

where θ is the Higgs-singlet mixing angle, and I_B is a loop function. The Higgs triple self-coupling λ_3 also deviates from the Standard Model prediction due to the Higgs-singlet mixing. Then the self-coupling is predicted to be [56]

$$\begin{aligned}\lambda_3 =& \big(6\lambda_H v\big)\cos^3\theta + \big(6a_{HS} + 6\lambda_{HS} v_S\big)\sin\theta\cos^2\theta \\ &+ \big(6\lambda_{HS} v\big)\sin^2\theta\cos\theta + \big(2a_S + 6\lambda_S v_S\big)\sin^3\theta\,.\end{aligned} \tag{1.15}$$

In the Standard Model we have $\lambda_3 = \lambda_{3,\text{SM}} \equiv 3m_h^2/v \simeq 191$ GeV. If the singlet is light, $m_S < m_h/2$, then the Higgs boson acquires an exotic decay channel, $h \to SS$, which may be invisible depending on the stability of S. The rate for this decay is

$$\Gamma(h \to SS) = \frac{\lambda_{211}^2}{32\pi m_h}\sqrt{1 - \frac{4m_S^2}{m_h^2}} \tag{1.16}$$

where

$$\begin{aligned}\lambda_{211} =& \big(2a_{HS} + 2\lambda_{HS} v_S\big)\cos^3\theta + \big(4\lambda_{HS} v - 6\lambda_H v\big)\sin\theta\cos^2\theta \\ &+ \big(6\lambda_S v_S + 2a_S - 4\lambda_{HS} v_S - 4a_{HS}\big)\sin^2\theta\cos\theta + \big(-2\lambda_{HS} v\big)\sin^3\theta\,.\end{aligned} \tag{1.17}$$

is the effective tri-linear coupling of the mass eigenstates. Measurements of the Higgs boson at the LHC already strongly constrain the invisible decay channel, which requires $\lambda_{211} << 1$ or $m_S > m_h/2$.

The complementarity between first order electroweak phase transition and precision Higgs observables is shown in Fig. 1.14 for the singlet extension of the Standard Model. Orange points correspond to models with a first order phase transition, $v(T_{\text{pt}})/T_{\text{pt}} \neq 0$. Blue points correspond to models with a strongly first order phase transition, $v(T_{\text{pt}})/T_{\text{pt}} \gtrsim 1$, which is a necessary requirement for electroweak baryogenesis (1.10). Red points correspond to models with a very strongly first order phase transition that can potentially be probed by the space-based gravitational wave interferometer telescope LISA.

Figure 1.14 shows that the models with a first order phase transition (all colored points) also generally predict large deviations in the hZZ coupling. For the models with a strongly first order phase transition (blue and red points) the effect on g_{hZZ} is large enough to be tested by the CEPC. Additionally, most of the parameter points also predict a large enhancement to the Higgs trilinear self-coupling that can be probed by a future 100 TeV hadron collider experiment, like the proposed SppC. The funnel region of orange points at $\lambda_3/\lambda_{3,\text{SM}} \approx 1$ corresponds to a "blind spot" where the Higgs-singlet mixing vanishes. Thus, apart from the blind spot, *the reach of the CEPC is sufficient to probe a first order electroweak phase transition across the entire parameter space*.

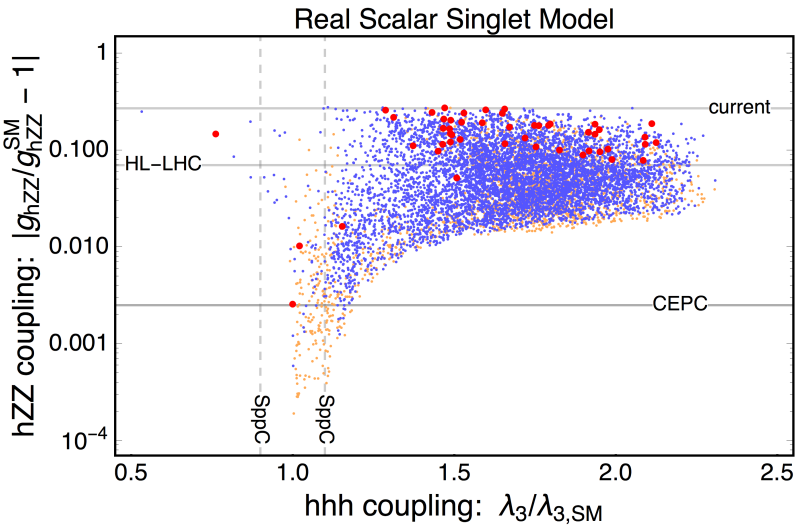

Figure 1.14: Collider observables in the real scalar singlet model. Points in theory space with a first order phase transition are shown in orange, points with a strongly first order phase transition are shown in blue, and points with a strongly first order phase transition that also produces detectable gravitational waves are shown in red. The figure is reproduced from Ref. [55].

The blind spot mentioned above corresponds to two scenarios. The Higgs-singlet mixing could vanish, because of an accidental cancellation between a_{HS} and $\lambda_{HS}v_S$. This corresponds to an artificially fine-tuned parameter space, that is not theoretically appealing. Alternatively, the mixing vanishes identically in the $\mathbb{Z}_2$ symmetric limit of the singlet extension. In this case, the relevant parameter space is shown in Fig. 1.13. The right panel shows the predicted deviation in the hZZ coupling away from the Standard Model expectation, which is on the edge of the CEPC sensitivity.

Another representation of the parameter space appears in Fig. 1.15, which shows a correlation between the phase transition temperature and the Higgs cubic self-coupling. For a similar analysis see also Ref. [57], but note that this article was published before the Higgs mass was determined.

Among all possible new physics that renders the electroweak phase transition to be first order, we focus on the singlet extension here, because it is the most challenging to test with collider experiments. To illustrate this point, one can allow the new scalar particles to carry an electric charge (similar to a two-Higgs doublet model). An analysis of this model has been performed in Ref. [55], and the results are shown in Fig. 1.16. The CEPC has enough sensitivity to test the entire interesting parameter space, and much of the space will also be tested by measurements at the LHC.

What will we learn from the CEPC?

The CEPC will probe the Higgs boson with unprecedented precision. While the LHC has taught us that the Higgs is responsible for electroweak symmetry breaking, measurements at the CEPC provide a unique opportunity to learn *how* electroweak symmetry breaking occurs. The nature of the electroweak phase transition is a question that we cannot settle using only measurements at the LHC and its upgrades. Simple and compelling extensions of the Standard Model can have a dramatic effect on the nature of the electroweak phase transition, while remaining completely inaccessible to the LHC. However, the presence

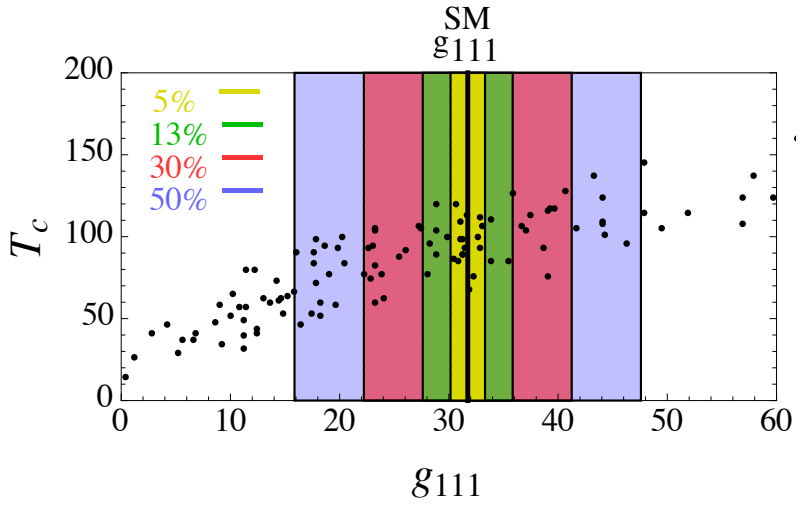

Figure 1.15: A correlation between the cubic self-coupling of the SM-like scalar boson and the critical temperature of the first order electroweak phase transition. To connection with the notation in the text, $g_{111} \to \lambda_3/(6\ \mathrm{GeV})$ and $T_c \to T_{\mathrm{pt}}/\mathrm{GeV}$. The figure is reproduced from Ref. [56].

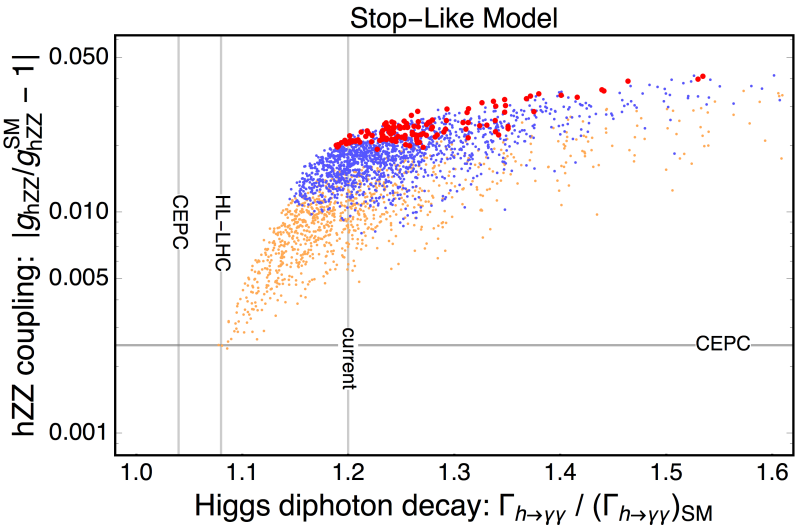

Figure 1.16: A model in which the new scalar particles are charged and uncolored. Such a model can be tested by the CEPC, but it is already strongly constrained by the LHC's measurement of the Higgs diphoton decay width. The figure is reproduced from Ref. [55].

of new particles coupled to the Higgs boson must affect the way that the Higgs boson couples to itself and to other Standard Model particles, such as the Z-boson. Therefore precision measurements of the Higgs couplings are precisely what's required to expose the new physics. In particular, the strength of the hZZ coupling, which will be measured at the 0.1% level by the CEPC, is an excellent litmus test for a first order electroweak phase transition.

1.3 Exploring new physics

Exotic new physics could interact with the Standard Model in multiple ways that could be tested at CEPC. Here we summarize and classify different possible scenarios, which are discussed in more detail in the following sections:

1. Exotic particles carry Standard Model charges. The classic example in the dark matter context is dark matter in electroweak multiplets: although dark matter must be neutral, it could be part of an SU(2) multiplet that also contains charged particles. Because CEPC is primarily a machine for Higgs and electroweak physics, this is a natural case to consider.

2. Renormalizable Standard Model portals: if there are no new particles with Standard Model gauge interactions and no new gauge groups that the Standard Model particles are charged under, exotic particles in the hidden (dark) sectors can still interact with the Standard Model via the gauge-singlet operators $H^\dagger H$ ("Higgs portal") [58–65], $B_{\mu\nu}$ ("hypercharge portal" or kinetic mixing) [66–72], and HL ("neutrino portal") [73–79].

3. Portals with additional Standard Model sector physics or new gauge groups that the Standard Model is charged under: if some exotic particle itself carries no Standard Model gauge charges, it may nonetheless interact with the Standard Model via unknown new particles with Standard Model charges. For instance, the existence of a second Higgs doublet that couples dominantly to leptons can make models of "leptophilic" dark matter possible. The second possibility is that there exists some new gauge group, e.g. $U(1)'$, that (some) Standard Model particles are charged under. Then there is a renormalizable coupling between the new gauge boson and the current made of the Standard Model particles. If the new gauge group is anomalous with the Standard Model particle content, there could also be a Wess-Zumino type interaction between the Z and the new gauge boson [80–89].

4. Effective theory and high dimensional operators: this approach is agnostic to which of the above three scenarios we consider. The theory only contains certain light exotic particles and the Standard Model. The other new physics that generates the coupling between them is not identified and is only encoded in Wilson coefficients. Examples include an axion-like particle (ALP) interacting with the Z boson or photon through dimension-five operators [90–102] and magnetic inelastic dark matter and Rayleigh dark matter models [103–107], in which the dark sector interacts with Z via even higher dimensional operators.

These different scenarios may result in modifications to precision Higgs and Z observables or to exotic Higgs and Z decays. The first type of signal has been discussed in Chapter 2. In sections 1.3.1 and 1.3.2, we will discuss the potential of CEPC for measuring exotic Higgs and Z decays. Then in section 1.3.3, we will focus on the implications for dark matter and dark sectors. In sections 4.5 and 4.6, we will discuss the potential of measuring exotic physics connected to neutrino and flavor physics.

1.3.1 Higgs exotic decays

Higgs boson can be an important portal to new physics beyond the Standard Model. Such new physics could manifest itself through Higgs exotic decays if some of the degrees of freedom are light. The Higgs boson BSM decays have a rich variety of possibilities. To organize this study on Higgs boson BSM decays. We focus on two-body Higgs decays into BSM particles, dubbed as X_i, $h \to X_1 X_2$, which are allowed to subsequently decay further, up to four-body final states. The cascade decay modes are classified into four cases, schematically shown in Fig. 1.17. These processes can be motivated by SM+singlet extensions, two-Higgs-doublet-models, SUSY models, Higgs portals, gauge extensions of the SM [108–110].

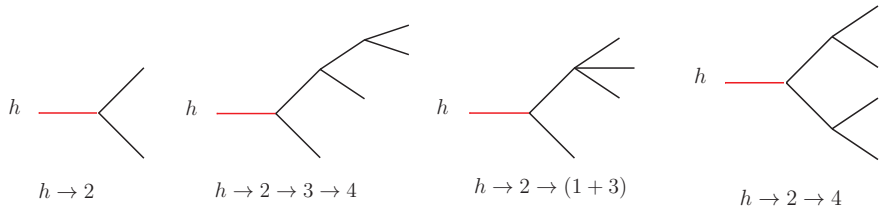

Figure 1.17: The topologies of the SM-like Higgs exotic decays.

For CEPC running at the center of mass energy $240 \sim 250$ GeV, the most important Higgs production mechanism is Z-Higgs associated production $e^+e^- \to Z^* \to Zh$. The Z boson with visible decays enables Higgs tagging using the "recoil mass" technique. A cut around the peak of the recoil mass spectrum would remove the majority of the SM background. To demonstrate a typical Higgs exotic search at CEPC, we show one benchmark processes from our analysis,$h \to jj + E_{\rm T}^{\rm miss}$ and $h \to b\bar{b} + E_{\rm T}^{\rm miss}$. In the last part of this section, we present the summary for Higgs exotic decay physics potential at CEPC for an integrated luminosity of 5 $\rm ab^{-1}$ and 10 $\rm ab^{-1}$ operated at 240 GeV. The details of these analysis can be found in Ref. [110].

For numerical analyses, we generate both the signal and the background events for a 240 GeV electron-positron collider with `MadGraph5` at parton level [111] We describe here our parameter choices for the detector effects, and our pre-selection cuts that are universal for the analyses for all Higgs exotic decay mode. All of the visible particles in the final state are required to have $|\cos\theta| < 0.98$, or equivalently $|\eta| < 2.3$. The final state particles are required to be well separated with $y_{ij} \equiv 2\min\left(E_i^2, E_j^2\right)(1-\cos\theta_{ij})/E_{vis}^2 \geqslant 0.001$. We only study the case where the Z boson decays into $\ell^+\ell^-$ where $\ell^\pm = e^\pm, \mu^\pm$. The signal events are required to contain at least a pair of opposite-sign same-flavor charged leptons with an opening angle greater than 80°, and satisfy $E_\ell > 5$ GeV and $|m_{\ell\ell} - m_Z| < 10$ GeV, where $m_{\ell\ell}$ is the invariant mass of the di-lepton system. The recoil mass is defined as $m^2_{\rm recoil} \equiv s - 2\sqrt{s}E_{\ell\ell} + m^2_{\ell\ell}$ where $E_{\ell\ell} = E_{\ell^+} + E_{\ell^-}$. The recoil mass is required to satisfy $|m_{\rm recoil} - m_h| < 5$ GeV. To suppress the ISR contribution to the backgrounds[1], for Higgs exotic decay modes without missing energy, we require the events to have the total visible energy $E_{vis} > 225$ GeV. We mimic the detector resolution effect by adding Gaussian smearing effects on the four-momentum of the particles, details can be found in Ref. [110].

[1]Corrections from beamstrahlung effect [112] and ISR effect [113] need to be carefully taken into account for certain processes relying a precise reconstruction of the recoil mass.

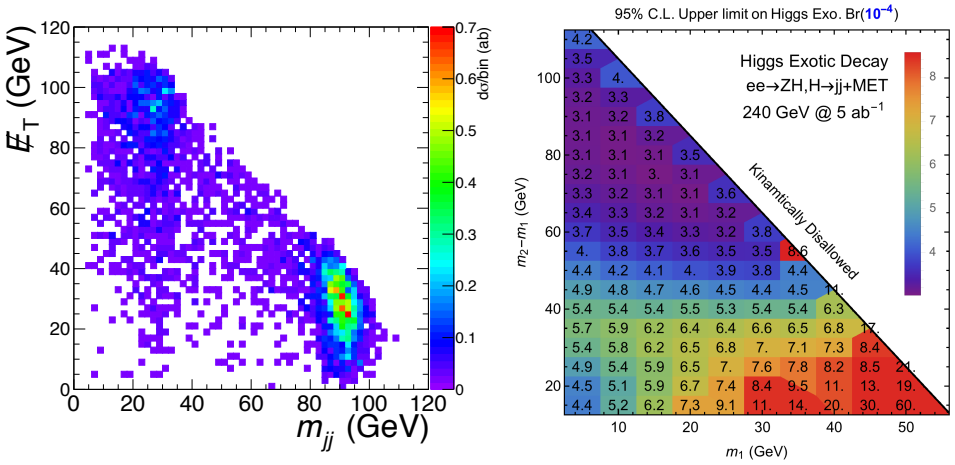

Figure 1.18: left panel: The invariant mass distribution of the SM backgrounds for $\ell^+\ell^-\nu_\ell\bar{\nu}_\ell jj$ in the m_{jj}-$E_{\rm T}^{\rm miss}$ plane. **Right panel:** The 95% C.L. upper limit on the Higgs exotic decay branching fractions into $jj + E_{\rm T}^{\rm miss}$ for various lightest detector-stable particle mass m_1 and mass splittings $m_2 - m_1$.

1.3.1.1 $h \to jj + \boldsymbol{E_{\rm T}^{\rm miss}}$

The SM-like Higgs boson decays into X_2X_1 with $X_2 \to X_1jj$ through an off-shell intermediate state gives raise to this exotic decay mode. Beyond the pre-selection cut and the recoil mass cut, we require that there are two additional jets which satisfy $E_j > 10\,\text{GeV}$ and $|\cos\theta_j| < 0.98$. The dominant background after the recoil mass cut will clearly be the Higgsstrahlung process with $h \to ZZ^* \to q\bar{q}\nu\bar{\nu}$. After the recoil mass cut, the SM background cross section is 0.063 fb. The dijet invariant mass (m_{jj}) distribution and the two-dimensional differential distribution of m_{jj} versus $E_{\rm T}^{\rm miss}$ of the SM background after the recoil mass cut are shown in the left panel of Fig. 1.18. There is a clear valley in the distribution between 35 to 75 GeV, in which none of the Z bosons from the SM-like Higgs boson decay are on-shell and thus the $h \to q\bar{q}\nu_\ell\bar{\nu}_\ell$ is doubly suppressed.

We use the likelihood function of the $m_{b\bar{b}}$-$E_{\rm T}^{\rm miss}$ distribution to derive the exclusive limit. The results are shown in the right panel of Fig. 1.18 in the plane of X_1, mass m_1, and the mass splitting between X_2 and X_1, $m_2 - m_1$ for $h \to jj + E_{\rm T}^{\rm miss}$. The exclusion limits on the branching fraction in the bulk region of the parameter space reach $3 \times 10^{-4} \sim 8 \times 10^{-4}$ for $h \to jj + E_{\rm T}^{\rm miss}$.

From the exclusion limits shown in the right panel of Fig. 1.18, we find that when the mass splitting $m_2 - m_1$ is around 80 GeV, the future lepton colliders have the strongest sensitivities on these Higgs exotic channels, reaching around 3.1×10^{-4} for $h \to jj + E_{\rm T}^{\rm miss}$. When X_1 is light and $m_2 - m_1$ is large, the energy is shared by the two jets and the X_1. Consequently, when the mass splitting $m_2 - m_1$ is around 80 GeV, the dijet invariant mass will be around 40∼60 GeV, falling in the "valley" of low SM background as shown in the left panel of Fig. 1.18. For heavier X_1, the MET will be lower due to less momentum available for the LSP. The optimal limits will be reached for an even smaller mass splitting.

1.3.2 Exotic Z decay

CEPC's Z pole run will offer unique possibilities to test new physics. We summarize the sensitivities of exotic Z decay branching ratios at CEPC including a hypothetical Tera Z, comparing them with those of HL-LHC, in Fig. 1.19. We have classified exotic Z decay channels by final states, the number of intermediate resonances, and different topologies. The final states we consider are $Z \to \not{E} + \gamma$, $\not{E} + \gamma\gamma$, $\not{E} + \ell^+\ell^-$, $\not{E} + JJ$, $(JJ)(JJ)$ and $\gamma\gamma\gamma$. Each pair of photons, charged leptons or jets can be a resonance, which we denoted with $()$. In Fig. 1.19, we go through all six categories of final states and for each category, we choose several typical decay topologies and the detailed process is labeled on the bar-chart. For CEPC and Tera Z, the sensitivity reach for exotic Z decay branching ratios (BR) are plotted as blue and red bars. The kinematic cuts are general p_T and angular cuts on reconstructed objects, and if there is a resonance in the pair of particles (including dark matter particles), an appropriate invariant mass cut will be applied. The cuts are optimized for each topology by checking the kinematic variable distributions. The sensitivity reach for the high luminosity LHC (HL-LHC) at 13 TeV with $\mathcal{L} = 3\ \mathrm{ab}^{-1}$ has been computed in a similar way. Details of the simulation can be found in Ref. [114].

The sensitivity to final states with missing energy reaches branching ratios 10^{-6} to $10^{-9.5}$ for CEPC and 10^{-7} to $10^{-11.5}$ for Tera Z. For each topology, the light blue and red shaded regions indicate the range from varying the model parameters, like mediator or dark matter mass. The light color regions with dashed boundary show the optimal sensitivity, while the dark color regions with solid boundary show the pessimistic benchmark of the model. In all the channels, future Z factories improve the sensitivity by several orders of magnitude above those of HL-LHC.

In general, CEPC has several advantages compared to a hadron collider like HL-LHC. First, an e^+e^- collider has a much cleaner environment compared to a hadron collider with a huge QCD background. Second, in the Drell-Yan production of a Z boson at a hadron collider, the decay products tends to be soft because the Z boson mass is small compared to the beam energy, which makes it hard to detect at HL-LHC. Therefore, it is natural that CEPC has better sensitivity compared to HL-LHC and provides a better opportunity to look into the dark sector physics through exotic Z decays.

We will present two case studies to demonstrate the great power of exotic Z decays to probe different dark (hidden) sectors [114]. (Further discussion of a variety of exotic Z decays appears in [115].) The first model contains fermionic dark matter interacting with a singlet real scalar S, which mixes with the Standard Model Higgs. The possible exotic Z decay channel in this case is $Z \to \tilde{s}Z^* \to (\bar{\chi}\chi) + \ell^+\ell^-$, where $\tilde{s}$ is the light scalar mass eigenstate (mostly the dark Higgs S) and χ is the fermionic dark matter. The second model is an axion-like particle a coupling to the Standard Model $U(1)_Y$ gauge field B_μ. Then the exotic Z decay is $Z \to a\gamma \to (\gamma\gamma)\gamma$. The final state is 3γ and in the case that m_a is too small to separate the two photons, the final state is 2γ. The sensitivity of exotic Z decays (as well as other possible probes) to key parameters in these two models is summarized in Fig. 1.20.

In the left panel of Fig. 1.20, there are two free parameters, the Higgs mixing angle $\sin\alpha$ and dark Higgs mass $m_{\tilde{s}}$. The other two parameters related to dark matter are fixed. One is the dark matter mass, fixed closed to half of $m_{\tilde{s}}$, which only affects the dark matter relic abundance but not other limits. The other one is the Yukawa coupling between dark matter χ and the dark Higgs $\tilde{s}$, which is taken to be $y_\chi = 0.1$ for illustrative purposes. We

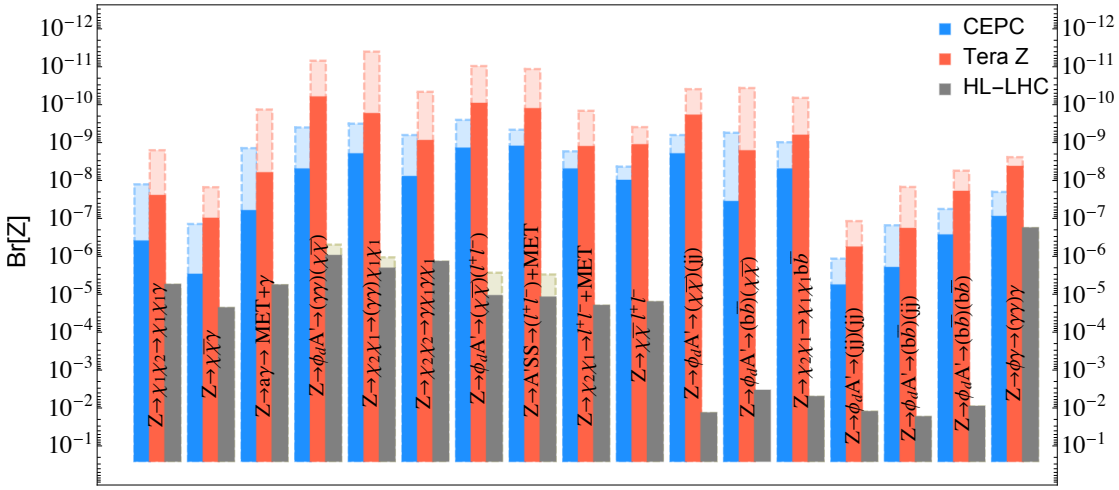

Figure 1.19: The sensitivity reach for branching ratio for various exotic Z decay topologies at CEPC (10^{10} Z), a possible extension to Tera Z (10^{12} Z), and the high luminosity LHC at 13 TeV with $\mathcal{L} = 3\ \mathrm{ab}^{-1}$. Adapted from ref. [114].

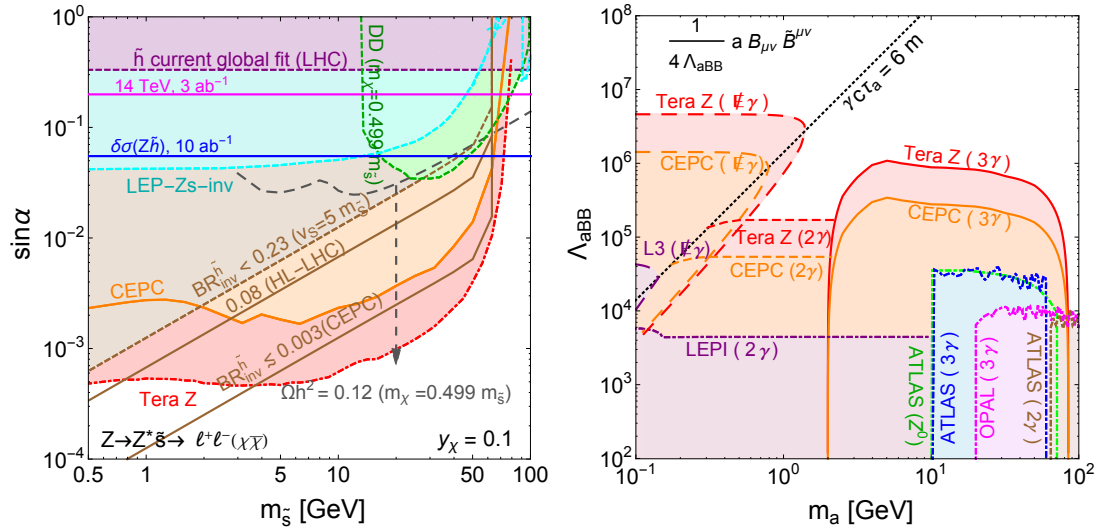

Figure 1.20: Z rare decays at CEPC, adapted from Adapted from ref. [114]. **Left**: the sensitivity to the dark Higgs mixing angle $\sin\alpha$ at CEPC (10^{10} Z) and at a Tera Z option (10^{12} Z) in a Higgs portal dark matter model, using the process $Z \to \ell^+\ell^-\tilde{s} \to \ell^+\ell^-(\bar{\chi}\chi)$. **Right**: the sensitivity to the coupling Λ_{aBB} for an axion-like particle (ALP) model as a function of the ALP mass m_a, where B is the hypercharge gauge field. The signal process is $Z \to \gamma a$, where a can decay to a pair of photons (3γ), be detected as one photon due to high boost (2γ), or be detected as missing energy due to its long lifetime ($\gamma \not{E}$).

look for the exotic Z decay process $Z \to \ell^+\ell^-\tilde{s} \to \ell^+\ell^-(\bar{\chi}\chi)$, which has been labeled as an orange solid line for the CEPC (10^{10} Z) option and a red dot-dashed line for the Tera Z (10^{12} Z) option, and compared with the LEP result with an integrated luminosity $114\ \mathrm{pb}^{-1}$ [116] labeled as "LEP-Zs-inv".

The dark Higgs can also be constrained using the modified SM Higgs coupling with mixing angle $\sin\alpha$, independent of the scalar mass $\tilde{s}$. The global fit to Higgs data at

the LHC 7 TeV and 8 TeV runs can constrain the single scaling factor to Higgs interactions, and this gives $\sin\alpha < 0.33$ [117] which is labeled as "$\tilde{h}$ current global fit (LHC)". The HL-LHC can extend the reach to $\sin\alpha < 0.28$ (0.20) using 300 fb^{-1} $(3$ ab$^{-1})$ luminosity [118]. In the future e^+e^- collider, the precision measurement of the Higgs bremsstrahlung cross-section $\sigma(Zh)$ can reach the accuracy of $\mathcal{O}(0.3\% - 0.7\%)$ expected from $5 - 10$ ab^{-1} [119–121], which can probe the scalar mixing down to $0.055 - 0.084$ [122], labeled as "$\delta\sigma(Zh)$". The next type of constraint comes from SM Higgs invisible decay. The current LHC limits from the Run I combination of ATLAS and CMS data constrains BR$(h \to$ inv$) \leq 0.23$ at 95% C.L. [123, 124]. Following the $\tilde{h}$ invisible decay branching ratio in the Higgs portal dark matter model, the limit on the mixing angle $\sin\alpha$ is labeled as "BR$^{\tilde{h}}_{\text{inv}} < 0.23$". We also add the HL-LHC (3 ab^{-1}) and future e^+e^- collider projections on invisible Higgs search, which lead to 95% C.L. limits BR$^{\tilde{h}}_{\text{inv}} \lesssim 0.08 \sim 0.16$ [125, 126] and BR$^{\tilde{h}}_{\text{inv}} \lesssim 0.003$ [120, 127] at ILC and CEPC. There are also constraints based on dark matter assumptions. The dark matter relic abundance [128] is satisfied on the dashed gray line, while the direct detection searches on spin-independent cross-sections (XENON1T [129], LUX [130], PANDAX-II [131], and CRESST-II [132]) excludes the region within the dashed green line.

In the right-panel of Fig. 1.20, we have searched for the exotic Z decay $Z \to \gamma a$, followed by $a \to \gamma\gamma$. In the 3γ signal, the ALP mass is heavy enough that the two photons are well separated and detectable. When the mass of the ALP is below $\mathcal{O}(1)$ GeV, the boost of the axion makes the two photons from the axion decay close enough together that they cannot be resolved. Hence, the 2γ search channel is more relevant. The current constraints on the two cases are given by LEP and LHC photon searches. In Fig. 1.20, the LEP I [133] constraint uses an inclusive diphoton search $e^+e^- \to 2\gamma + X$ covering the small mass region. In the higher mass region, the boost of the axion decreases and the 3γ channel is considered. The LEP II (OPAL) constraints have 2γ and 3γ data [134], which are employed to put bounds on the process $e^+e^- \to \gamma/Z^\star \to a\gamma \to 2\gamma + \gamma$. ATLAS 3γ and $Z \to 3\gamma$ [135, 136] searches can be translated to an ALP bound, as derived in [137]. There is also the possibility that the ALP decays outside of the detector, which is relevant for a $\not{E} + \gamma$ search. In this case the strongest bound comes from the LEP L3 collaboration with 137 pb^{-1} data at the Z pole [138]. It can limit the BR of the exotic decay $Z \to \gamma\not{E}$ down to 1.1×10^{-6} if the photon energy is greater than ~ 30 GeV. It directly excludes $\Lambda_{\text{aBB}} < 4.3 \times 10^4$ for $Z \to \not{E} + \gamma$ decay, and is labeled as "L3 $(\not{E}\gamma)$" in the right panel of Fig. 1.20. The sensitivity curves are plotted as an orange solid line for CEPC (10^{10} Z) and a red dot-dashed line for a Tera Z (10^{12} Z) option.

These comparisons show that exotic Z decays at a future Z-factory could provide the leading sensitivities compared to other dark matter detection experiments, current limits from collider searches, and estimated sensitivities of high luminosity run of the LHC (HL-LHC).

1.3.3 Dark matter and hidden sectors

Observations tell us that the majority of matter in the universe is dark. Because the abundance of dark matter in the universe is within an order of magnitude of the abundance of ordinary matter, it is natural to suspect that dark matter and ordinary matter should be related in some way. A variety of models, including the classic thermal relic WIMP, attempt to explain the abundance of dark matter in terms of its interactions with ordinary matter.

In some models, there is a richer "dark sector" consisting not only of dark matter itself but of new force-carrying particles that can mediate self-interactions between dark matter particles or interactions of dark matter with ordinary matter.

Different classes of possibilities for how dark matter interacts with the Standard Model have been summarized in section 1.3. Below we discuss each of these possibilities in turn. This categorization of studies may be useful in the future for identifying DM scenarios at CEPC that have not yet been fully studied.

There are major efforts underway to search for dark matter via direct detection, indirect detection, and searches at the LHC and lower energy but high luminosity collider and fixed-target experiments. It is possible that one of these experiments will discover a dark matter signal before CEPC operates. Even in that case, CEPC can play a crucial role in discovering the *nature* of the dark matter particle. Direct detection, for example, may tell us a spin-independent scattering rate, but without knowledge of the local dark matter density or whether the particle we are seeing constitutes all of the dark matter or is just a component, limited knowledge of particle physics would be gleaned from the discovery. The role of CEPC in such a case could be to tell us that dark matter interacts directly with the Higgs boson or weak gauge bosons, for instance. Below we will emphasize both cases in which CEPC can *measure* dark matter properties and supplement other experiments and cases in which CEPC could play the crucial role in *discovering* a DM signal for the first time.

1.3.3.1 Dark matter in electroweak multiplets

CEPC's strength is electroweak physics, both through precision measurements of properties of W and Z bosons and through its primary role as a Higgs factory. Studies of the CEPC's capabilities for detecting new electroweak physics include [19, 22, 38, 139–145]. Hence, the most natural place to begin is with CEPC searches for dark matter particles that are in electroweak multiplets (e.g. doublets or triplets of $\mathrm{SU}(2)_L$) or mixtures of electroweak multiplets (including admixtures of a singlet). Studies on this topic include [146–151].

One question is whether other, dedicated dark matter experiments will cover the full parameter space of dark matter in electroweak multiplets. Dark matter direct detection experiments, like the currently-operating Xenon1T [129] and PandaX [152], are currently probing much of the parameter space for spin-independent dark matter scattering on nucleons mediated by Higgs exchange. The current bound on the DM-nucleon cross section of a few times $10^{-46}\ \mathrm{cm}^2$ corresponds to an $h\chi\chi$ coupling in the Lagrangian with coefficient of order 10^{-2}. Future experiments like DARWIN [153] will potentially push the search down to the neutrino floor, corresponding to $h\chi\chi$ couplings of order 10^{-3}. This will probe a large swath of the parameter space for electroweak dark matter.

As noted above, CEPC could help to measure DM properties even if a direct detection experiment makes the discovery first. Still more interesting are possibilities in which electroweak DM could be *missed* by direct detection experiments but seen by CEPC. There are two main scenarios to consider where this could happen. The first is if DM is a nearly pure electroweak multiplet, such as a pseudo-Dirac higgsino. Such particles have very small interactions with the Higgs, so their direct detection rate is loop-suppressed and at about the level of the neutrino floor [154]. These particles would also be very difficult to detect at the LHC [155]. Indirect detection may constrain them, but at low mass their thermal abundance is low, and even a significant non-thermal abundance may fall below

current constraints [156, 157]. A second possibility is that DM lies in a mixed electroweak multiplet with couplings to the Higgs, but the coupling of the lightest mass eigenstate has a small coupling to the Higgs, either accidentally or due to an approximate symmetry. This is referred to as a *blind spot* for direct detection [158, 159]. For instance, a mostly-wino dark matter particle in a supersymmetric theory has vanishing tree-level coupling to the Higgs boson if $M_2 = -\mu \sin(2\beta)$. In some cases, a spin-independent blind spot may be covered by spin-dependent scattering. Blind spots might also be uncovered by collider searches [160].

Robust blind spots for both spin-dependent and spin-independent scattering arise in some theories due to approximate *parity* or *custodial* symmetries. In the MSSM, this occurs for higgsino dark matter at $\tan\beta = 1$ and $\mathrm{sign}(\mu M_{1,2}) < 0$. In closely related theories, these blind spots have been understood to result from custodial symmetries [147]. These robust direct detection blind spots are excellent opportunities for CEPC to play a role in dark matter physics, so let us explain the physics in somewhat more detail. They arise for pseudo-Dirac DM, i.e. theories with a Dirac mass term of the form $\mu\chi_1\chi_2$ which can be written as a sum of two Majorana mass terms, $\mu(\chi_+\chi_+ - \chi_-\chi_-)$ where $\chi_\pm = \frac{1}{\sqrt{2}}(\chi_1 \pm \chi_2)$. In such a theory the Z boson couples off-diagonally, $Z_\mu(\chi_+^\dagger \overline{\sigma}^\mu \chi_- + \mathrm{h.c.})$. Mixing or higher-dimension operators can split the mass eigenstates, but in the custodially symmetric limit, the eigenstates remain χ_+ and χ_- rather than mixtures thereof. There is a parity symmetry under which χ_+ and the Z are odd but χ_- and h are even, which forbids an $h\chi_+\chi_+$ coupling. Hence when χ_+ is the lighter mass eigenstate, both spin-dependent and spin-independent scattering are turned off.

A number of studies have been carried out on two particular models of electroweak dark matter, the doublet–singlet and doublet–triplet models (e.g. [161–163]). The doublet–singlet model introduces a singlet fermion S (with zero hypercharge) with Majorana mass $-\frac{1}{2}m_S SS$ and two electroweak doublet Weyl fermions $D_{1,2}$ with opposite hypercharges $\mp 1/2$ and Dirac mass $-m_D\epsilon_{ij}D_1^i D_2^j$, together with mixing through the SM Higgs:

$$y_1 HSD_1 - y_2 H^\dagger S D_2 + \mathrm{h.c.} \tag{1.18}$$

The doublet–triplet model introduces the same doublet fields as well as an SU(2) triplet with zero hypercharge, T, with a Majorana mass $-\frac{1}{2}m_T T^i T^i$ and mixing with the doublet through the Higgs:

$$y_1(H\sigma^i D_1)T^i - y_2(H^\dagger\sigma^i D_2)T^i + \mathrm{h.c.} \tag{1.19}$$

Both of these models have blind spots for both spin-independent *and* spin-dependent direct detection in the pseudo-Dirac case when $m_D < m_{S,T}$ (all mass parameters taken to be positive) and $y_1 = y_2$. An explicit rewriting of the Lagrangian that makes a custodial symmetry manifest in this limit has been given in [147]. This blind spot can also be understood in terms of a parity symmetry at the point $y_1 = y_2$ along the lines explained in the previous paragraph.

In the SUSY context we can identify the fields S, D, and T with the bino, higgsino, and wino. In this case the couplings y_1 and y_2 are equivalent to $g^{(\prime)}\cos\beta$ and $g^{(\prime)}\sin\beta$ in the doublet–triplet (doublet–singlet) case. These relatively small couplings tend to lead to small signals at CEPC. However, it is also interesting to consider extensions of the MSSM with an *additional* doublet and singlet that mix to serve as dark matter. Such theories can help to explain why the observed Higgs mass is heavier than expected in the simplest SUSY theories [164], which offers a motivation for considering the larger values of $y_{1,2}$ that could be probed at CEPC.

Precision electroweak physics at the Z pole is most sensitive to the S and T parameters. Although these operators appear in studying the propagators of gauge fields, they originate from new physics that couples to the Higgs. For instance, in the basis of [165], the S parameter is related to the operators $H^\dagger \sigma^i H W^i_{\mu\nu} B^{\mu\nu}$, $(H^\dagger \sigma^i \overleftrightarrow{D}_\mu H) D^\nu W^i_{\mu\nu}$, and $(H^\dagger \overleftrightarrow{D}_\mu H)\partial^\nu B_{\mu\nu}$; the T parameter, to $(H^\dagger \overleftrightarrow{D}_\mu H)^2$. These operators are generated in the doublet–singlet or doublet–triplet model because the fermions mix by coupling to the Higgs boson. On the other hand, for a pure electroweak multiplet like the pseudo-Dirac higgsino, Higgs couplings are very small and S and T are suppressed. The T parameter is also suppressed in models with a good approximate custodial symmetry. In such theories, other electroweak precision observables like the W and Y operators $(D^\mu W^i_{\mu\nu})^2$ or $(\partial^\mu B_{\mu\nu})^2$ may be relatively important, though they are generated with small coefficients and are harder to probe. In this case, observables at 240 GeV from processes like $e^+e^- \to \mu^+\mu^-$ [166] or $e^+e^- \to W^+W^-$ [148, 167] may be more effective probes of electroweak dark matter than Z-pole observables.

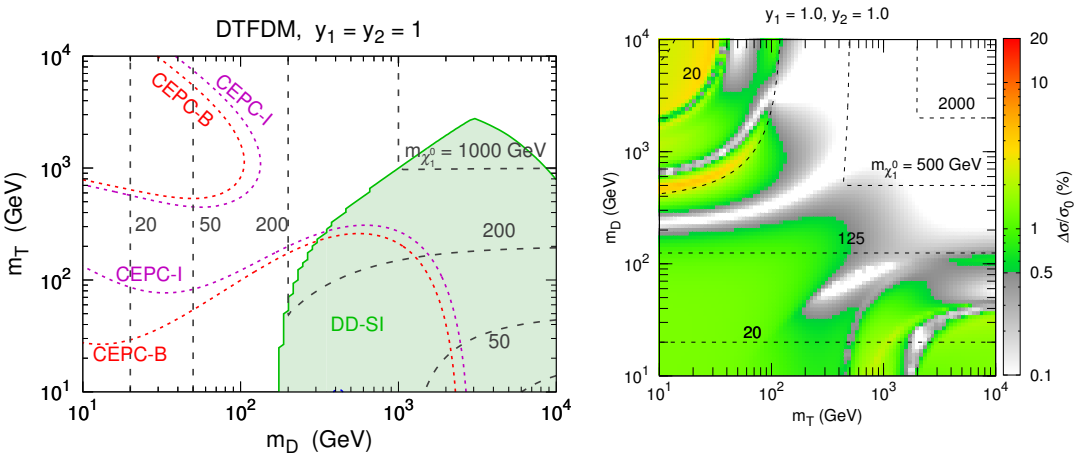

Figure 1.21: Left: CEPC electroweak precision (S, T) fit probe of the doublet–triplet model at the custodially symmetric point $y_1 = y_2 = 1$, taken directly from Figure 5a of [147]. When the dark matter particle is mostly triplet ($m_D \gg m_T$), spin-independent direct detection is a powerful probe (shaded green region). When the dark matter particle is mostly doublet, the tree-level direct detection rate vanishes but CEPC's measurement of the S parameter becomes a powerful probe (dashed contours). **Right:** CEPC probe of the same model via the Higgsstrahlung cross section $\sigma(Zh)$, taken directly from Figure 11b of [150]. We see that in a large part of parameter space with $m_T \gg m_D$, where the direct detection rate is low due to custodial symmetry, there are observable (percent-level or higher) deviations in the Zh cross section.

The doublet–singlet and doublet–triplet models at the CEPC have been discussed in [147], which focuses on the S and T parameters (and also discusses a quadruplet–triplet model with similar properties).[2] They have shown that CEPC can probe a large region of parameter space where the dark matter mass is below 200 GeV, and certain regions of parameter space with even larger masses. In particular, the S parameter allows a probe of the custodially symmetric region that is hidden from direct detection. We show some results from this paper in the left-hand panel of Figure 1.21. A related study in [150] considers effects

[2]Earlier papers discussing electroweak and Higgs constraints on similar models include [168–172].

of doublet–singlet and doublet–triplet dark matter on Higgs observables, including the Zh cross section, the $h \to \gamma\gamma$ decay rate, and the Higgs invisible width. Away from the custodially symmetric point in the doublet–singlet model, when $y_1 = 0.5$ and $y_2 = 1.5$, CEPC's measurement of the total Zh cross section probes up to 200 GeV lightest neutralino mass. For $y_1 = y_2 = 1$, with custodial symmetry, deviations are smaller and m_D is probed only up to about 125 GeV. In the doublet–triplet case, the region of parameter space bounded by the Zh measurement is illustrated in the right-hand panel of Figure 1.21. Aspects of a slightly different doublet–singlet model, with the singlet taken to be a Dirac fermion, have also been discussed in Ref. [146]. They focus on the region with mostly singlet DM, in which case the doublet may be thought of as allowing a completion of a "Higgs portal" model. In this case, the most important constraints come from the T parameter. They also present results for a wider range of doublet and singlet masses including cases where dark matter is mostly doublet.

In the case in which DM resides in a nearly pure electroweak multiplet, the S and T parameters and the $h \to \gamma\gamma$ rate are no longer useful probes. For the case of nearly pure higgsinos, Ref. [148] has studied the prospects of an $e^+e^- \to W^+W^-$ measurement at CEPC as a constraint. This measurement is sensitive not only to corrections to the photon and Z propagators but to loop corrections to the triple gauge coupling vertex. Ref. [148] claims that a 0.1% precision measurement of $e^+e^- \to W^+W^-$ at CEPC could probe higgsino dark matter up to about 210 GeV. However, the scatter plot in Figure 1 of that reference suggests that many models with even heavier higgsinos will be accessible. A more detailed future exploration of the parameter space probed by the W^+W^- measurement would be useful. The rate of $e^+e^- \to \mu^+\mu^-$ at 240 GeV can also be a sensitive probe of deviations in the propagators of photons and Z bosons; in particular, for new physics contributing to the W and Y parameters but not to S and T, it may be superior to electroweak precision studies on the Z pole thanks to the larger center-of-mass energy. A detailed study of this probe of electroweak physics has been carried out in [166]. Their conclusion is that if systematic uncertainties can be controlled to achieve a 0.1% precision on the rate, pseudo-Dirac higgsinos may be excluded up to a mass of about 200 GeV. This is encouraging, since pseudo-Dirac doublets are among the most difficult electroweak particles to probe in any experiment. In particular, the LHC is not expected to reach far above 200 GeV (though this will depend in part on how well systematic uncertainties can be understood). The results of Ref. [166] may not apply directly to CEPC due to their assumptions about beam polarization, so a further dedicated CEPC study of this process is warranted.

Another interesting possibility is that light singlet dark matter mixing with heavier electroweak-charged particles. A particular example arises for mostly-bino dark matter in the MSSM [173], $\tilde{\chi}_1^0$, which could have a non-thermal relic abundance. Because the bino is a pure singlet, it couples to the Standard Model only through small mixing parameters and is difficult to detect directly. However, in some cases it can be detected through the invisible width of the Higgs boson. The parameter space probed by dark matter direct detection and CEPC is shown in the right panel of Fig. 1.22. This figure illustrates that CEPC could probe the region allowed by the current direct detection with a sensitivity to $\mathrm{Br}(h \to \tilde{\chi}_1^0\tilde{\chi}_1^0) \gtrsim 0.24\%$,

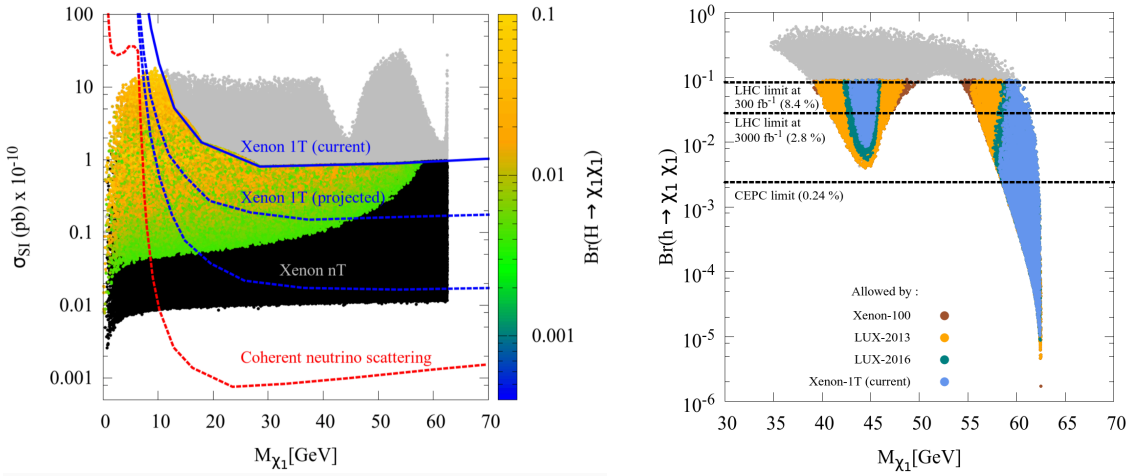

Figure 1.22: Nonthermal neutralino dark matter and invisible Higgs decays, adapted from [173]. **Left:** The spin-independent (SI) WIMP-nucleon cross-section vs $M_{\tilde{\chi}_1^0}$ for all points allowed by collider and relic density constraints. The color code characterizes the value of $\mathrm{Br}(h \to \tilde{\chi}_1^0\tilde{\chi}_1^0)$, while black points have $\mathrm{Br}(h \to \tilde{\chi}_1^0\tilde{\chi}_1^0) < 0.4\%$. The solid blue line shows the current limit from LUX-2016 [174] and the dashed blue line shows the reach for Xenon1T [175] and Xenon-nT [175]. **Right:** The Higgs to invisible branching ratio $\mathrm{Br}(h \to \tilde{\chi}_1^0\tilde{\chi}_1^0)$ vs. the LSP mass $M_{\tilde{\chi}_1^0}$. The grey (colored) points distinguish the points allowed before (after) the Higgs signal strength constraints. Blue, green, yellow, red points are allowed by the current limits on SI WIMP-nucleon cross-section from Xenon1T, LUX-2016, LUX-2013 and Xenon-100. From top to bottom, the black-dashed line represents the reach of the LHC with 300 fb^{-1}, LHC with 3000 fb^{-1}, and CEPC.

1.3.3.2 Renormalizable Standard Model portals

If the dark matter does not reside in an electroweak multiplet, it could still couple to the SM through coupling to gauge-invariant, renormalizable SM "portal" operators

$$H^\dagger H, B^{\mu\nu}, HL, \tag{1.20}$$

where H is the SM higgs doublet, $B^{\mu\nu}$ is the hypercharge field strength and L is a lepton doublet. These three portals are usually referred to as the Higgs portal, the kinetic mixing (or hypercharge) portal and the lepton (neutrino) portal. These simple portal dark matter scenarios predict rich phenomenology and a plethora of experimental signatures. They have been established as well defined dark matter benchmarks and experimental targets, in addition to the traditional electroweak WIMP scenario.

CEPC, with all the powerful direct and indirect probes it could provide, could potentially play an important role in detecting and testing these SM portals to dark matter. Below we will present estimates of the CEPC potential for the Higgs and kinetic mixing portals based on the studies in the existing literature.

The simplest Higgs portal model contains a real singlet scalar ϕ serving as dark matter [60]. The scalar ϕ couples to the SM through $c_s\phi^2 H^\dagger H$ with c_s a dimensionless number. It is odd under a $\mathbb{Z}_2$ symmetry which stabilizes it. At a lepton collider, ϕ could be pair produced in either the associated production with Z-bremsstrahlung $e^+e^- \to Zh^{(*)} \to Z\phi\phi$ or in the Z fusion $e^+e^- \to e^+e^-h^{(*)} \to e^+e^-\phi\phi$. The resulting signals are jets or leptons plus missing energy. When $m_\phi < m_h/2$, ϕ's are produced from on-shell Higgs decays and contribute to the invisible width of the Higgs. When $m_\phi > m_h/2$, the production goes through an off-shell Higgs and the search is more challenging. Based on results

in Ref. [176], CEPC will be sensitive to the on-shell Higgs decays to two ϕ's and probe the Higgs portal coupling down to 10^{-3} for $m_\phi < 60$ GeV assuming a a jet energy resolution of 3%. The reach is comparable to that of the current generation of dark matter direct detection experiments such as PandaX and Xenon1T when $m_\phi \subset (10 - 60)$ GeV and is superior when $m_\phi < 10$ GeV since direct detection is no longer effective due to the energy thresholds. CEPC's sensitivity, in particular that of the exotic Z decay, to fermionic Higgs portal dark matter has been discussed in section 1.3.2.

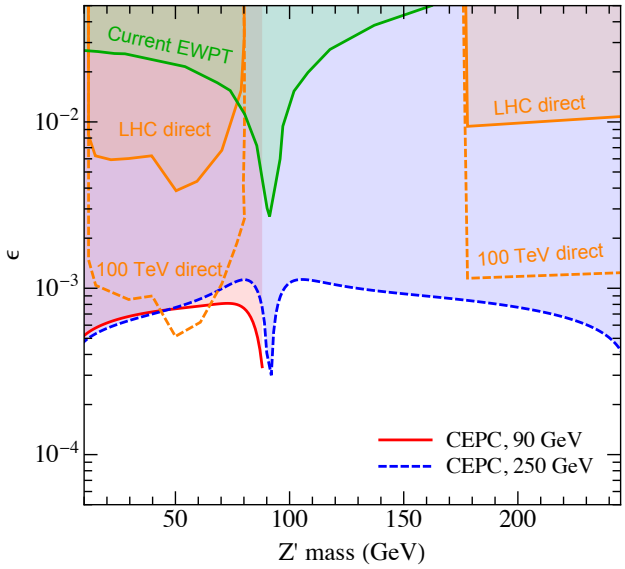

Figure 1.23: Dark photons via radiative return at CEPC. This figure, adapted from [177], shows 95% C.L. bounds on the mixing parameter ϵ with *hypercharge* as a function of the dark photon (Z') mass. The CEPC $\sqrt{s} = 90$ GeV and 250 GeV projections correspond to 0.5 ab^{-1} and 5 ab^{-1} respectively; the 100 TeV projection is for 3 ab^{-1}. Constraints from electroweak precision (EWPT) and direct searches taken from [178].

Next, let us consider the kinetic mixing portal scenario, in which the hidden sector containing the dark matter is charged under a broken dark Abelian gauge symmetry, $U(1)_D$. $U(1)_D$ could mix with the SM hypercharge $U(1)_Y$ through the operator

$$\frac{1}{2}\frac{\epsilon}{\cos\theta} Z_{D\mu\nu} B^{\mu\nu}, \tag{1.21}$$

where ϵ is the kinetic mixing parameter and θ is the weak mixing angle. The heavy gauge boson associated with $U(1)_D$, often called the dark photon, could be searched for at a lepton collider in quite a few ways. First, the dark photon introduces two effects in the fit of precision electroweak observables: a shift in the Z mass observable and a shift of the Z couplings to SM fermions. The Z-pole program at CEPC could improve the sensitivity to electroweak observables by a factor of 10 compared to LEP and push the reach of ϵ down to $\sim 10^{-3}$ for $m_{Z_D} < 90$ GeV [178]. A more powerful way is to search for dark photons directly through the radiative return processes such as $e^+e^- \to \gamma Z_D \to \gamma\mu^+\mu^-$. The search can be implemented by simply counting the number of events in the dimuon invariant mass spectrum in both the Z-pole and Higgs programs at CEPC. The direct searches probe $\epsilon \subset (3 \times 10^{-4} - 10^{-3})$ depending on m_{Z_D} in the entire mass range up to 250 GeV that could be covered by CEPC [177], as illustrated in Fig. 1.23. Another

Parameter	Signal process		Background (pb)		Signal region
ϵ	$\tilde{Z}\tilde{K}$	$\tilde{Z} \to \bar{\ell}\ell$, $\tilde{K} \to \bar{\chi}\chi$	$\bar{\ell}\ell\bar{\nu}\nu$	0.929	$N_\ell \geq 2$, $\lvert m_{\ell\ell} - m_Z \rvert < 10$ GeV, and $\lvert m_{\text{recoil}} - m_{\tilde{K}} \rvert < 2.5$ GeV
		$\tilde{Z} \to \bar{\ell}\ell$, $\tilde{K} \to \bar{\ell}\ell$	$\bar{\ell}\ell\bar{\ell}\ell$	0.055	$N_\ell \geq 4$, $\lvert m_{\ell\ell} - m_Z \rvert < 10$ GeV, and $\lvert m_{\ell\ell} - m_{\tilde{K}} \rvert < 2.5$ GeV
	$\tilde{A}\tilde{K}$	$\tilde{K}$ inclusive decay	$\gamma f\bar{f}$	23.14	$N_\gamma \geq 1$, and $\lvert E_\gamma - (\frac{\sqrt{s}}{2} - \frac{m_{\tilde{K}}^2}{2\sqrt{s}}) \rvert < 2.5$ GeV
		$\tilde{K} \to \bar{\ell}\ell$	$\gamma\bar{\ell}\ell$	12.67	$N_\gamma \geq 1$, $N_\ell \geq 2$, $\lvert E_\gamma - (\frac{\sqrt{s}}{2} - \frac{m_{\tilde{K}}^2}{2\sqrt{s}}) \rvert < 2.5$ GeV, and $\lvert m_{\ell\ell} - m_{\tilde{K}} \rvert < 5$ GeV
		$\tilde{K} \to \bar{\chi}\chi$	$\gamma\bar{\nu}\nu$	3.45	$N_\gamma \geq 1$, $\lvert E_\gamma - (\frac{\sqrt{s}}{2} - \frac{m_{\tilde{K}}^2}{2\sqrt{s}}) \rvert < 2.5$ GeV, and $\not{E} > 50$ GeV
	$\tilde{Z}H_0$	$H_0 \to \tilde{K}\tilde{Z}$ with $\tilde{K} \to \bar{\chi}\chi$, $\tilde{Z} \to \bar{\ell}\ell$	$\bar{\ell}\bar{\ell}\ell\ell\bar{\nu}\nu$	1.8×10^{-5}	$N_\ell \geq 4$, $\lvert m_{\ell\ell} - m_Z \rvert < 10$ GeV, and $\lvert m_{\text{recoil}} - m_{\tilde{K}} \rvert < 2.5$ GeV
$\sin\alpha$	$\tilde{Z}S$	$\tilde{Z} \to \bar{\ell}\ell$ $S \to \tilde{K}\tilde{K} \to 4\chi$	$\bar{\ell}\ell\bar{\nu}\nu$	0.87	$N_\ell \geq 2$, $\lvert m_{\ell\ell} - m_Z \rvert < 10$ GeV, and $\lvert m_{\text{recoil}} - m_S \rvert < 2.5$ GeV

Table 1.1: Double Dark Portal model: summary of the different vector + scalar and vector + vector production modes studied, along with the most salient cuts to identify the individual signals. All background processes include up to one additional photon to account for initial and final state radiation. Background rates are given for $\sqrt{s} = 250$ GeV, and visible particles are required to satisfy preselection cuts given in the main text of [122].

possible direct probe is the rare Z decay: $Z \to h_D Z_D \to Z_D Z_D Z_D$, where h_D is the dark Higgs. The reach of this has been discussed in section 1.3.2.

In the remainder of this subsection we will discuss a case study of a model with two renormalizable Standard Model–dark sector couplings, the Double Dark Portal model of [122]. This model rests on the observation that one possible origin for the mass of a $U(1)_D$ dark gauge boson is through the VEV of a dark Higgs scalar Φ carrying $U(1)_D$ charge. The $U(1)_D$ gauge boson kinetically mixes with the photon (with mixing parameter ϵ) while the dark Higgs Φ mixes with the Higgs through a $\lambda_{HP}|\Phi|^2|H|^2$ quartic potential. A dark fermion χ with Dirac mass m_χ carrying U(1)$_D$ dark charge can play the role of dark matter. We denote the two scalar mass eigenstates of this model by H_0 (mostly Higgs) and S (mostly Φ) with mixing angle α. We denote the vector mass eigenstates by $\tilde{Z}_\mu$ (mostly the SM Z boson) and $\tilde{K}_\mu$ (mostly the dark photon). Both of the renormalizable portal couplings lead to attractive discovery prospects at CEPC from a variety of channels summarized in Table 1.1.

This model contains several couplings allowing transitions from the Standard Model to the dark sector, proportional to an insertion of a mixing parameter. Vertices proportional to α include H_0SS; H_0H_0S; $\tilde{K}_\mu\tilde{K}^\mu H_0$; and $\tilde{Z}_\mu\tilde{Z}^\mu S$. Vertices proportional to ϵ include $\tilde{Z}_\mu\tilde{K}^\mu S$ and $\tilde{Z}_\mu\tilde{K}^\mu H_0$. If $4m_\chi < 2m_{\tilde{K}} < m_S$, then both the dark photon $\tilde{K}$ and dark Higgs S will dominantly decay invisibly, with visible branching ratios suppressed by $e^2\epsilon^2/g_D^2$ and $\tan^2\alpha/g_D^2$ respectively. Hence, the Double Dark Portal model contains invisible Higgs decay modes $H_0 \to SS \to 4\tilde{K} \to 8\chi$ and $H_0 \to 2\tilde{K} \to 4\chi$, in addition to the possible exotic decay $H_0 \to \tilde{Z}\tilde{K}$ which is either partially visible or invisible depending on the $\tilde{Z}$ decay channel. A precision measurement of the invisible branching fractions of the Higgs boson can significantly constrain the model, as summarized in Fig. 1.24. Precision observation of the Higgsstrahlung rate with $\mathcal{O}(0.3\% - 0.7\%)$ accuracy [119–121] will constrain the scalar mixing angle at the level $\sin\alpha \lesssim 0.055 - 0.084$.

Direct searches for dark sector particles are possible in the channels $\tilde{Z}H_0$, $\tilde{Z}S$, $\gamma\tilde{K}$ and $\tilde{Z}\tilde{K}$. The sensitivity of CEPC searches for these signals and comparisons to existing constraints from BaBar, LEP, and LHC are summarized in Fig. 1.25. The $\tilde{Z}\tilde{K}$ final state can

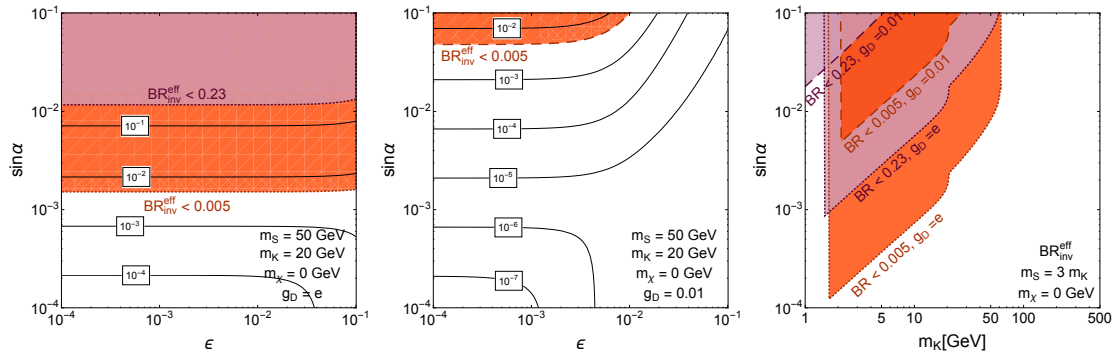

Figure 1.24: Adapted from ref. [122]. **Left and center:** Rates for the invisible branching fraction of the 125 GeV Higgs in the $\sin\alpha$ vs. ϵ plane, setting $m_S = 50$ GeV, $m_K = 20$ GeV, and $g_D = e$ (left) and 0.01 (center). **Right:** Exclusion regions in the $\sin\alpha$ vs. m_K plane from the search for an invisible decay of the 125 GeV Higgs by ATLAS and CMS giving $\text{BR}_{\text{inv}} < 0.23$ [123, 124], and projected reach from a future e^+e^- machine giving $\text{BR}_{\text{inv}} < 0.005$ [118–120, 179].

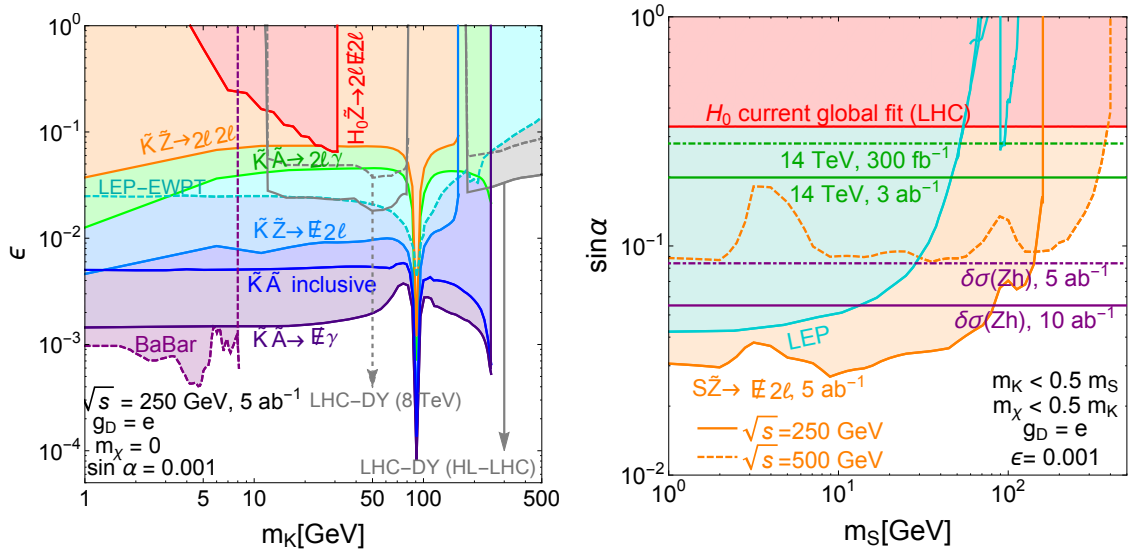

Figure 1.25: Adapted from ref. [122]. **Left:** Projected exclusion regions in the ϵ vs. m_K plane from multiple complementary searches of $\tilde{K}$ production. Solid lines enclose expected exclusion regions with $L = 5$ ab^{-1} of $\sqrt{s} = 250$ GeV e^+e^- machine data. Dashed lines indicate existing limits from the LEP $e^-e^+ \to \ell^-\ell^+$ contact operator search, LEP electroweak precision tests (LEP-EWPT), BaBar $\tilde{K}$ invisible decay search (BaBar) and LHC Drell-Yan constraints (LHC-DY). The 3 ab^{-1} HL-LHC projection for Drell-Yan constraints is also shown as a solid line. Note m_K is approximately the $m_{\tilde{K}}$ mass eigenvalue. **Right:** Exclusion reach from the $\tilde{Z}S$, $\tilde{Z} \to \ell^+\ell^-$ search in the recoil mass distribution for invisible S decays in the $\sin\alpha$ vs. m_S plane using 5 ab^{-1} of e^+e^- data at $\sqrt{s} = 250$ GeV or 500 GeV. We also show comparisons to the current fit, $\sin\alpha < 0.33$ [117], future LHC projections of 0.28 (0.20) using 300 fb^{-1} (3 ab^{-1}) luminosity [118], and precision $\delta\sigma(Zh)$ measurements constraining 0.084 (0.055) using 5 ab^{-1} (10 ab^{-1}) [119–121]. We plot the excluded region from LEP searches for invisible low mass Higgs in ZS channel in cyan [116, 180–182].

be searched for using the recoil mass in events containing $Z \to \ell^+\ell^-$. The radiative return process $e^+e^- \to \gamma\tilde{K}$ allows a search for events with a monochromatic photon together with $\tilde{K} \to \bar{\chi}\chi, \ell^+\ell^-$. The left panel of Fig. 1.25 shows that searches with invisible $\tilde{K}$ are more effective than those with $\tilde{K} \to \ell^+\ell^-$, due to the larger branching fraction. The figure also shows that a search for $H_0 \to \tilde{Z}\tilde{K}(\to \bar{\chi}\chi)$ is less effective. Finally, the right-hand

panel of Fig. 1.25 shows the reach of a search for the S-strahlung process $e^+e^- \to \tilde{Z}S$ in the mixing angle $\sin\alpha$. This search is exactly analogous to the previous search at LEP-II for a purely invisible decaying Higgs [116]. Improved sensitivity could be obtained by varying the $\sqrt{s}$ of the collider to maximize the $\sigma(e^+e^- \to \tilde{Z}S)$ rate for the test S mass (see also Ref. [183]).

1.3.3.3 Portals with additional SM-sector physics

While the renormalizable SM portals are simple, they are not the only possibilities. Portals between the dark and visible sectors could be formed by additional particles with Standard Model gauge charges. These can offer interesting variations on the renormalizable portal. One example of such a portal is the leptonic Higgs portal [184]. This model includes an elementary scalar, S, which only couples to the SM leptons, $g_\ell S\bar{l}l$.[3] Note that this operator is not SM gauge invariant and has to be UV completed. One possible simple UV completion is to couple a SM singlet to two Higgs doublets with one of the doublets only coupling to leptons and the other one only coupling to quarks. At a lepton collider, assuming that the couplings g_ℓ are proportional to the corresponding lepton mass, S could be produced in association with τ leptons, $e^+e^- \to \tau^+\tau^- + (S \to e^+e^-, \mu^+\mu^-, \tau^+\tau^-)$. Current beam dump and lepton colliders only probe m_S to a few GeV. CEPC could be capable of extending the sensitivity to much heavier S up to ~ 250 GeV. In the particular lepton-specific two Higgs doublet UV completion, the mixing between the singlet S and the higgs boson h leads to exotic Higgs decays such as $h \to SS \to 4\tau, 2\mu 2\tau$. For the 4τ final state, CEPC could test a branching fraction as small as 10^{-4} at 95% C.L., improving the sensitivity by three orders of magnitude compared to even HL-LHC [185]! This is translated to a factor of 30 improvement in testing the coupling g_ℓ fixing all the other parameters. Another similar possibility is a leptonic portal arising from some gauge bosons coupling to SM lepton-flavor currents [186].

In general, the dark matter portal models could give rise to exotic Higgs decays. A thorough review of the models leading to exotic Higgs decays and the status of LHC searches could be found in Ref. [108]. Supersymmetric exotic decays of the Higgs boson have been studied in Refs. [185, 187]. The potential of detecting exotic Higgs decays in 14 different final states at CEPC has been presented in Ref. [185]. In every final state, we expect at least one order of magnitude improvement in sensitivity compared to HL-LHC and in quite a few channels, we expect 3-4 orders of magnitude improvement at CEPC. More details are discussed in section 1.3.1.

A characteristic feature of many models that go beyond renormalizable portals is the possibility of new sources of flavor violation. For example, nonrenormalizable (dipole moment) operators could allow one SM fermion to decay to a dark photon and another SM fermion of different flavor, e.g. $\mu^\pm \to e^\pm\gamma_d$ or $t \to c\gamma_d$ [188]. Renormalizable completions of such models introduce new "messenger" particles that interact with the SM gauge groups and the dark photon. The induced flavor-violating decays could be searched for at CEPC.

Another possibility that could be tested at the CEPC is flavor-violating dark matter in which dark matter couples dominantly to muons [189]. The dark multiplet contains a

[3] A variant of the model with S dominantly coupling to the muon and proton with tiny couplings to the electron and neutron might explain the proton radius puzzle and the muon anomalous magnetic moment discrepancy.

scalar and a vector-like fermion and couples to the muon through a Yukawa interaction. The neutral component of the scalar serves as the dark matter candidate. The interaction generates a loop correction to the $\gamma\mu^+\mu^-$ and $Z\mu^+\mu^-$ couplings that could be measured as deviations in the cross section of $e^+e^- \to \mu^+\mu^-$. Choosing the Yukawa coupling to be about 1, a 2% precision measurement of the cross section can probe dark matter mass within 20 GeV around 120 GeV. Related models include flavored dark matter [190, 191], in which dark matter particle carries flavor quantum numbers and has renormalizable contact interactions with the SM fields. In particular, electron-flavored dark matter could be produced copiously at a lepton collider associated with a photon if its mass is below ~ 120 GeV.

1.3.3.4 Effective theory

So far, our discussion of dark matter has been organized based on details of the model. However, one could also take a portal-agnostic or "model-independent" approach, simply searching for a generic signal like a single photon plus missing energy [192]. This could arise if DM is part of an electroweak multiplet, due to loops of the charged $\mathrm{SU}(2)_L$ partners of dark matter and W bosons. It could also arise if completely new charged particles, independent of DM, exist and couple to DM. Results could be expressed simply in terms of effective operators, without committing to a particular UV completion. A variety of studies of such signals at e^+e^- colliders have been carried out, e.g. [193–196].

In an effective theory approach, such signals arise from dimension-7 effective operators coupling fermionic dark matter to pairs of SM gauge bosons. The operators that can be efficiently constrained by searches at CEPC are

$$\begin{aligned}\mathcal{L}_{\mathrm{S}} &\supset \frac{1}{\Lambda^3_{\gamma\gamma}}\bar{\chi}\chi A^{\mu\nu}A_{\mu\nu} + \frac{1}{\Lambda^3_{\gamma Z}}\bar{\chi}\chi A^{\mu\nu}Z_{\mu\nu},\\ \mathcal{L}_{\mathrm{P}} &\supset \frac{1}{\Lambda^3_{\gamma\gamma}}\bar{\chi}i\gamma_5\chi A^{\mu\nu}\widetilde{A}_{\mu\nu} + \frac{1}{\Lambda^3_{\gamma Z}}\bar{\chi}i\gamma_5\chi A^{\mu\nu}\widetilde{Z}_{\mu\nu},\end{aligned} \tag{1.22}$$

where the field strengths $A_{\mu\nu}$ and $Z_{\mu\nu}$ and their duals $\widetilde{A}_{\mu\nu}$ and $\widetilde{Z}_{\mu\nu}$ couple to the scalar (S) and the pseudoscalar (P) fermionic dark matter bilinears. The Λ factors in the coefficients represent the approximate mass scale of new physics (up to loop factors). Similar operators can be also be written for the $\mathrm{SU}(2)_L$ gauge fields, but the WW couplings may not be as efficiently probed by e^+e^- collisions at the Z pole.

The diphoton operator dominates processes with low momentum transfer because the photon is massless. It is much more stringently constrained by direct detection than its DM-γZ and DM-ZZ counterparts. For DM lighter than half of m_Z, indirect detection using diffuse gamma rays is also more sensitive to the diphoton operator. Collider searches, on the other hand, can more effectively probe Z couplings. The high-luminosity Z pole run at CEPC offers a unique opportunity to test the DM couplings to the Z boson. For a light DM mass, the resonantly produced $\bar{\chi}\chi\gamma$ system is best searched for in the channel of monophoton + missing energy.

Ref. [197] studies the proposed Z pole runs' prospective limits on effective DM-γZ and $\gamma\gamma$ couplings in the monophoton channel. The major SM background $e^+e^- \to \bar{\nu}\nu\gamma$ can be effectively controlled by optimizing the cut on the single photon's p_T. The corresponding constraints on Λ are illustrated in Figs. 1.26 and 1.27. The best sensitivity is obtained for light dark matter mass. In case only one operator is considered, the projected sensitivity

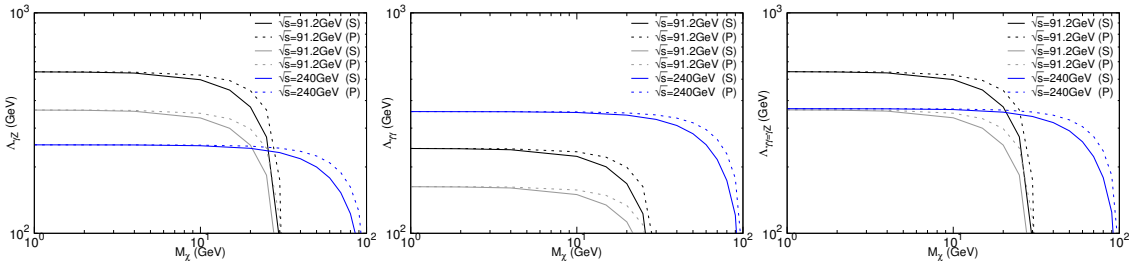

Figure 1.26: CEPC 3σ reach in the $m_\chi - \Lambda$ plane, adapted from ref. [197]. The black, gray, and blue lines refer to $\sqrt{s} = 91.2$ GeV with 2.5 ab^{-1}, 91.2 GeV with 25 fb^{-1}, and 240 GeV with 5 ab^{-1} respectively. The three panels from left to right correspond to pure $\Lambda_{\gamma Z}$ interaction, pure $\Lambda_{\gamma\gamma}$ interaction, and $\Lambda_{\gamma Z} = \Lambda_{\gamma\gamma}$ interaction. The photon is required to have $|\eta| < 3$ and a $p_T > 25\,(35)$ GeV for $91.2\,(240)$ GeV collision energy to optimize the sensitivity for a low m_χ. The solid lines are for a scalar operator and the dashed lines for the pseudoscalar case.

for $\Lambda_{\gamma Z}$ is 360 GeV, 540 GeV for 25 fb^{-1} (giga Z) and 2.5 ab^{-1} (tera Z) luminosities at the Z pole. In comparison, $\Lambda_{\gamma\gamma}$ is best probed at higher energy runs, and a limit of 360 GeV is obtained for a 5 ab^{-1} run at 240 GeV center of mass energy. In general, both $\Lambda_{\gamma Z}$ and $\Lambda_{\gamma\gamma}$ would be present and their relative size is model dependent.

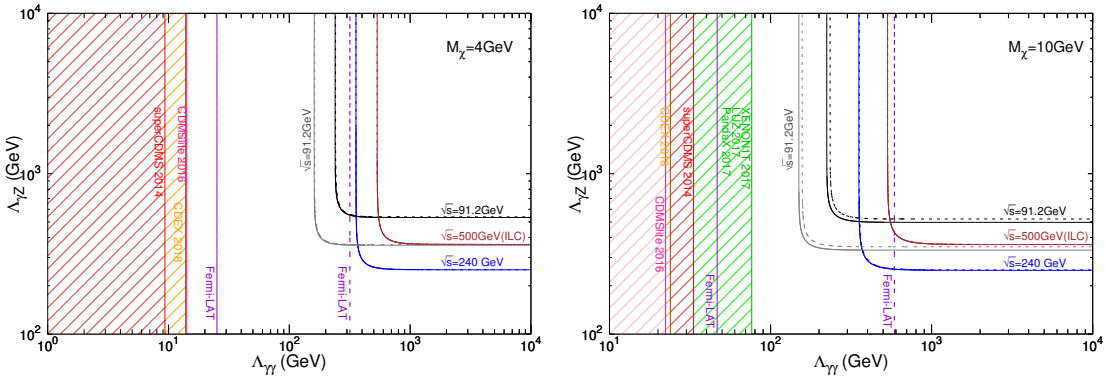

Figure 1.27: $\Lambda_{\gamma\gamma} - \Lambda_{\gamma Z}$ limits for direct, indirect detection and CEPC runs from ref. [197]. In the left (right) panel, the DM mass is $m_\chi = 4\,(10)$ GeV. Solid and dashed curves show the constraints for scalar and pseudoscalar types of operators, respectively. Red, orange, and pink dashed areas indicate the bounds from SuperCDMS [198], CDEX [199], and CDMSlite [200]. The green dashed area shows the bound from XENON1T [129], LUX [130], and PandaX [152] (which are in close proximity to each other). The purple (dashed) line denotes the Fermi-LAT bound from the R3 region [201]. For CEPC limits, curves are as indicated in Fig. 1.26. The brown line denotes the ILC 3σ sensitivity with an integrated luminosity of 500 fb^{-1} at $\sqrt{s} = 500$ GeV with cuts $10^\circ < \theta_\gamma < 170^\circ$ and $p_T(\gamma) > 90$ GeV. Note that the XENON1T/LUX/PandaX limit only appears in the m_χ=10 GeV case.

Fig. 1.27 further shows the direct and indirect detection limits together with CEPC's constraint in the $\Lambda_{\gamma\gamma} - \Lambda_{\gamma Z}$ plane. For direct detection, we adopt the calculation of the spin-independent scattering rate via the scalar operator from Ref. [106, 202], which takes into account the diphoton exchange that dominates over γZ contributions. We choose benchmark DM masses at 4 and 10 GeV that are accessible to major nuclear recoil experiments. For indirect detection, we show the 95% CL constraint from the gamma ray line search at Fermi-LAT [201]. The nonrelativistic DM annihilation cross section into two photons ($\bar{\chi}\chi \to \gamma\gamma$) is dominated by $\Lambda_{\gamma\gamma}$ for m_χ below $m_Z/2$. The $\Lambda_{\gamma Z}$ dependence only

Table 1.2: The current and projected limits on selected Higgs exotic decay modes for the (HL-)LHC and CEPC with 5 ab^{-1} integrated luminosity, based upon results from Ref. [110]. The projections for the HL-LHC are collected in the third column, where the limits for 100 fb^{-1} and 300 fb^{-1} alone are shown in parentheses and square brackets respectively.

Decay Mode	95% C.L. limit on Br		
	LHC	HL-LHC	CEPC
$E_{\mathrm{T}}^{\mathrm{miss}}$	0.23	0.056	0.014
$(b\bar{b})+E_{\mathrm{T}}^{\mathrm{miss}}$	–	[0.2]	1×10^{-4}
$(jj)+E_{\mathrm{T}}^{\mathrm{miss}}$	–	–	4×10^{-4}
$(\tau^+\tau^-)+E_{\mathrm{T}}^{\mathrm{miss}}$	–	[1]	8×10^{-5}
$b\bar{b}+E_{\mathrm{T}}^{\mathrm{miss}}$	–	[0.2]	2×10^{-4}
$jj+E_{\mathrm{T}}^{\mathrm{miss}}$	–	–	5×10^{-4}
$\tau^+\tau^-+E_{\mathrm{T}}^{\mathrm{miss}}$	–	–	8×10^{-5}
$(b\bar{b})(b\bar{b})$	1.7	(0.2)	6×10^{-4}
$(c\bar{c})(c\bar{c})$	–	(0.2)	8×10^{-4}
$(jj)(jj)$	–	[0.1]	2×10^{-3}
$(b\bar{b})(\tau^+\tau^-)$	[0.1]	[0.15]	4×10^{-4}
$(\tau^+\tau^-)(\tau^+\tau^-)$	[1.2]	$[0.2\sim0.4]$	2×10^{-4}
$(jj)(\gamma\gamma)$	–	[0.01]	1×10^{-4}
$(\gamma\gamma)(\gamma\gamma)$	$[7\times10^{-3}]$	4×10^{-4}	8×10^{-5}

emerges in a tiny correction as part of the $\bar{\chi}\chi \to \gamma(\gamma^*/Z^* \to \bar{f}f)$ process, and can be ignored at the DM masses shown.

1.3.3.5 Miscellaneous

Merge these references into the neutrino section once it's complete?

Batell/McCullough "natural neutrinos" (does this belong here or in a different section?) [203]

Lepton flavor violation from neutral scalar at CEPC [204] should be cited somewhere, maybe not here

1.3.3.6 Summary and outlook

We summarize the set of Higgs exotic decays in Table 1.2, including current and projected LHC constraints, and limits from our study for the CEPC with 5 ab^{-1} integrated luminosity. For the LHC constraints, we tabulate both the current limits and projected limits on these exotic decay channels from various references. We choose to focus on comparison for particular benchmark points, which is sufficient to demonstrate the qualitative difference between the LHC and CEPC.

In the summary in Table 1.2 and the corresponding Fig. 1.28, the exotic Higgs decay channels are selected such that they are hard to be constrained at the LHC. The improvements on the limits of the Higgs exotic decay branching fractions vary from one to four orders of magnitude for these channels. The lepton colliders can improve the limits on the Higgs invisible decays beyond the HL-LHC projection by one order of magnitude, reaching the SM invisible decay branching fraction of 0.12% from $h \to ZZ^* \to \nu\bar{\nu}\nu\bar{\nu}$ [205]. After subtraction of the SM contribution to the Higgs to invisible decays, a 95% C.L. up-

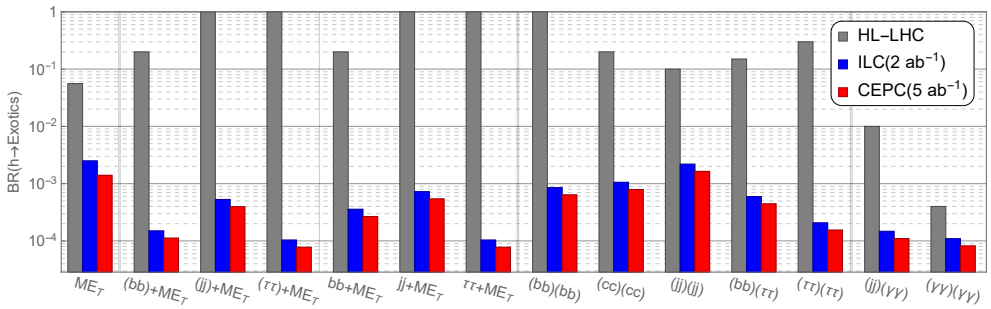

Figure 1.28: The 95% C.L. upper limit on selected Higgs exotic decay branching fractions at HL-LHC, ILC and CEPC, based on Ref [110]. The benchmark parameter choices are the same as in Table 1.2. We put several vertical lines in this figure to divide different types of Higgs exotic decays.

per limit can be placed on BSM Higgs For the Higgs exotic decays into hadronic particle plus missing energy, $b\bar{b} + E_{\mathrm{T}}^{\mathrm{miss}}$, $jj + E_{\mathrm{T}}^{\mathrm{miss}}$ and $\tau^+\tau^- + E_{\mathrm{T}}^{\mathrm{miss}}$, the future lepton colliders improve on the HL-LHC sensitivity for these channels by roughly three to four orders of magnitude. This great advantage benefits a lot from low QCD background and the Higgs tagging from recoil mass technique at future lepton colliders. As for the Higgs exotic decays without missing energy, the improvement varies between two to three orders of magnitude, except for the one order of magnitude improvement for the $(\gamma\gamma)(\gamma\gamma)$ channel. Being able to reconstruct the Higgs mass from the final state particles at the LHC does provide additional signal-background discrimination power and hence the improvement from CEPC on Higgs exotic decays without missing energy is less impressive than for those with missing energy. Furthermore, as discussed earlier, leptons and photons are relatively clean objects at the LHC and the sensitivity at the LHC on these channels will be very good. CEPC complements the HL-LHC for hadronic channels and channels with missing energy.

1.3.4 Neutrino connection

1.3.4.1 Neutrino Mass Models

The CEPC is an excellent tool to study the physics associated with the neutrino mass generation as a portal to unknown new physics during both, the 240 GeV and Z-pole runs. It can therefore be used as a discovery machine for new physics that evades the detection at hadronic colliders, including feebly coupled “hidden sector" extensions of the SM that can address fundamental questions in particle physics and cosmology.

1.3.4.2 Introduction

The experimental observation of neutrino flavor oscillations [206, 207] indicates that neutrinos have a nonzero mass. Global fits to neutrino oscillation experiments (cf. e.g. [208, 209]) allow to fix two neutrino mass square differences as well as all mixing angles in the Pontecorvo-Maki-Nakagawa-Sakata matrix V_ν (assuming it to be unitary), while the absolute neutrino mass scale is constrained from cosmology to be in the sub-eV range, cf. e.g. [210]. The data immediately poses the questions why the neutrinos are so much lighter than all other fermions, and why the elements of the neutrino mass mixing matrix are so different from the quark mixing matrix.

Since the Standard Model (SM) of particle physics cannot account for the neutrino masses $m_i \neq 0$ in a renormalizable way, the neutrino oscillations provide compelling evidence from the laboratory for physics beyond the SM. While the origin of the charged third generation fermions of the SM is well established by the Higgs boson measurements, the origin of neutrino masses is unknown and calls for a more fundamental theory of nature, into which the SM is embedded. Moreover, neutrinos may be Majorana fermions [211], fundamentally different from their charged fermion counterparts with experimentally verifiable consequences related to violation of lepton number, discoverable at colliders [212]. It may also be connected to the open question in cosmology, the *baryon asymmetry of the universe* (BAU), i.e., the tiny excess $\sim 10^{-10}$ [128] of matter over antimatter in the early universe, cf. sec. 1.3.4.10.

Under the assumption that the *New Physics scale* Λ associated with the mass of the lightest new particle involved in the generation of neutrino masses is much larger than the typical energy $E_\nu \sim \mathrm{MeV}$ in neutrino oscillation experiments,[4] the neutrino oscillations can be described in the framework of Effective Field Theory (EFT). The relevant operators $\mathcal{O}_i^{[n]}$ have mass dimension $n > 4$, are suppressed by powers of Λ^{n-4}, and have Wilson coefficients $c_i^{[n]}$ which are matrices in flavour space. In this framework the smallness of neutrino masses can be a consequence of any combination of the following reasons:

I) *High-Scale Seesaw Mechanism:* Large values of Λ automatically lead to small m_i. The three tree level implementations of the idea [215] are known as: type-I [73, 74, 216–219], SM plus right-handed neutrinos N; type-II [219–223], SM plus scalar $SU(2)_L$ triplet Δ_L; type-III [224], SM plus fermionic $SU(2)_L$ triplet field Σ_L.

II) *Small numbers:* The $\mathcal{O}_i^{[n]}$ can remain small (for all values of Λ, including those accessible to the CEPC) if the Wilson coefficients $c_i^{[n]}$ are small. In particular, if the neutrinos are Dirac particles their masses can be generated by the Higgs mechanism in exactly the same way as all other fermion masses with tiny Yukawa couplings. Tiny constants can be avoided e.g. when the neutrino interactions are created dynamically due to the spontaneous breaking of a flavor symmetry by flavons [225], or when the $\mathcal{O}_i^{[n]}$ are created radiatively, cf. e.g. [226–230].

III) *Low-Scale Seesaw Mechanism:* A low scale Λ and $\mathcal{O}(1)$ couplings between the SM and the new particles can be realized when symmetries give rise to cancellations in the neutrino mass matrix. For instance the $B - L$ symmetry of the SM can keep the $\mathcal{O}_i^{[n]}$ small for Λ below the TeV scale [231–233]. Specific models that implement this idea include the inverse [234–236] and linear [237, 238] seesaw, the Neutrino Minimal Standard Model [239, 240] and scale invariant models [241].

Here the terms "high scale" and "low scale" scenarios should be understood with respect to the CEPC collision energy; for values of Λ far above 240 GeV the EFT treatment introduced here to describe neutrino oscillation experiments can also be applied to the CEPC phenomenology, while lower values imply that the new particles can be found at the CEPC and have to be described dynamically.

[4] Scenarios with $\Lambda < E_\nu$ are in principle feasible, cf. e.g. refs. [213, 214] and references therein, but strongly constrained by the success of the high level of consistency in global fits to neutrino oscillation data that assume only three light neutrinos [208, 209].

The original setting for the seesaw mechanism were grand unified theories, based on $SO(10)$ [217], and $SU(5)$ [216], as well as the minimal Left-Right (LR) symmetric model [73, 74] and flavor/family symmetries [218]. The large scale of grand unification typically sets the mass scale Λ related to neutrino physics beyond the direct reach of colliders, however parts of multiplets may lie much below the GUT scale. For example, the minimal $SU(5)$ model with the addition of 24_F on top of the original Georgi-Glashow model, needs a light fermionic triplet in order for gauge couplings to unify [242, 243], motivating type III searches at the TeV scales. Other well known examples are for instance $B - L$ symmetry, additional "neutrinophilic" Higgs doublets, and flavor symmetries. Such neutrino mass physics generally predicts the existence of new particles, which could at least in principle be discovered and studied at the CEPC.

1.3.4.3 Lepton number violation

If neutrinos are Majorana particles, the mechanism that generates their mass can mediate LNV processes at colliders if the scale Λ is below or near the collision energy [212].

Type I Seesaw: Observing the violation of lepton number from heavy neutrino mass eigenstates (N_i) in the process $e^+e^- \to N\nu$ at lepton colliders is possible in principle due to the different kinematics of LNV and LNC processes as was demonstrated for the ILC [244]. In particular for heavy neutrino N_i masses $M_i > M_Z$, the process $e^+e^- \to \nu\ell jj$ is a promising signature at lepton colliders [245–247] and has been studied specifically for CEPC [248].

The subleading production process for heavy neutrinos at lepton colliders $e^+e^- \to N\ell^\pm W^\mp$ allows for same sign dileptons for $N \to \ell^\pm W^{(*)}$ and $W \to$ hadrons [247].

The observation of the interesting "inverse neutrinoless double β decay" [249], would require same sign lepton collisions [250]. It is worth pointing out, that LNV in Type I Seesaw mechanism is suppressed by the smallness of the light neutrino masses [232, 233]. It has been proposed that the suppression of LNV may be alleviated by the process of heavy neutrino-antineutrino oscillations, which occurs for heavy neutrinos with masses below m_W and with $U^2 < \mathcal{O}(10^{-5})$ [251–253].

Signals in Type II Seesaw: The triplet scalar multiplet Δ_L in the type II seesaw contains three complex fields: the neutral CP-even and CP-odd states, singly charged and the doubly charged components. The appealing feature of the model is the direct connection between LH neutrino masses and mixing parameters [254, 255] and the Majorana Yukawa matrix $M_\nu = Y_\Delta \langle \Delta_L \rangle$, that may lead to cFLV signals [256].

Collider phenomenology of this setup is set by the final state that mainly depends on the triplet vev [257] and the mass splittings of its components [258]. If the masses are degenerate, the dominant decay mode is to leptons if the triplet vev is small $\lesssim 10^{-4}$ GeV. This decay mode tests the flavor structure of the neutrino mass matrix and leads to significant flavor dependent bounds up to 870 GeV at the LHC [259]. For the triplet vev above $\gtrsim 10^{-4}$ GeV, the states decay to pairs of gauge bosons. A relatively small mass splitting, allowed by the EW precision tests, triggers cascade decay modes [258], which produce soft hadronic and multi-lepton final states [260]. Signal in the WW lead to weak lower bounds at the LHC, $m_{\Delta_L^{++}} \gtrsim 90$ GeV [261] or less, depending on the lepton flavor. Similarly, the cascade decays [258, 262] are not easy to look for in hadronic colliders [263], however they may be observable in cleaner lepton collisions [264].

At lepton colliders, the triplet components can be produced pair-wise through $e^+e^- \to S\overline{S}$, $S, S' = \Delta_L^0, \Delta_L^\pm, \Delta_L^{\pm\pm}$ or in single production in association with two same-sign leptons $e^+e^- \to \Delta_L^{\pm\pm}\ell^\mp\ell^\mp$, see [265, 266]. Another possible production mode is via vector-boson fusion $e^+e^- \to \ell\,\ell' S\,S'$, where $\ell, \ell' = e^\pm, \nu$, as discussed in [267].

The doubly charged scalar bosons $\Delta_L^{\pm\pm}$ can couple to the electrons and positrons directly and contribute to Bhabha scattering in the t-channel [265, 268].

Running the lepton colliders with same-sign beams may strongly enhance the production of the doubly charged components in the s-channel [265, 269], see [270] for the recent work.

Exotic Higgs decays with same-sign leptons: The mixing of the SM Higgs doublet with the $SU(2)_R$ triplet Higgs that gives Majorana mass to right-handed neutrinos in the Left-Right Symmetric Model (LRSM) [271–274] may lead to LNV decays of $h \to NN$ [275]. Subsequent and possibly displaced decay of $N \to \ell^\pm jj$, can lead to a $\Delta L = 2$ LNV and potentially charged lepton flavor violating (cFLV) final states with two same sign-leptons and up to four jets. Due to the soft final states and displacement, such searches may be challenging at the LHC, however lepton colliders are much more suitable to detect such signals due to the absence of triggers and lower QCD backgrounds.

The presence of the mixing also allows for an enhanced production of the $SU(2)_R$ triplet $pp \to \Delta_R^0 \to NN$ at the LHC [276] with varying kinematics, depending on its mass. Moreover, one may be able observe a truly exotic Higgs decay with $h \to \Delta_R^0\Delta_R^0 \to 4N$, where lepton number can be broken to up to four units [276]. The production at lepton colliders may proceed through the Higgs mixing $e^+e^- \to Z\Delta_R^0 \to NNZ$ for $\sqrt{s} \lesssim 100$ GeV and in the VBF channel that produces the $NN\nu\bar{\nu}$ final state with lepton number violation (LNV) and missing energy [276]. At $\sqrt{s} = 240$ GeV and $\mathcal{L} = 5$ ab, one may expect from a few 100 to more than 5000 NNZ events, depending on the masses of triplets and heavy neutrinos, as well as the Higgs-triplet mixing. Such events are essentially background free at lepton colliders because of the LNV final state, Z tagging and characteristic displacement. Similarly, the quadruple production of N's can proceed through Higgs-triplet triple vertex with the potential of observing $\mathcal{O}(10^4)$ events with the branching ratio of Higgs to $\Delta_R^0\Delta_R^0$ at 1% level.

1.3.4.4 Charged lepton flavor violation

Neutrino oscillations violate lepton flavor, which is transferred to the charged leptons via perturbation theory, such that the violation of the charged lepton flavor (cLFV) is a prediction [277].

Mixed flavor leptonic Higgs or Z boson decays: Observables at high energy that can measure cLFV are exotic decays of the Z boson into two charged leptons of different flavor, $Z \to e^\pm\mu^\mp$, $e^\pm\tau^\mp$, $\mu^\pm\tau^\mp$ [278, 279]. Also the decays of the Higgs boson into two charged leptons of different flavor are possible [280, 281]. The processes $h \to e^\pm\mu^\mp$, $e^\pm\tau^\mp$, $\mu^\pm\tau^\mp$ are lepton flavor violating Higgs decays that can be measured at the CEPC for branching ratios as small as $1.2 \times 10^{-5} \div 1.6 \times 10^{-4}$ [282].

Lepton universality violation in W boson decays: The branching ratios of the W bosons should be identical for the three different leptons[5], which is due to the lepton universality in the SM. Another probe of lepton universality is given by the decays of the τ lepton. Mixing of the active neutrinos with neutral fermions from the Type I or III seesaw can lead to violations of lepton universality, cf. e.g. [284]. Charged scalar particles can affect the measurement of lepton-universality observables from W boson branching ratios [285].

Mixed flavor final states with and without resonance: An observable cLFV process at lepton colliders is given by $e^+e^- \to \ell_\alpha^\pm \ell_\beta^\mp \, (+H)$. These processes receive contributions from electrically neutral scalars, for instance from neutrinophillic Two Higgs Doublet models, Type II-based Seesaw models, $B-L$ or left-right symmetry. A dedicated study of of such cLFV processes involving neutral scalars can be found in ref. [204]. The most stringent constraints and the CEPC prospects in both the on-shell and off-shell modes collected in Fig. 1.29.

1.3.4.5 Higgs boson properties

Anomalous Higgs boson production: For $M_i > m_h$ additional Higgs bosons can be produced from heavy neutrino decays in processes $e^+e^- \to Z^* \to N\nu \to H\nu\nu$. This can yield an enhancement of the SM mono-Higgs channel of up to $\sim 2\%$ when applying "standard" filters [286, 287]. The CEPC sensitivity via additional Higgs bosons from dedicated analyses is shown by the yellow line in Fig. 1.30.

Heavy neutrinos can also contribute significantly to the process $e^+e^- \to HWW$ [288]. The heavy charged leptons from the Type III Seesaw are expected to modify the Higgs potential [289, 290] and can lead to significant contributions to the process $e^+e^- \to HH$ [291].

In $B-L$ and $L-R$ symmetric models the additional neutral scalar particles may reduce the standard Higgs boson production cross section due to their mixing. In the minimal LRSM model at TeV scales, Higgs couplings, such as the triple Higgs vertex can be dominated by loops [276, 292] of charged triplets and heavy neutrinos, leading to several 10% or even $\mathcal{O}(1)$ corrections of the hhh vertex with respect to the SM, if the neutral triplet-Higgs mixing is at a 10% level.

Invisible Higgs boson decays: N_i can leave measurable imprints in precision measurements of the Higgs boson branching ratios. In Type I Seesaw for N_i with $M < m_h$ the Higgs boson can decay into a light and a heavy neutrino mass eigenstate, which can account for up to 30% of the Higgs decays [293] without violating present constraints [294]. The sensitivity from searches via Higgs branching ratio measurements, considering the precision from Ref. [121], are shown by the red line in Fig. 1.30.

Leptonic Higgs decays with cLFV or LNV: As mentioned above cLFV decays also add loop-induced additional channels to the total Higgs decay width, cf./ sec. 1.3.4.4, and processes where the Higgs couples to two N_i can give rise to exotic LNV decay channels, cf. 1.3.4.3.

[5]Current LEP data features a branching $\mathrm{Br}(W \to \tau\nu)$ that is larger than $\mathrm{Br}(W \to \ell_{e,\mu}\nu)$ by $\sim 2\sigma$ [283].

Higgs decays into two N_i : In $B-L$ and $L-R$ symmetric models, additional neutral scalars can mix with the Higgs boson. This can give rise to additional decay channels into two N_i , which can be observable, depending on their masses and lifetimes. Such signatures were studied in the context of LRSM [275, 276] and $B-L$ models [295, 296].

Anomalous diphoton decays: In the Type II Seesaw the additional scalar particles couple directly to the Higgs boson, such that the singly and doubly charged components contribute to its loop-induced coupling to the photon [258, 297–299]. Also Type III Seesaw contains additional charged particles that can contribute to the Higgs-to-diphoton branching ratio, see e.g. [300]. In the LRSM, the doubly charged component of the $SU(2)_R$ triplet couples rather strongly to the SM Higgs, leading to a $\mathcal{O}(100\ \text{GeV})$ lower bound on its mass [292].

Modified Higgs self couplings: In Type I Seesaw the N_i with masses M_i of a few TeV can modify the trilinear Higgs self-coupling up to 30 percent [301]. One would expect this modification also for the low-scale Type III Seesaw [289, 290].

1.3.4.6 Modifications of electroweak precision observables

Neutrino mass physics can modify the theory predictions for the electroweak observables, which may be observable even if the new mass scale is above the CEPC center-of-mass energy. These can either occur due to virtual exchange of the new particles (which may be represented by higher dimensional operators in an EFT approach [302, 303]) or due to the production of new particles that mix with SM particles (e.g. with the active neutrinos or the SM Higgs boson).

In the context of the type I seesaw mechanism the mixings $\theta_{ai} = vY_{ai}/M_i$ of n_s heavy right handed neutrinos ν_{Ri} with the SM neutrinos ν_{La} leads to an effective violation of unitarity in the 3×3 mixing matrix V_ν, which is a submatrix of the $(3+n_s) \times (3+n_s)$ leptonic mixing matrix $\mathcal{U}$ [284, 304–306]. This affects all the electroweak precision observables (EWPO). Such tests are mostly independent of the heavy neutrino masses M_i and they test different combinations of the active-sterile mixing parameters [284, 293, 307, 308]. We show the corresponding possible sensitivity of the CEPC by solid and dashed blue lines in Fig. 1.30, considering a total integrated luminosity of 0.1 ab^{-1}. In addition to the modified EWPO, one also expects violations of lepton universality and (apparent) violations of the unitarity of the Cabibbo-Kobayashi-Maskawa matrix [284, 294, 309–312].

In the context of type II seesaw, the EWPTs are affected both by the triplet vev, as well as by the mass splittings [258] that enter the oblique T parameter. In the minimal LRSM, this splitting is predicted to be large and leads to a lower bound on the entire $SU(2)_L$ triplet multiplet [292].

1.3.4.7 Displaced secondary vertices

Single displaced vertex in Type I Seesaw: For masses below m_W, the N_i lifetime scales as $\tau_{N_i} \propto |\sum_a |\theta_{ai}|^2|^{-2} G_F^{-2} M_i^{-5}$ and their decays give rise to a visibly displaced secondary vertex in a large part of the allowed parameter space. [6] Displaced vertex signatures have

[6] The sensitivity of a standard detector could be increased with additional detectors of the MATHUSLA [313] or FASER [314] type.

been studied in detail for the case of the Type I Seesaw, and the CEPC specific results from refs. [253, 315] are shown in figure 1.30. It is worth noting that with a longer Z pole run the sensitivity for $M_i < m_Z$ can be significantly increased, cf. figure 1.31. The sensitivity of a standard detector could be increased with additional detectors of the MATHUSLA [313, 316] or FASER [314] type.

Long lived neutral scalars: Due to mixing with the Higgs boson, the electrically neutral scalars in gauged $U(1)_{B-L}$ [317] or the neutral scalar from $SU(2)_R$ [318] can decay via the SM Yukawa couplings into the SM fermions. For masses in the GeV range, the resulting proper lifetimes can easily be $\mathcal{O}(1)$ cm, such that their decays give rise to displaced secondary vertices.

Multiple displaced vertices: Pair production of N in exotic Higgs decays may lead to two displaced vertices, each containing a lepton and two jets at parton level, as pointed out in the context of LRSM [275, 276] and models with $B - L$ symmetry [295, 296]. Rare exotic decays of the SM-like Higgs boson to a pair of triplets with subsequent decay to $4N$s leads to up to four displaced vertices with rather soft final states, which lepton colliders may be much more suited for than the LHC.

The associated production of the scalar triplet at $e^+e^- \to Z^* \to Z\Delta_R^0$ leads to two displaced vertices when $\Delta_R^0 \to NN$, while Z decay gives additional prompt leptons/jets or missing energy.

1.3.4.8 Extra gauge bosons

Extended theoretical frameworks generally predict more and stronger signals from heavy neutrinos. In particular the gauged $B - L$ symmetry, which contains an extra Z' gauge boson, may give rise to a modified rate the processes $e^+e^- \to \ell^+\ell^-$ at lepton colliders [319–321].

The Left-Right symmetric model contains the parity-symmetric W_R and Z_{LR} charged and neutral gauge bosons. The charged bosons are strongly constrained by B and K meson mixing and CP-odd observables, cf. e.g. [322], as well the neutron EDM constraints [323], with current bounds in the 3 TeV range. The neutral gauge boson Z_{LR} is typically heavier in minimal LR models.

In many instances, the LHC searches are catching up with flavor limits. In particular the 'golden channel' $pp \to W_R \to \ell N$ [324] features a dynamic parameter space [325] that ranges from prompt N production to merged neutrino jets [326–328], displaced vertices [329, 330] and a single prompt lepton with missing energy, where current bounds range up to 5 TeV, see [330] for the complete coverage of parameter space of W_R and N masses.

Additional gauge bosons can give rise to additional production mechanisms for N_i that is not suppressed by small Yukawa couplings, but possibly by the large gauge boson masses or their small couplings to the SM, cf. e.g. [295].

1.3.4.9 Monte Carlo Tools for seesaws at CEPC

The aforementioned seesaw scenarios have been implemented in various `FeynRules` [331–333]-based model files that are compatible with the general purpose event generators `Herwig` [334], `MadGraph5_aMC@NLO` [111], `Sherpa` [335], and `Whizard` [336]. In particular, publicly available Universal FeynRules Object (UFO) [337] libraries are available for models of heavy neutrinos [338], including those with extra gauge bosons [328,

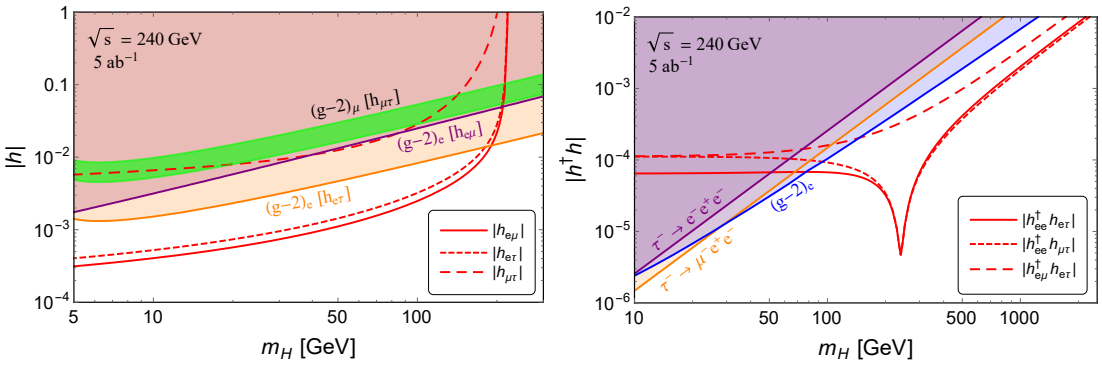

Figure 1.29: Prospects of probing the effective cFLV couplings $h_{\alpha\beta}$ ($\alpha \neq \beta$) from searches of $e^+e^- \to \ell_\alpha^\pm \ell_\beta^\mp H$ (left) and $e^+e^- \to \ell_\alpha^\pm \ell_\beta^\mp$ (right) at CEPC with $\sqrt{s} = 240$ GeV and $\mathcal{L} = 5$ ab^{-1}. Here we have assumed 10 cFLV signal events, and the shaded regions are excluded by electron and muon $g-2$, the rare decays $\tau \to eee$ and $\tau \to ee\mu$. In the left panel we have assumed a BR of 50% from H decay to be visible, and the green band could explain the $(g-2)_\mu$ discrepancy at the 2σ level. See text and [204] for more details.

339–342]; models with triplet scalars [341, 343, 344], including the Higgs gluon fusion and Higgs-triplet mixing [345], as well as models with triplet leptons [346–349].

1.3.4.10 Leptogenesis

1.3.4.11 Motivation

Global fits to present neutrino oscillation data prefer charge-parity (CP) violation in the leptonic sector at the $2 \div 2.5\sigma$ level, cf. [208, 209]. The CP violation in the leptonic sector may be related [350] to the observed *baryon asymmetry of the universe* (BAU), i.e., the tiny excess $\eta_B \sim 10^{-10}$ [128] of matter over antimatter in the early universe over that formed the origin of the baryonic matter in the universe after mutual annihilation of all other particles and antiparticles, cf. e.g. [351].

The idea that a matter-antimatter asymmetry in the early universe is primarily generated in the lepton sector [352] and then transferred into a baryon asymmetry via sphaleron processes [353] is known as *leptogenesis* and provides an explanation for the observed BAU and connects one of the deepest mysteries in cosmology to the properties of neutrinos.

For Λ above the collision energies at the CEPC, it is impossible to discover the new particles responsible for the generation of the BAU, but observing a combination of LNV and cFLV signatures at scales accessible to the CEPC could still rule out such "high scale leptogenesis" scenarios because particles with LNV interactions near the electroweak scale could wash out baryon asymmetries that were produced at high scales [354, 355].

If, in contrast, Λ is within reach of the CEPC, one can directly probe the mechanism of leptogenesis by studying the properties of the new particles [356]. One of the best studied scenarios that accommodates leptogenesis is based on the low-scale type I seesaw model. The Yukawa couplings Y_{ai} that couple the right-handed neutrinos N_i to the Higgs and the left-handed neutrinos ν_{La} in general are complex and are a potential source of CP violation. Hence, the N_i may be the common origin on neutrino masses and baryonic matter in the universe. In the mass range M_i around and below the collider-accessible TeV scale, leptogenesis can proceed in two different ways. For M_i above the electroweak scale, the BAU can be generated during the freeze-out and decay of the ν_{Ri} [357] ("freeze-out scenario"). For masses below the electroweak scale the BAU can be generated in

CP-violating oscillations [240, 358] and Higgs decays [359] during the N_i production ("freeze-in scenario"). The latter effectively also describes leptogenesis in the *Neutrino Minimal Standard Model* (νMSM) [239, 240], a complete model where a third heavy neutrino composes the Dark Matter [75, 76] and does not contribute significantly to neutrino mass generation and leptogenesis due to strong observational constraints [360]. Due to its minimality, part of the relevant parameter space of this model is in principle fully testable at colliders [361, 362], and significant fractions of the parameter space can be probed with the CEPC [253]. For M_i below the electroweak scale, this analysis could be done with an accuracy on the percent level at the Z pole with 10/ab [253].

1.3.4.12 Lepton Number violation

Lepton number violation is a crucial ingredient of any leptogenesis scenario. Typical signatures at the CEPC may involve same sign dilepton final states, either in prompt or displaced decays, cf. sec. 1.3.4.3. An observation of such processes in all three SM flavours or a combination of LNV in some channel and different cLFV signatures could potentially falsify high scale leptogenesis scenarios [354, 355].

Many low scale models rely on an approximate lepton number conservation to explain the smallness of the neutrino masses in the regime of coupling constants that is accessible to the CEPC [231–233], which parametrically suppresses the rate of LNV processes discussed in sec. 1.3.4.3 in prompt decays. For particles with quasi-degenerate masses and comparable lifetimes, as they e.g. appear in resonant leptogenesis scenarios of the νMSM, it has been proposed that this suppression may be overcome by the long time that they have to undergo coherent oscillations within the detector [251, 252, 363]. Since the amount of lepton number violation is proportional to the mass splitting, indirect measurements may be possible from a comparison of the rates for lepton number violating and conserving processes [251, 363] or by observing heavy neutrino-antineutrino oscillations in the detector [252] in displaced vertex searches at the CEPC [253]. The reach of such searches at CEPC in the minimal seesaw model is shown in Fig. 1.31, cf. also 1.30.

1.3.4.13 Lepton flavor violation

Measurements of cLFV (cf. sec. 1.3.4.4) are crucial to test high scale leptogenesis models at the CEPC because an efficient washout of the asymmetries in all flavours at temperatures above the electroweak scale is crucial to rule out such scenarios as the origin of the BAU [355].

Low scale leptogenesis scenarios typically rely on flavour effects and therefore tend to make predictions for the rates of cLFV. In the minimal type I seesaw with $n_s = 2$ (or the νMSM), leptogenesis significantly restricts the flavour mixing pattern of heavy neutrinos N_i with experimentally accessible mixing angles [362]. The accuracy on the percent level at which the flavour mixing pattern can be probed in displaced vertex searches with $10\,\mathrm{ab}^{-1}$ at the Z pole are sufficient to probe large fractions of the parameter region for which heavy neutrinos can be discovered.

1.3.4.14 Displaced decays from long lived heavy neutrinos

For heavy neutrino masses below the electroweak scale, where leptogenesis proceeds in the "freeze in" manner, the N_i couplings should be comparably small to avoid a complete washout of the BAU in the early universe ($|\theta_{ai}|^2 < 10^{-8} \times 10\mathrm{GeV}/M_i$ [364], where larger values can be allowed due to strong hierarchies in their couplings to individual SM

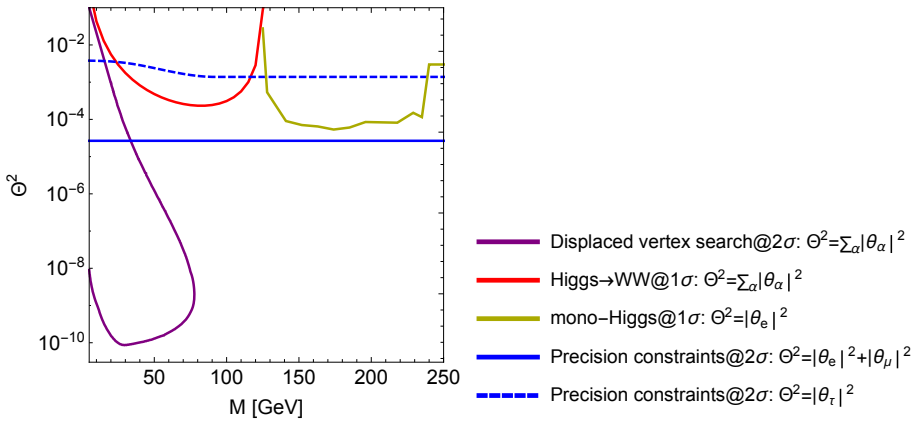

Figure 1.30: Sensitivities to the active-sterile mixing θ and masses M of sterile neutrinos at the CEPC for different signatures. The blue (solid and dashed) lines and the purple line denote electroweak precision measurements [284, 293, 307, 308] and displaced vertex searches [315] at the Z pole run with an integrated luminosity of 10 ab^{-1}, respectively. The yellow and red lines stem from the measurements of Higgs production [286, 287] and decay [293], respectively, for an integrated luminosity of 5 ab^{-1} at $\sqrt{s}$ =240 GeV.

flavours [365]). Hence, most of the parameter space of active-sterile neutrino mixing and masses that is compatible with low scale leptogenesis in this scenario gives rise to long lifetimes of the heavy neutrino mass eigenstates, which can be found with high sensitivity via displaced vertex searches at CEPC. The reach of such searches at CEPC is compared to the parameter region where leptogenesis is feasible in the minimal seesaw model in Fig. 1.31.

1.3.5 Extended Higgs Sector

While all the indications from the current measurements seem to confirm the validity of the SM up to the electroweak scale of a few hundred GeV, and the observed Higgs boson is SM-like, there are compelling arguments, both from theoretical and observational points of view, in favor of the existence of new physics beyond the Standard Model (BSM). As such, searching for new Higgs bosons would be of high priority since they are present in many extensions of theories beyond the SM. One of the most straightforward, but well-motivated extensions is the two-Higgs-doublet model (2HDM) [368], in which there are five massive spin-zero states in the spectrum ($h, H^0, A^0, H^\pm$) after the electroweak symmetry breaking. Extensive searches for BSM Higgs bosons have been actively carried out, especially in the LHC experiments [21, 369–379]. Unfortunately, no signal observation has been reported thus far. This would imply either the non-SM Higgs bosons are much heavier and essentially decoupled from the SM, or their interactions are accidentally aligned with the SM configuration [380, 381]. In either situation, it would be challenging to directly observe those states in experiments.

Complementary to the direct searches, precision measurements of SM parameters and the Higgs properties could lead to relevant insights on new physics. High precision achieved at future Higgs factories with about 10^6 Higgses, and possible Z pole measurements with $10^{10} - 10^{12}$ Z bosons [139, 382–385] would hopefully shed light on the new physics associated with the electroweak sector. Identifying the light CP-even Higgs h to be the experimentally observed 125 GeV Higgs, the couplings of h to the SM fermions

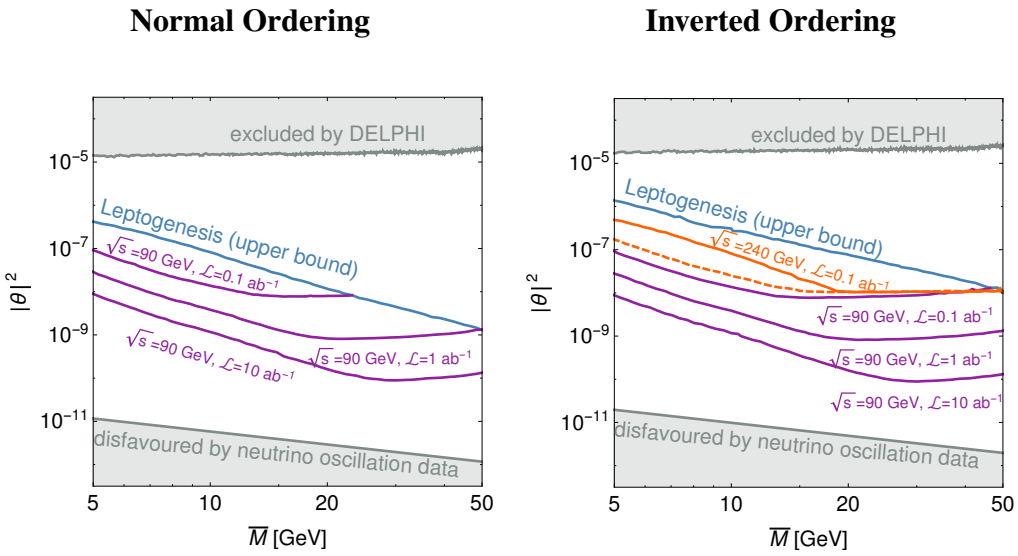

Figure 1.31: The grey area is ruled out by the DELPHI experiment [366, 367] (top) and current neutrino oscillation data (bottom). The blue "BAU" line shows the largest possible $\sum_a |\theta_{ai}|^2$ for which the baryon asymmetry of the universe can be generated in the minimal type I seesaw model with $n_s = 2$ with given $\bar{M} = (M_1 + M_2)/2$ and $|M_2 - M_1|/(M_2 + M_1) < 0.1$. This upper limit is expected to be much higher [365] and practically identical to the DELPHI constraint with $n_s = 3$ heavy neutrinos, so that the CEPC at 240 GeV can enter the cosmologically interesting parameter region for both hierarchies. Above the colored contour lines the CEPC is expected to observe at least four displaced vertex events from N_i compatible with neutrino masses and BAU. The orange lines show the regions accessible with $\sqrt{s} = 240$ GeV for the most optimistic and most pessimistic flavour mixing patters consistent with light neutrino oscillation data. The purple lines indicate the regions accessible with $\sqrt{s}$ at the Z pole, which do not depend on the flavour mixing pattern. The figure is based on the results found in ref. [253].

and gauge bosons receive two contributions: tree-level values, which are controlled by the mixing angles α of the CP-even Higgses and $\tan\beta$, ratios of the vacuum expectation values of two Higgses: $\tan\beta = v_1/v_2$, and loop contributions with heavy Higgses running in the loop. Of particular interest is the so-called "alignment limit" [380, 386] of $\cos(\beta-\alpha) = 0$, in which the light CP-even Higgs couplings are identical to the SM ones at the tree-level, regardless the other scalar masses. Loop corrections, however, could lead to deviations of the couplings of h to SM particles, even at the alignment limit.

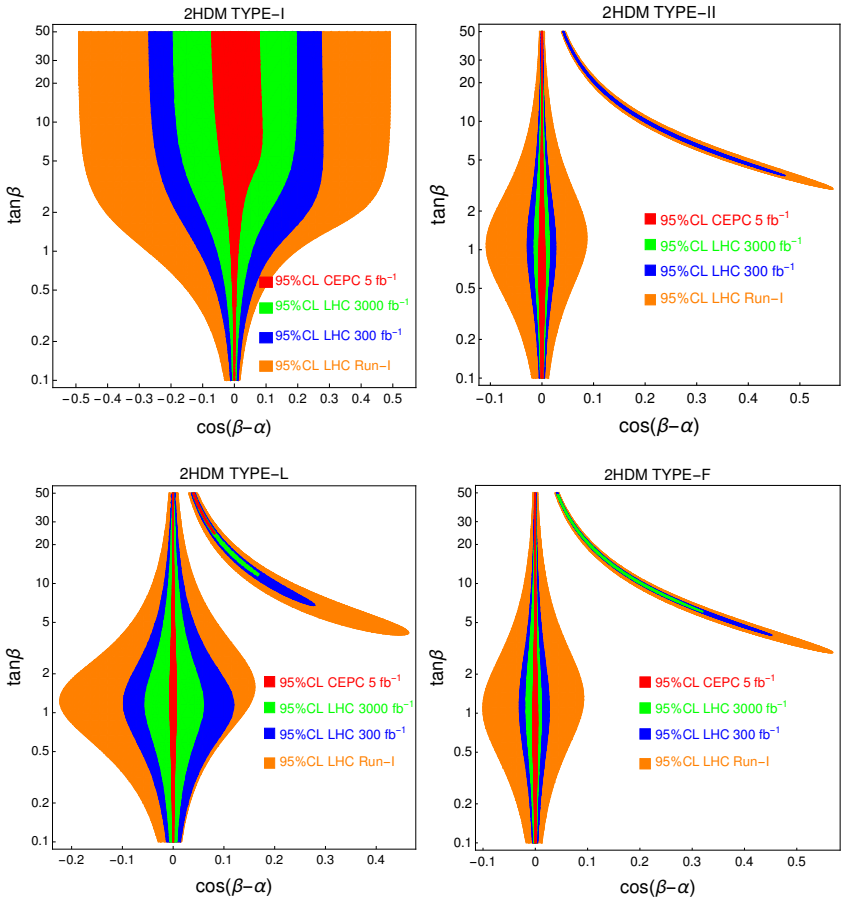

Figure 1.32: The allowed region in the plane of $\cos(\beta-\alpha)$ vs. $\tan\beta$ at 95% C.L. for the four types of 2HDM, given LHC and CEPC Higgs precision measurements. For future measurements, it is assumed that the measurements agree with SM predictions. The special "arm" regions for the Type-II, L and F are the wrong-sign Yukawa regions. Plots are taken from Ref. [19].

There is a plethora of articles in the literature to study the effects of the heavy Higgs states on the Higgs couplings in Models with extended Higgs sector [19, 368, 387–395]. With a global fit to the Higgs rate measurements at the LHC as well as the CEPC, assuming that no deviation to the SM values is observed at future measurements, the 95% C.L. region in the $\cos(\beta-\alpha)$ vs. $\tan\beta$ plane for various types of 2HDM (depending on how the two Higgs doublets are coupled to the quark and lepton sectors) are shown in Fig. 1.32 for tree-level only effects. $\cos(\beta-\alpha)$ in all four types are tightly constrained at both small and large values of $\tan\beta$, except for Type-I, in which constraints are relaxed at large $\tan\beta$ due to suppressed Yukawa couplings.

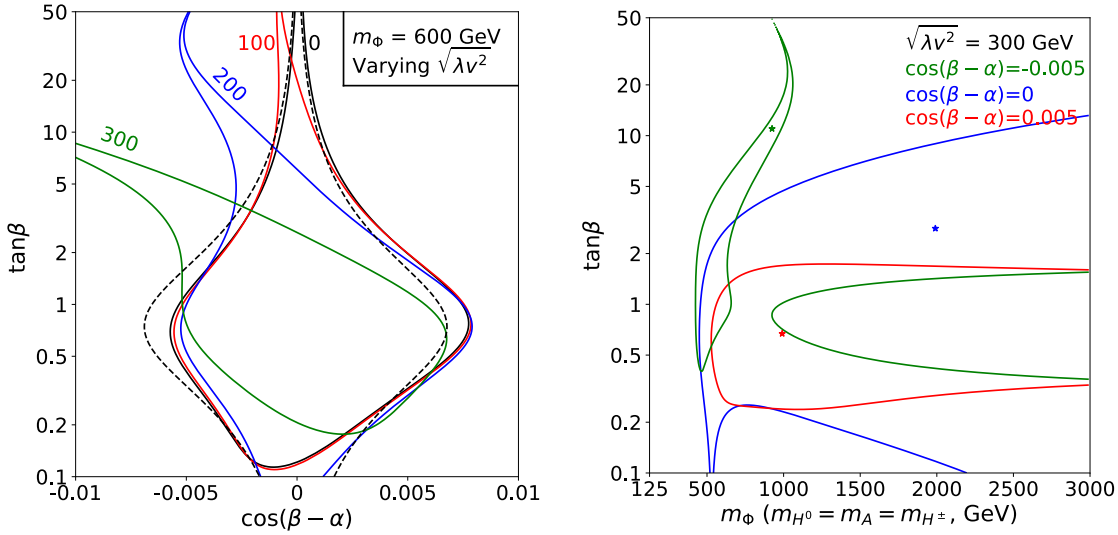

Figure 1.33: Three-parameter fitting results at 95% C.L. with CEPC precision for Type-II 2HDM. The left panel shows the parameter space $\cos(\beta-\alpha)$ vs. $\tan\beta$, varying the value $\sqrt{\lambda v^2}$ with $m_A = m_H = m_{H^\pm} = m_\Phi = 600$ GeV. The tree-level only global fit results are shown by the dashed black lines for comparison. The right panel shows the m_Φ vs. $\tan\beta$ plane, varying the value of $\cos(\beta-\alpha)$ with $\sqrt{\lambda v^2} = 300$ GeV. The colored stars show the corresponding best fit point. Plots are taken from Ref. [395].

To fully explore the Higgs factory potential in search for new physics beyond the SM, both the tree-level deviation and loop corrections need to be considered. Fig. 1.33 shows the 95% C.L. global fit results to all CEPC Higgs rate measurements in the Type-II 2HDM parameter space, including both tree level and loop corrections. Degenerate Heavy Higgs masses $m_A = m_H = m_{H^\pm} = m_\Phi$ are assumed such that Z-pole precision measurements are automatically satisfied. The left panel shows $\cos(\beta-\alpha)$ vs. $\tan\beta$ parameter space with regions enclosed by curves are allowed if no deviation from the SM prediction is observed. Black, red, blue and green curves are for model parameter $\sqrt{\lambda v^2} = \sqrt{m_\Phi^2 - m_{12}^2/s_\beta c_\beta} =$ 0, 100, 200, and 300 GeV, respectively. The tree-level only global fit results are shown by the dashed black lines for comparison. $|\cos(\beta-\alpha)|$ is typically constrained to be less than about 0.008 for $\tan\beta \sim 1$. For smaller and larger values of $\tan\beta$, the allowed range of $\cos(\beta-\alpha)$ is greatly reduced. Loop effects from heavy Higgses tilt the value of $\cos(\beta-\alpha)$ towards negative, especially in the large $\tan\beta$ region.

The right panel of Fig. 1.33 shows the 95% C.L. allowed region in m_Φ vs. $\tan\beta$ plane, with $\cos(\beta-\alpha) = -0.005$ (green), 0 (blue) and 0.005 (red). In the alignment limit of $\cos(\beta-\alpha) = 0$, the heavy Higgs mass $m_\Phi > 500$ GeV are still allowed for $\tan\beta \lesssim 10$. Once deviating away from the alignment limit, the constraints on the heavy Higgs mass get tighter. Comparing to the direct searches of the heavy Higgs bosons at hadron colliders [21, 369–379], The reach in the heavy Higgs mass and couplings at future Higgs factories can be complementary to the direct search limits at the LHC, especially for intermediate values of $\tan\beta$.

Going beyond the degenerate mass case, both the Higgs and Z-pole precision variables are sensitive to the mass splittings between the charged Higgs and the neutral ones. Fig. 1.34 shows the 95% C.L. range of $\Delta m_A = m_A - m_H$ vs. $\Delta m_C = m_{H^\pm} - m_H$ plane, focusing on the $\cos(\beta-\alpha)$ dependence (given by different colored lines), for Higgs and

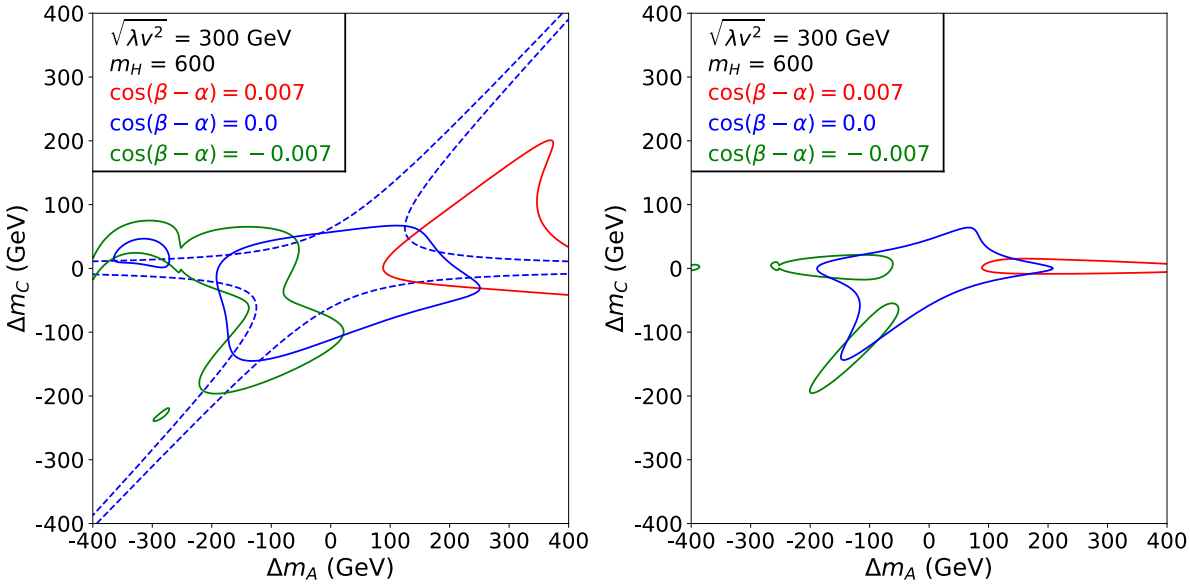

Figure 1.34: Three-parameter fitting 95% C.L. range of $\Delta m_A = m_A - m_H$ vs. $\Delta m_C = m_{H^\pm} - m_H$ pane, focusing on the $\cos(\beta - \alpha)$ dependence (given by different colored lines), for Higgs and Z-pole precision constraints individually (left panel), and combined constraints (right panel) in the Type-II 2HDM. Plots are taken from Ref. [395].

Z-pole precision constraints individually in (left panel), and combined constraints (right panel), with $m_H = 600$ GeV and $\sqrt{\lambda v^2} = 300$ GeV. For the Higgs precision fit, the alignment limit (blue curve) leads to both Δm_A and Δm_C around 0 within a few hundred GeV range. Even for small deviation away from the alignment limit, Δm_A is constrained to be positive for $\cos(\beta - \alpha) = 0.007$, and negative for $\cos(\beta - \alpha) = -0.007$. The Z pole precision measurements (shown in region enclosed by blue dashed curves) constrain either $\Delta m_C \sim 0$ or $\Delta m_C \sim \Delta m_A$, equivalent to $m_{H^\pm} \sim m_{H,A}$. The dependence on $\cos(\beta - \alpha)$ is almost non-noticeable given the small range of $\cos(\beta - \alpha)$ allowed under the current LHC Higgs precision measurements. Combining both the Higgs and Z pole precisions (right panel), the range of $\Delta m_{A,C}$ are further constrained to a narrower range. The expected accuracies at the Z-pole and at a Higgs factory are quite complementary in constraining heavy Higgs mass splittings.

1.4 QCD precision measurement

As a fundamental force in nature, strong force is responsible for the generation of proton mass. The discovery in 1970s of Quantum Chromodynamics (QCD) as a correct theory for describing strong force marks a great achievement in the history of human civilization. Despite forty years of intense study and numerous progress, QCD remains the least understood quantum field theory of nature, in particular in its non-perturbative domain. Even at high energy where the strong force becomes weak due to the property of asymptotic freedom, it is still challenge to obtain quantitative description of QCD phenomena. For example, the "fine structure constant" of QCD, α_s, is eight order of magnitude less constrained than the fine structure constant of QED, and is currently the least constrained fundamental force of nature, including gravity. Improving the precision in our understand-

ing of QCD has direct impact to our understanding of nature, ranging from the production and decay of the Higgs boson, the partonic structure of proton, and the stability of the Standard Model vacuum.

QCD can be studied at lepton, lepton-hadron, and hadron collider. Traditionally, hadron colliders such as the Large Hadron Collider (LHC) has been described as QCD machine, because both initial state and final state at hadron colliders are intimately connected to QCD. However, the strong-interaction nature of initial state also adds additional complications to the description of hard scattering, including the need for the detailed knowledge of Parton Distribution Functions (PDFs), as well as removal/subtraction of the effects from multiple scattering or underlying events. These complications are absent at lepton collider, making it an ideal environment for studying QCD at highest precision. In the past lepton collider has played important role in the study of QCD, from the direct observation of gluon jet to the precise extraction of α_s from collider experiment. Compared with LEP, the largest e^+e^- collider ever built, CEPC has substantial improvement in statistics and systematics, therefore allow QCD study at unprecedented precision. The increase in collision energy will also allow exploration of QCD phenomena at previously unaccessible territory at lepton collider. Besides those well-known problems from the LEP era, many new directions on QCD and jet have been opened since the LHC era due increasing attention in the study of structure of jet, either as a way to disentangle new physics from QCD background, or as a probe of QCD dynamics. CEPC will be an ideal machine to address many of these questions at high precision, due to the absent of complications from multiple scattering and underlying events.

Combined with the remarkable progress in QCD theory, ranging from new methods for efficient calculation of cross section, to development of effective field theory for collider process, to new ideas for simulating scattering processes on Lattice, it is expected that CEPC will marks a new chapter in QCD reserach.

1.4.1 Precision α_s determination

The strong coupling constant α_s is perhaps the most important parameter in QCD. It enters the perturbative predictions of QCD on every observable, in particular cross sections for scattering processes with hadronic final state at CEPC. A precision determination of α_s at CEPC with unprecedented experimental uncertainties will be an important contribution to the world efforts of α_s determination. At lepton collider, α_s can be measured in a number ways. The represented ones include hadronic Z decay, hadronic τ decay, QCD jet rates, and QCD event shape measurement. Summary of α_s determination from these observables using LEP data can be found in Ref. [283].

A distinct feature of CEPC compared with previous lepton collider is the increase of center-of-mass energy. The measurements which can benefit from increased energy are event shape observables, for which non-perturbative corrections are typically scale as $c\Lambda_{\mathrm{QCD}}/Q$, where c is an $\mathcal{O}(1)$ parameter which can not be calculated from first principle with current understanding of QCD. There exist two different approaches in the modeling of non-perturbative hadronization effects for event shapes. One based on corrections for non-perturbative hadronization effects using QCD inspired Monte Carlo tools [396–400], the other based on analytic modeling of non-perturbative shape function [401–405]. Neither of the two treatments can be regarded fully satisfactory. In the Monte Carlo approach, there is mismatch in the parton level definition of Monte Carlo simulation and fixed order

calculation. In the analytic power correction approach, the associated systematics has not been fully verified. Therefore, by going to higher center-of-mass energy, the impact of hardonization effects can be reduced, and the uncertainties associated with them can also be reduced.

As an example of α_s determination from event shape observable using analytic power correction, we quote the recent determination based on C parameter [405]:

$$\alpha_s(m_Z) = 0.1123 \pm 0.0002_{\rm exp} \pm 0.0007_{\rm hadr} \pm 0.0014_{\rm pert}\,, \tag{1.23}$$

where hadronization effects and perturbative uncertainties are the main source of uncertainties contributed to α_s determination. While the perturbative uncertainties can be expected to be reduced further in the coming years, given the remarkable progress in the calculation of higher order corrections and in the resummation of large logarithms, the reduction of hadronization uncertainty is likely coming from an increase of center-of-mass energy.

Currently, for thrust [402, 406], C parameter [404, 405], and heavy-jet-mass distribution [407], the best theoretical prediction is at the level of N^{3}LL resummation matched to NNLO in fixed order perturbation theory. A notable recent progress is the calculation of Energy-Energy Correlation (EEC) at NNLO. EEC is an event shape observable which exhibits the so-called rapidity divergence, and leads to additional logarithms to be resummed, compared with thrust et al.. Very recently, a determination of α_s using NNLL resummation matched to NNLO, and Monte Carlo for the modeling of power corrections, has been done, with the result [408]:

$$\alpha_s(m_Z) = 0.11750 \pm 0.00018_{\rm exp} \pm 0.00102_{\rm hadr} \pm 0.00257_{\rm ren} \pm 0.00078_{\rm res}\,, \tag{1.24}$$

where hadronization effects are important source of uncertainties. Since the analysis in Ref. [408] only uses data at or below Z pole, it is expected that future from CEPC at $250\ \mathrm{GeV}$ can significantly reduce the hadronization uncertainty. Additional scale and resummation uncertainties can also be reduced in the future by incorporating N^{3}LL resummation [409].

1.4.2 Jets rates at CEPC

Another distinct feature of CEPC compared with LEP is its unprecedented luminosity, in particular above Z pole. The high luminosity opens the door for the precision study of multi-jet production at e^+e^- collider.

As an example, we show in Fig. 1.35 the four-jet production cross sections at CEPC ($\sqrt{s} = 250\,\mathrm{GeV}$) with the Durham jet algorithm as a function of the resolution parameter y_{cut}, calculated using NLOjet++ [410]. The cross sections are at the level of a few pb to tens pb for the range of y_{cut} considered. The colored bands represent the scale variations calculated by varying the renormalization scale from $\sqrt{s}/2$ to $2\sqrt{s}$. The NLO predicitons show a smaller scale variation as comparing to the LO ones. The cross sections diverge for small resolution parameter where further QCD resummations are needed to stabilize the theoretical predictions. The right plot shows the projected statistical uncertainties assuming an integrated luminosity of 1 and 5 ab^{-1}. The statistical uncertainties are at the level of one per mille or better for y_{cut} below 10^{-2} due to the large luminosity. The scale uncertainties of the NLO predictions are large in comparison and about 10%, which can be reduced with QCD resummation [410]. The n-jet rate have been employed to

measure the strong coupling constant α_s at LEP [411]. The four-jet cross sections are propotional to α_s^2 at leading order, thus the statistical uncertainties in the measurement of α_s are estimated to be well below one per mille. On the hand, the theoretical uncertainties will play a dominant role and need further investigations. Currently, NNLO predictions for e^+e^- to three jets are available [412–416]. Along this line there have been remarkable progress in the calculation of two-loop amplitudes with five external particles [417, 418], and its associate integrals [419, 420]. Although there is still substantial work to be done, a NNLO calculation for four jet production can be expected in the future. There has also been progress in resumming the large logarithms in jet rates. A Monte Carlo approach for resumation has been proposed and used to resum the large logarithms in two-jet rates in Ref. [421], which can achieve resummation at NNLL level. It would be very interesting to extend this approach to three and four jet rates.

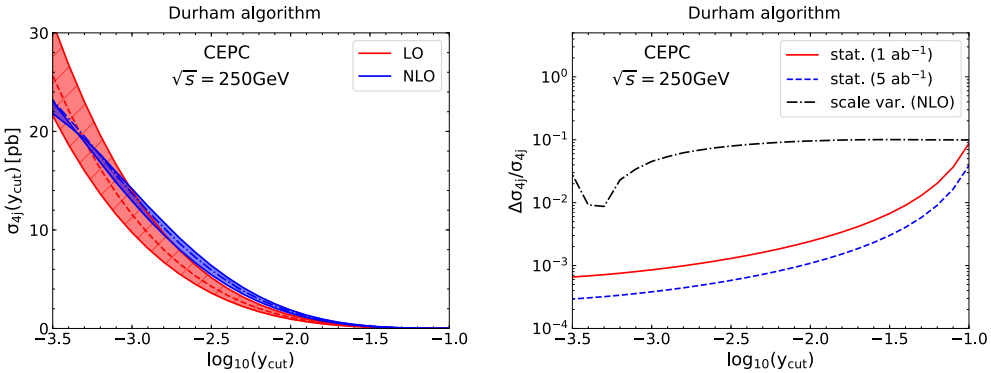

Figure 1.35: Left plot: four-jet production cross sections at CEPC ($\sqrt{s} = 250\,\mathrm{GeV}$) with the Durham jet algorithm as a function of the resolution parameter y_{cut}; Right plot: scale variation and expected statistical uncertainties for the same cross sections normalized to the central values.

1.4.3 Non-global logarithms

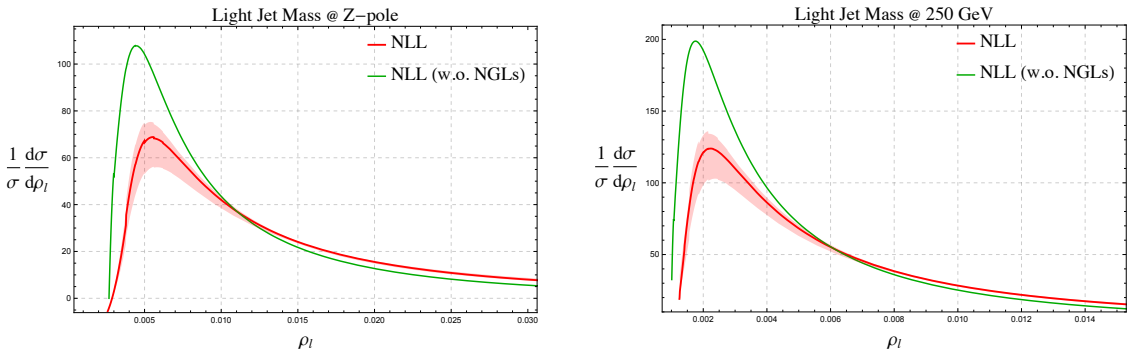

Figure 1.36: Normalized light-jet-mass distribution at Z-pole (Left) and 250 GeV (Right). Green curves are NLL results without NGLs, and red bands are full NLL results with scale uncertainties.

Besides the precision extraction of α_s from jetty final states, there has also be significant interests in understanding some novel aspects of QCD dynamics from jet processes at lepton collider. An important example is the study on Non-global logarithms (NGL) [422, 423].

Non-global logarithms are significant obstacles to study soft physics at high energy colliders. E.g. jet physics, energy flow measurements, hadronization and so on. And therefore it is important to develop theoretical framework to understand their structures. NGLs are first pointed out by Dasgupta and Salam in Ref.[422], where they developed Monte-Carlo algorithm to resum leading-logarithmic(LL) NGLs in the large N_C limit. After that, based on strong energy ordering limit Banfi, Marchesini and Smye derived an integral-differential evolution equation which can also resum LL NGLs [423]. Since then, there are many efforts trying to improve theoretical predictions [424–429], including sub-leading N_c effects[430–432] and some fixed-order calculations[433, 434].

Recently, there are several developments in these fields[435–443]. E.g. the effective field theory developed in Ref. [437], which is the first time to write down the factorisation formula for non-global observables and give an any order renormalization group evolution equation for NGLs.

As electron positron collider CEPC will provide new opportunities, which can precisely measure NGLs in many observables. As shown in Fig. 1.36 we show normalized light-jet-mass distribution at Z-pole (Left) and 250 GeV (Right). Green curves are NLL results without NGLs, and red bands are full NLL results with scale uncertainties. Obviously, after including NGLs theoretical predicitons are reduced significantly, and especially this reduction is magnificent at 250 GeV. Therefore CPEC CEPC will give us the first opportunity to measure NGLs.

1.4.4 QCD event shapes and light quark Yukawa coupling

Higgs boson in the SM decays dominantly to various hadronic final states with a total branching fraction of more than 80%. That provides a new source for QCD studies at CEPC Higgs factory, especially with the unique color-neutral digluon state. Table. 1.3 summarizes the estimated number of events for different hadronic decay modes of the Higgs boson, assuming the tagged Z boson decaying into electrons or muons and an integrated luminosity of 5 fb^{-1} and $\sqrt{s} = 250\,\mathrm{GeV}$. The traditional hadronic event shapes, e.g., thrust distribution, can be well measured due to the high statistics. At lepton colliders one can reconstruct the kinematics fully and then boost all final states back to rest frame of the Higgs boson. On theory side those distributions can be calculated with high precision by QCD resummation matched with fixed-order results. There exist uncertainties from non-perturbative QCD effects like from model of hadronizations which are usually estimated by MC event generators. Left plot of Fig. 1.37 shows the normalized distribution of the variable thrust for several different hadronic decay channels of the Higgs boson, including gg, $q\bar{q}$, $b\bar{b}$, and $W(q\bar{q})W^*(q\bar{q})$ [444]. The distribution peaks at $\tau \sim 0.02$ for light-quark decay channel. The peak shifts to $\tau \sim 0.05$ for the gluon channel, corresponding to a scaling of roughly C_A/C_F. The distribution is much broader for the gluon case due to the stronger QCD radiation. The distribution for the $b\bar{b}$ channel is very close to the $q\bar{q}$ case, except at very small τ, where the mass and hadronization effects become important. For the WW^* channel there exist already four quarks at leading order and the distribution is concentrated in the large-τ region.

Different shapes of the thrust distribution from diquark and digluon final states motivates the idea of using global event shapes to probe the Yukawa couplings of light quarks [444], namely strange, up and down quarks. The provided discrimination can largely reduce background due to Higgs boson decays into two gluons while backgrounds

$Z(l^+l^-)H(X)$	gg	$b\bar{b}$	$c\bar{c}$	$WW^*(4h)$	$ZZ^*(4h)$	$q\bar{q}$
BR [%]	8.6	57.7	2.9	9.5	1.3	~ 0.02
N_{event}	6140	41170	2070	6780	930	14

Table 1.3: The decay branching ratios of the SM Higgs boson with a mass of 125 GeV to different hadronic channels [205] and the corresponding expected numbers of events in ZH production, with subsequent decays at a e^+e^- collider with $\sqrt{s} = 250$ GeV and an integrated luminosity of 5 ab^{-1}. h represents any of the quarks except the top quark and q are light quarks.

from Higgs boson decays into heavy quarks can be suppressed with the usual heavy-flavor tagging algorithms. It is of great challenging to probe the light-quark Yukawa couplings due to their smallness since the projected number of events with full luminosity of CEPC is only 14 as shown in Table. 1.3. The expected exclusion limits on decay branching ratios of Higgs boson to light quarks are shown in the right plot of Fig. 1.37, indicated by intersections with the vertical line and normalized to the branching ratio to digluon. The results can be translated into an upper limit of 0.48% on the decay branching ratios or 5 times of its value in standard model for Yukawa coupling of strange quark.

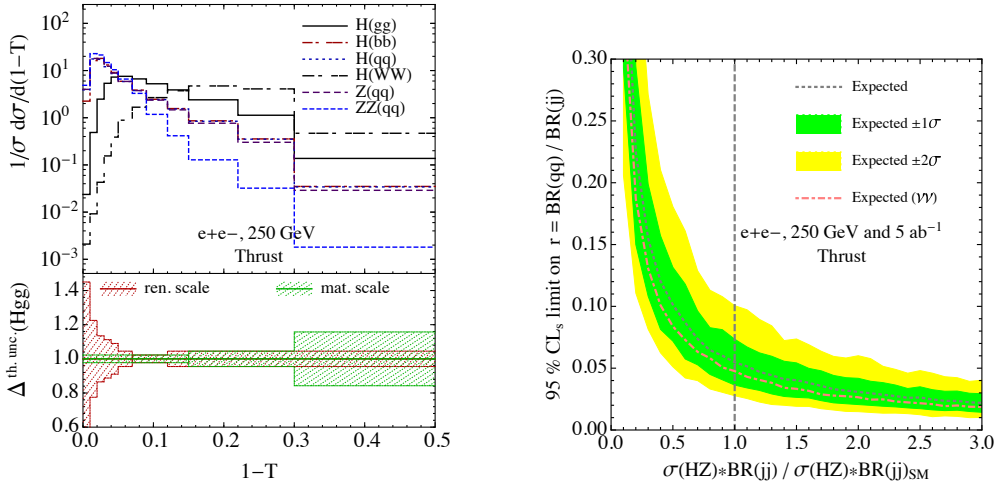

Figure 1.37: Left plot: normalized distributions of thrust in hadronic decays of the Higgs boson, in $e^+e^- \to q\bar{q}$ with a CMS energy of 125 GeV and in $e^+e^- \to Zq\bar{q}$ with a CMS energy of 250 GeV; Right plot: expected 95% $\mathrm{CL_s}$ exclusion limit on r as a function of the total cross section of the Higgs boson decay to jj normalized to the SM value.

References

[1] The ATLAS Collaboration, G. Aad et al., *Observation of a new particle in the search for the Standard Model Higgs boson with the ATLAS detector at the LHC*, Phys. Lett. B **716** (2012) 1–29, arXiv:1207.7214 [hep-ex].

[2] The CMS Collaboration, S. Chatrchyan et al., *Observation of a new boson at a mass of 125 GeV with the CMS experiment at the LHC*, Phys. Lett. **B716** (2012) 30–61, arXiv:1207.7235 [hep-ex].

[3] P. A. M. Dirac, *New basis for cosmology*, Proc. Roy. Soc. Lond. **A165** (1938) 199–208.

[4] K. G. Wilson, *The Renormalization Group and Strong Interactions*, Phys. Rev. **D3** (1971) 1818.

[5] L. Susskind, *Dynamics of Spontaneous Symmetry Breaking in the Weinberg-Salam Theory*, Phys. Rev. **D20** (1979) 2619–2625.

[6] G. 't Hooft, *Naturalness, chiral symmetry, and spontaneous chiral symmetry breaking*, NATO Sci. Ser. B **59** (1980) 135–157.

[7] P. Fayet, *Supersymmetry and Weak, Electromagnetic and Strong Interactions*, Phys. Lett. **64B** (1976) 159.

[8] P. Fayet, *Spontaneously Broken Supersymmetric Theories of Weak, Electromagnetic and Strong Interactions*, Phys. Lett. **69B** (1977) 489.

[9] S. Dimopoulos and H. Georgi, *Softly Broken Supersymmetry and SU(5)*, Nucl. Phys. **B193** (1981) 150–162.

[10] D. B. Kaplan, H. Georgi, and S. Dimopoulos, *Composite Higgs Scalars*, Phys. Lett. **136B** (1984) 187–190.

[11] N. Arkani-Hamed, A. G. Cohen, E. Katz, A. E. Nelson, T. Gregoire, and J. G. Wacker, *The Minimal moose for a little Higgs*, JHEP **08** (2002) 021, arXiv:hep-ph/0206020 [hep-ph].

[12] B. Bellazzini, C. Csáki, and J. Serra, *Composite Higgses*, Eur. Phys. J. **C74** (2014) no. 5, 2766, arXiv:1401.2457 [hep-ph].

[13] S. Weinberg, *Implications of Dynamical Symmetry Breaking*, Phys. Rev. **D13** (1976) 974–996. [Addendum: Phys. Rev.D19,1277(1979)].

[14] N. Arkani-Hamed, S. Dimopoulos, and G. R. Dvali, *The Hierarchy problem and new dimensions at a millimeter*, Phys. Lett. **B429** (1998) 263–272, arXiv:hep-ph/9803315 [hep-ph].

[15] I. Antoniadis, N. Arkani-Hamed, S. Dimopoulos, and G. R. Dvali, *New dimensions at a millimeter to a Fermi and superstrings at a TeV*, Phys. Lett. **B436** (1998) 257–263, arXiv:hep-ph/9804398 [hep-ph].

[16] L. Randall and R. Sundrum, *A Large mass hierarchy from a small extra dimension*, Phys. Rev. Lett. **83** (1999) 3370–3373, arXiv:hep-ph/9905221 [hep-ph].

[17] L. Randall and R. Sundrum, *An Alternative to compactification*, Phys. Rev. Lett. **83** (1999) 4690–4693, arXiv:hep-th/9906064 [hep-th].

[18] P. W. Graham, D. E. Kaplan, and S. Rajendran, *Cosmological Relaxation of the Electroweak Scale*, Phys. Rev. Lett. **115** (2015) no. 22, 221801, arXiv:1504.07551 [hep-ph].

[19] J. Gu, H. Li, Z. Liu, S. Su, and W. Su, *Learning from Higgs Physics at Future Higgs Factories*, JHEP **12** (2017) 153, arXiv:1709.06103 [hep-ph].

[20] A. Djouadi, L. Maiani, G. Moreau, A. Polosa, J. Quevillon, and V. Riquer, *The post-Higgs MSSM scenario: Habemus MSSM?*, Eur. Phys. J. **C73** (2013) 2650, arXiv:1307.5205 [hep-ph].

[21] J. Baglio, A. Djouadi, and J. Quevillon, *Prospects for Higgs physics at energies up to 100 TeV*, Rept. Prog. Phys. **79** (2016) no. 11, 116201, arXiv:1511.07853 [hep-ph].

[22] J. Fan, M. Reece, and L.-T. Wang, *Precision Natural SUSY at CEPC, FCC-ee, and ILC*, JHEP **08** (2015) 152, arXiv:1412.3107 [hep-ph].

[23] J. Fan and M. Reece, *A New Look at Higgs Constraints on Stops*, JHEP **06** (2014) 031, arXiv:1401.7671 [hep-ph].

[24] N. Craig, M. Farina, M. McCullough, and M. Perelstein, *Precision Higgsstrahlung as a Probe of New Physics*, JHEP **03** (2015) 146, arXiv:1411.0676 [hep-ph].

[25] R. Essig, P. Meade, H. Ramani, and Y.-M. Zhong, *Higgs-Precision Constraints on Colored Naturalness*, JHEP **09** (2017) 085, arXiv:1707.03399 [hep-ph].

[26] G. F. Giudice, C. Grojean, A. Pomarol, and R. Rattazzi, *The Strongly-Interacting Light Higgs*, JHEP **06** (2007) 045, arXiv:hep-ph/0703164 [hep-ph].

[27] A. Thamm, R. Torre, and A. Wulzer, *Future tests of Higgs compositeness: direct vs indirect*, JHEP **07** (2015) 100, arXiv:1502.01701 [hep-ph].

[28] N. Craig, S. Knapen, and P. Longhi, *Neutral Naturalness from Orbifold Higgs Models*, Phys. Rev. Lett. **114** (2015) no. 6, 061803, arXiv:1410.6808 [hep-ph].

[29] G. Burdman, Z. Chacko, H.-S. Goh, and R. Harnik, *Folded supersymmetry and the LEP paradox*, JHEP **02** (2007) 009, arXiv:hep-ph/0609152 [hep-ph].

[30] Z. Chacko, H.-S. Goh, and R. Harnik, *The Twin Higgs: Natural electroweak breaking from mirror symmetry*, Phys. Rev. Lett. **96** (2006) 231802, arXiv:hep-ph/0506256 [hep-ph].

[31] T. Cohen, N. Craig, G. F. Giudice, and M. Mccullough, *The Hyperbolic Higgs*, JHEP **05** (2018) 091, arXiv:1803.03647 [hep-ph].

[32] H. Cai, H.-C. Cheng, and J. Terning, *A Quirky Little Higgs Model*, JHEP **05** (2009) 045, arXiv:0812.0843 [hep-ph].

[33] N. Craig, C. Englert, and M. McCullough, *New Probe of Naturalness*, Phys. Rev. Lett. **111** (2013) no. 12, 121803, arXiv:1305.5251 [hep-ph].

[34] T. Flacke, C. Frugiuele, E. Fuchs, R. S. Gupta, and G. Perez, *Phenomenology of relaxion-Higgs mixing*, arXiv:1610.02025 [hep-ph].

[35] X.-m. Zhang, *Operators analysis for Higgs potential and cosmological bound on Higgs mass*, Phys. Rev. **D47** (1993) 3065–3067, arXiv:hep-ph/9301277 [hep-ph].

[36] C. Grojean, G. Servant, and J. D. Wells, *First-order electroweak phase transition in the standard model with a low cutoff*, Phys. Rev. **D71** (2005) 036001, arXiv:hep-ph/0407019 [hep-ph].

[37] C. Delaunay, C. Grojean, and J. D. Wells, *Dynamics of Non-renormalizable Electroweak Symmetry Breaking*, JHEP **04** (2008) 029, arXiv:0711.2511 [hep-ph].

[38] Q.-H. Cao, F. P. Huang, K.-P. Xie, and X. Zhang, *Testing the electroweak phase transition in scalar extension models at lepton colliders*, Chin. Phys. **C42** (2018) no. 2, 023103, arXiv:1708.04737 [hep-ph].

[39] F. P. Huang, P.-H. Gu, P.-F. Yin, Z.-H. Yu, and X. Zhang, *Testing the electroweak phase transition and electroweak baryogenesis at the LHC and a circular electron-positron collider*, Phys. Rev. **D93** (2016) no. 10, 103515, arXiv:1511.03969 [hep-ph].

[40] F. P. Huang, Y. Wan, D.-G. Wang, Y.-F. Cai, and X. Zhang, *Hearing the echoes of electroweak baryogenesis with gravitational wave detectors*, Phys. Rev. **D94** (2016) no. 4, 041702, arXiv:1601.01640 [hep-ph].

[41] S. R. Coleman and E. J. Weinberg, *Radiative Corrections as the Origin of Spontaneous Symmetry Breaking*, Phys.Rev. **D7** (1973) 1888–1910.

[42] J. R. Espinosa and M. Quiros, *Novel Effects in Electroweak Breaking from a Hidden Sector*, Phys. Rev. **D76** (2007) 076004, arXiv:hep-ph/0701145 [hep-ph].

[43] C. Caprini et al., *Science with the space-based interferometer eLISA. II: Gravitational waves from cosmological phase transitions*, JCAP **1604** (2016) no. 04, 001, arXiv:1512.06239 [astro-ph.CO].

[44] A. G. Cohen, D. Kaplan, and A. Nelson, *Progress in electroweak baryogenesis*, Ann.Rev.Nucl.Part.Sci. **43** (1993) 27–70, arXiv:hep-ph/9302210 [hep-ph].

[45] M. Carena, M. Quiros, and C. E. M. Wagner, *Opening the window for electroweak baryogenesis*, Phys. Lett. **B380** (1996) 81–91, arXiv:hep-ph/9603420 [hep-ph].

[46] J. R. Espinosa, *Dominant two loop corrections to the MSSM finite temperature effective potential*, Nucl. Phys. **B475** (1996) 273–292, arXiv:hep-ph/9604320 [hep-ph].

[47] D. Curtin, P. Jaiswal, and P. Meade, *Excluding Electroweak Baryogenesis in the MSSM*, JHEP **08** (2012) 005, arXiv:1203.2932 [hep-ph].

[48] D. J. H. Chung, A. J. Long, and L.-T. Wang, *125 GeV Higgs boson and electroweak phase transition model classes*, Phys. Rev. **D87** (2013) no. 2, 023509, arXiv:1209.1819 [hep-ph].

[49] J. R. Espinosa and M. Quiros, *The Electroweak phase transition with a singlet*, Phys. Lett. **B305** (1993) 98–105, arXiv:hep-ph/9301285 [hep-ph].

[50] J. Choi and R. R. Volkas, *Real Higgs singlet and the electroweak phase transition in the Standard Model*, Phys. Lett. **B317** (1993) 385–391, arXiv:hep-ph/9308234 [hep-ph].

[51] J. McDonald, *Electroweak baryogenesis and dark matter via a gauge singlet scalar*, Phys. Lett. **B323** (1994) 339–346.

[52] S. Profumo, M. J. Ramsey-Musolf, and G. Shaughnessy, *Singlet Higgs phenomenology and the electroweak phase transition*, JHEP **08** (2007) 010, arXiv:0705.2425 [hep-ph].

[53] D. Curtin, P. Meade, and C.-T. Yu, *Testing Electroweak Baryogenesis with Future Colliders*, JHEP **11** (2014) 127, arXiv:1409.0005 [hep-ph].

[54] M. McCullough, *An Indirect Model-Dependent Probe of the Higgs Self-Coupling*, Phys. Rev. **D90** (2014) no. 1, 015001, arXiv:1312.3322 [hep-ph]. [Erratum: Phys. Rev.D92,no.3,039903(2015)].

[55] P. Huang, A. J. Long, and L.-T. Wang, *Probing the Electroweak Phase Transition with Higgs Factories and Gravitational Waves*, Phys. Rev. **D94** (2016) no. 7, 075008, arXiv:1608.06619 [hep-ph].

[56] S. Profumo, M. J. Ramsey-Musolf, C. L. Wainwright, and P. Winslow, *Singlet-catalyzed electroweak phase transitions and precision Higgs boson studies*, Phys. Rev. **D91** (2015) no. 3, 035018, arXiv:1407.5342 [hep-ph].

[57] A. Noble and M. Perelstein, *Higgs self-coupling as a probe of electroweak phase transition*, Phys. Rev. **D78** (2008) 063518, arXiv:0711.3018 [hep-ph].

[58] V. Silveira and A. Zee, *Scalar Phantoms*, Phys. Lett. **161B** (1985) 136–140.

[59] J. McDonald, *Gauge singlet scalars as cold dark matter*, Phys. Rev. **D50** (1994) 3637–3649, arXiv:hep-ph/0702143 [HEP-PH].

[60] C. P. Burgess, M. Pospelov, and T. ter Veldhuis, *The Minimal model of nonbaryonic dark matter: A Singlet scalar*, Nucl. Phys. **B619** (2001) 709–728, arXiv:hep-ph/0011335 [hep-ph].

[61] B. Patt and F. Wilczek, *Higgs-field portal into hidden sectors*, arXiv:hep-ph/0605188 [hep-ph].

[62] Y. G. Kim and K. Y. Lee, *The Minimal model of fermionic dark matter*, Phys. Rev. **D75** (2007) 115012, arXiv:hep-ph/0611069 [hep-ph].

[63] V. Barger, P. Langacker, M. McCaskey, M. J. Ramsey-Musolf, and G. Shaughnessy, *LHC Phenomenology of an Extended Standard Model with a Real Scalar Singlet*, Phys. Rev. **D77** (2008) 035005, arXiv:0706.4311 [hep-ph].

[64] Y. G. Kim, K. Y. Lee, and S. Shin, *Singlet fermionic dark matter*, JHEP **05** (2008) 100, arXiv:0803.2932 [hep-ph].

[65] J. M. Cline, K. Kainulainen, P. Scott, and C. Weniger, *Update on scalar singlet dark matter*, Phys. Rev. **D88** (2013) 055025, arXiv:1306.4710 [hep-ph]. [Erratum: Phys. Rev.D92,no.3,039906(2015)].

[66] L. B. Okun, *Limits of Electrodynamics: Paraphotons?*, Sov. Phys. JETP **56** (1982) 502. [Zh. Eksp. Teor. Fiz.83,892(1982)].

[67] B. Holdom, *Two U(1)'s and Epsilon Charge Shifts*, Phys. Lett. **166B** (1986) 196–198.

[68] K. R. Dienes, C. F. Kolda, and J. March-Russell, *Kinetic mixing and the supersymmetric gauge hierarchy*, Nucl. Phys. **B492** (1997) 104–118, arXiv:hep-ph/9610479 [hep-ph].

[69] M. Pospelov, A. Ritz, and M. B. Voloshin, *Secluded WIMP Dark Matter*, Phys. Lett. **B662** (2008) 53–61, arXiv:0711.4866 [hep-ph].

[70] N. Arkani-Hamed and N. Weiner, *LHC Signals for a SuperUnified Theory of Dark Matter*, JHEP **12** (2008) 104, arXiv:0810.0714 [hep-ph].

[71] N. Arkani-Hamed, D. P. Finkbeiner, T. R. Slatyer, and N. Weiner, *A Theory of Dark Matter*, Phys. Rev. **D79** (2009) 015014, arXiv:0810.0713 [hep-ph].

[72] M. Pospelov, *Secluded U(1) below the weak scale*, Phys. Rev. **D80** (2009) 095002, arXiv:0811.1030 [hep-ph].

[73] P. Minkowski, $\mu \to e\gamma$ *at a Rate of One Out of* 10^9 *Muon Decays?*, Phys. Lett. **67B** (1977) 421–428.

[74] R. N. Mohapatra and G. Senjanovic, *Neutrino Mass and Spontaneous Parity Violation*, Phys. Rev. Lett. **44** (1980) 912.

[75] S. Dodelson and L. M. Widrow, *Sterile-neutrinos as dark matter*, Phys. Rev. Lett. **72** (1994) 17–20, arXiv:hep-ph/9303287 [hep-ph].

[76] X.-D. Shi and G. M. Fuller, *A New dark matter candidate: Nonthermal sterile neutrinos*, Phys. Rev. Lett. **82** (1999) 2832–2835, arXiv:astro-ph/9810076 [astro-ph].

[77] D. E. Kaplan, M. A. Luty, and K. M. Zurek, *Asymmetric Dark Matter*, Phys. Rev. **D79** (2009) 115016, arXiv:0901.4117 [hep-ph].

[78] A. Falkowski, J. Juknevich, and J. Shelton, *Dark Matter Through the Neutrino Portal*, arXiv:0908.1790 [hep-ph].

[79] J. F. Cherry, A. Friedland, and I. M. Shoemaker, *Neutrino Portal Dark Matter: From Dwarf Galaxies to IceCube*, arXiv:1411.1071 [hep-ph].

[80] J. A. Harvey, C. T. Hill, and R. J. Hill, *Standard Model Gauging of the Wess-Zumino-Witten Term: Anomalies, Global Currents and pseudo-Chern-Simons Interactions*, Phys. Rev. **D77** (2008) 085017, arXiv:0712.1230 [hep-th].

[81] R. J. Hill, *Some new implications of the anomalous baryon current in the Standard Model*, in *Proceedings, 43rd Rencontres de Moriond on Electroweak Interactions*

and Unified Theories: La Thuile, Italy, March 1-8, 2008, pp. 355–362. 2008. arXiv:0806.3673 [hep-ph]. http://lss.fnal.gov/cgi-bin/find_paper.pl?conf-08-202.

[82] A. Dedes and K. Suxho, *Heavy Fermion Non-Decoupling Effects in Triple Gauge Boson Vertices*, Phys. Rev. **D85** (2012) 095024, arXiv:1202.4940 [hep-ph].

[83] B. Batell, P. deNiverville, D. McKeen, M. Pospelov, and A. Ritz, *Leptophobic Dark Matter at Neutrino Factories*, Phys. Rev. **D90** (2014) no. 11, 115014, arXiv:1405.7049 [hep-ph].

[84] J. A. Dror, R. Lasenby, and M. Pospelov, *New constraints on light vectors coupled to anomalous currents*, Phys. Rev. Lett. **119** (2017) no. 14, 141803, arXiv:1705.06726 [hep-ph].

[85] A. Ismail, A. Katz, and D. Racco, *On dark matter interactions with the Standard Model through an anomalous Z?*, JHEP **10** (2017) 165, arXiv:1707.00709 [hep-ph].

[86] J. A. Dror, R. Lasenby, and M. Pospelov, *Dark forces coupled to nonconserved currents*, Phys. Rev. **D96** (2017) no. 7, 075036, arXiv:1707.01503 [hep-ph].

[87] A. Ismail and A. Katz, *Anomalous Z' and Diboson Resonances at the LHC*, arXiv:1712.01840 [hep-ph].

[88] A. Ekstedt, R. Enberg, G. Ingelman, J. LÃűfgren, and T. Mandal, *Minimal anomalous $\mathrm{U}(1)$ theories and collider phenomenology*, arXiv:1712.03410 [hep-ph].

[89] M. Fabbrichesi, E. Gabrielli, and B. Mele, *Z boson decay into light and darkness*, arXiv:1712.05412 [hep-ph].

[90] R. D. Peccei and H. R. Quinn, *CP Conservation in the Presence of Instantons*, Phys. Rev. Lett. **38** (1977) 1440–1443.

[91] S. Weinberg, *A New Light Boson?*, Phys. Rev. Lett. **40** (1978) 223–226.

[92] F. Wilczek, *Problem of Strong p and t Invariance in the Presence of Instantons*, Phys. Rev. Lett. **40** (1978) 279–282.

[93] J. M. Frere, D. R. T. Jones, and S. Raby, *Fermion Masses and Induction of the Weak Scale by Supergravity*, Nucl. Phys. **B222** (1983) 11–19.

[94] A. E. Nelson and N. Seiberg, *R symmetry breaking versus supersymmetry breaking*, Nucl. Phys. **B416** (1994) 46–62, arXiv:hep-ph/9309299 [hep-ph].

[95] J. Bagger, E. Poppitz, and L. Randall, *The R axion from dynamical supersymmetry breaking*, Nucl. Phys. **B426** (1994) 3–18, arXiv:hep-ph/9405345 [hep-ph].

[96] J. P. Conlon, *The QCD axion and moduli stabilisation*, JHEP **05** (2006) 078, arXiv:hep-th/0602233 [hep-th].

[97] P. Svrcek and E. Witten, *Axions In String Theory*, JHEP **06** (2006) 051, arXiv:hep-th/0605206 [hep-th].

[98] Y. Nomura and J. Thaler, *Dark Matter through the Axion Portal*, Phys. Rev. **D79** (2009) 075008, arXiv:0810.5397 [hep-ph].

[99] A. Arvanitaki, S. Dimopoulos, S. Dubovsky, N. Kaloper, and J. March-Russell, *String Axiverse*, Phys. Rev. **D81** (2010) 123530, arXiv:0905.4720 [hep-th].

[100] J. Jaeckel and A. Ringwald, *The Low-Energy Frontier of Particle Physics*, Ann. Rev. Nucl. Part. Sci. **60** (2010) 405–437, arXiv:1002.0329 [hep-ph].

[101] B. S. Acharya, K. Bobkov, and P. Kumar, *An M Theory Solution to the Strong CP Problem and Constraints on the Axiverse*, JHEP **11** (2010) 105, arXiv:1004.5138 [hep-th].

[102] A. Ringwald, *Exploring the Role of Axions and Other WISPs in the Dark Universe*, Phys. Dark Univ. **1** (2012) 116–135, arXiv:1210.5081 [hep-ph].

[103] K. Sigurdson, M. Doran, A. Kurylov, R. R. Caldwell, and M. Kamionkowski, *Dark-matter electric and magnetic dipole moments*, Phys. Rev. **D70** (2004) 083501, arXiv:astro-ph/0406355 [astro-ph]. [Erratum: Phys. Rev.D73,089903(2006)].

[104] E. Masso, S. Mohanty, and S. Rao, *Dipolar Dark Matter*, Phys. Rev. **D80** (2009) 036009, arXiv:0906.1979 [hep-ph].

[105] S. Chang, N. Weiner, and I. Yavin, *Magnetic Inelastic Dark Matter*, Phys. Rev. **D82** (2010) 125011, arXiv:1007.4200 [hep-ph].

[106] N. Weiner and I. Yavin, *How Dark Are Majorana WIMPs? Signals from MiDM and Rayleigh Dark Matter*, Phys. Rev. **D86** (2012) 075021, arXiv:1206.2910 [hep-ph].

[107] N. Weiner and I. Yavin, *UV completions of magnetic inelastic and Rayleigh dark matter for the Fermi Line(s)*, Phys. Rev. **D87** (2013) no. 2, 023523, arXiv:1209.1093 [hep-ph].

[108] D. Curtin et al., *Exotic decays of the 125 GeV Higgs boson*, Phys. Rev. **D90** (2014) no. 7, 075004, arXiv:1312.4992 [hep-ph].

[109] LHC Higgs Cross Section Working Group Collaboration, D. de Florian et al., *Handbook of LHC Higgs Cross Sections: 4. Deciphering the Nature of the Higgs Sector*, arXiv:1610.07922 [hep-ph].

[110] Z. Liu, L.-T. Wang, and H. Zhang, *Exotic decays of the 125 GeV Higgs boson at future e^+e^- lepton colliders*, Chin. Phys. **C41** (2017) no. 6, 063102, arXiv:1612.09284 [hep-ph].

[111] J. Alwall, R. Frederix, S. Frixione, V. Hirschi, F. Maltoni, O. Mattelaer, H. S. Shao, T. Stelzer, P. Torrielli, and M. Zaro, *The automated computation of tree-level and next-to-leading order differential cross sections, and their matching to parton shower simulations*, JHEP **07** (2014) 079, arXiv:1405.0301 [hep-ph].

[112] Q. Xiu, H. Zhu, X. Lou, and T. Yue, *Study of beamstrahlung effects at CEPC*, Chin. Phys. **C40** (2016) no. 5, 053001, arXiv:1505.01270 [physics.acc-ph].

[113] M. Greco, T. Han, and Z. Liu, *ISR effects for resonant Higgs production at future lepton colliders*, Phys. Lett. **B763** (2016) 409–415, arXiv:1607.03210 [hep-ph].

[114] J. Liu, L.-T. Wang, X.-P. Wang, and W. Xue, *Exposing Dark Sector with Future Z-Factories*, arXiv:1712.07237 [hep-ph].

[115] W.-F. Chang, J. N. Ng, and G. White, *Prospects for Detecting light bosons at the FCC-ee and CEPC*, arXiv:1803.00148 [hep-ph].

[116] L3 Collaboration, M. Acciarri et al., *Search for neutral Higgs boson production through the process e+ e- → Z* H0*, Phys. Lett. **B385** (1996) 454–470.

[117] ATLAS, CMS Collaboration, G. Aad et al., *Measurements of the Higgs boson production and decay rates and constraints on its couplings from a combined ATLAS and CMS analysis of the LHC pp collision data at $\sqrt{s} = 7$ and 8 TeV*, JHEP **08** (2016) 045, arXiv:1606.02266 [hep-ex].

[118] S. Dawson et al., *Working Group Report: Higgs Boson*, in *Proceedings, 2013 Community Summer Study on the Future of U.S. Particle Physics: Snowmass on the Mississippi (CSS2013): Minneapolis, MN, USA, July 29-August 6, 2013*. 2013. arXiv:1310.8361 [hep-ex]. http://inspirehep.net/record/1262795/files/arXiv:1310.8361.pdf.

[119] TLEP Design Study Working Group Collaboration, M. Bicer et al., *First Look at the Physics Case of TLEP*, JHEP **01** (2014) 164, arXiv:1308.6176 [hep-ex].

[120] CEPC-SPPC Study Group Collaboration, *CEPC-SPPC Preliminary Conceptual Design Report. 1. Physics and Detector*, . http://cepc.ihep.ac.cn/preCDR/main_preCDR.pdf.

[121] M. Ruan, *Higgs Measurement at e^+e^- Circular Colliders*, Nucl. Part. Phys. Proc. **273-275** (2016) 857–862, arXiv:1411.5606 [hep-ex].

[122] J. Liu, X.-P. Wang, and F. Yu, *A Tale of Two Portals: Testing Light, Hidden New Physics at Future e^+e^- Colliders*, JHEP **06** (2017) 077, arXiv:1704.00730 [hep-ph].

[123] ATLAS Collaboration, G. Aad et al., *Constraints on new phenomena via Higgs boson couplings and invisible decays with the ATLAS detector*, JHEP **11** (2015) 206, arXiv:1509.00672 [hep-ex].

[124] CMS Collaboration, V. Khachatryan et al., *Searches for invisible decays of the Higgs boson in pp collisions at sqrt(s) = 7, 8, and 13 TeV*, JHEP **02** (2017) 135, arXiv:1610.09218 [hep-ex].

[125] *Projections for measurements of Higgs boson cross sections, branching ratios and coupling parameters with the ATLAS detector at a HL-LHC*, ATL-PHYS-PUB-2013-014, CERN, Geneva, Oct, 2013. http://cds.cern.ch/record/1611186.

[126] CMS Collaboration, *Projected Performance of an Upgraded CMS Detector at the LHC and HL-LHC: Contribution to the Snowmass Process*, in *Proceedings, 2013 Community Summer Study on the Future of U.S. Particle Physics: Snowmass on the Mississippi (CSS2013): Minneapolis, MN, USA, July 29-August 6, 2013*. 2013. arXiv:1307.7135 [hep-ex]. https://inspirehep.net/record/1244669/files/arXiv:1307.7135.pdf.

[127] K. Fujii et al., *Physics Case for the 250 GeV Stage of the International Linear Collider*, arXiv:1710.07621 [hep-ex].

[128] Planck Collaboration, P. A. R. Ade et al., *Planck 2015 results. XIII. Cosmological parameters*, Astron. Astrophys. **594** (2016) A13, arXiv:1502.01589 [astro-ph.CO].

[129] XENON Collaboration, E. Aprile et al., *First Dark Matter Search Results from the XENON1T Experiment*, Phys. Rev. Lett. **119** (2017) no. 18, 181301, arXiv:1705.06655 [astro-ph.CO].

[130] LUX Collaboration, D. S. Akerib et al., *Results from a search for dark matter in the complete LUX exposure*, Phys. Rev. Lett. **118** (2017) no. 2, 021303, arXiv:1608.07648 [astro-ph.CO].

[131] PandaX-II Collaboration, A. Tan et al., *Dark Matter Results from First 98.7 Days of Data from the PandaX-II Experiment*, Phys. Rev. Lett. **117** (2016) no. 12, 121303, arXiv:1607.07400 [hep-ex].

[132] CRESST Collaboration, G. Angloher et al., *Results on light dark matter particles with a low-threshold CRESST-II detector*, Eur. Phys. J. **C76** (2016) no. 1, 25, arXiv:1509.01515 [astro-ph.CO].

[133] J. Jaeckel and M. Spannowsky, *Probing MeV to 90 GeV axion-like particles with LEP and LHC*, Phys. Lett. **B753** (2016) 482–487, arXiv:1509.00476 [hep-ph].

[134] OPAL Collaboration, G. Abbiendi et al., *Multiphoton production in e+ e- collisions at s**(1/2) = 181-GeV to 209-GeV*, Eur. Phys. J. **C26** (2003) 331–344, arXiv:hep-ex/0210016 [hep-ex].

[135] ATLAS Collaboration, G. Aad et al., *Search for Scalar Diphoton Resonances in the Mass Range* $65 - 600$ *GeV with the ATLAS Detector in* pp *Collision Data at* $\sqrt{s} = 8\,TeV$, Phys. Rev. Lett. **113** (2014) no. 17, 171801, arXiv:1407.6583 [hep-ex].

[136] ATLAS Collaboration, G. Aad et al., *Search for new phenomena in events with at least three photons collected in pp collisions at $\sqrt{s}$ = 8 TeV with the ATLAS detector*, Eur. Phys. J. **C76** (2016) no. 4, 210, arXiv:1509.05051 [hep-ex].

[137] S. Knapen, T. Lin, H. K. Lou, and T. Melia, *Searching for Axionlike Particles with Ultraperipheral Heavy-Ion Collisions*, Phys. Rev. Lett. **118** (2017) no. 17, 171801, arXiv:1607.06083 [hep-ph].

[138] L3 Collaboration, M. Acciarri et al., *Search for new physics in energetic single photon production in e^+e^- annihilation at the Z resonance*, Phys. Lett. **B412** (1997) 201–209.

[139] J. Fan, M. Reece, and L.-T. Wang, *Possible Futures of Electroweak Precision: ILC, FCC-ee, and CEPC*, JHEP **09** (2015) 196, arXiv:1411.1054 [hep-ph].

[140] L. Bian, J. Shu, and Y. Zhang, *Prospects for Triple Gauge Coupling Measurements at Future Lepton Colliders and the 14 TeV LHC*, JHEP **09** (2015) 206, arXiv:1507.02238 [hep-ph].

[141] J. Ellis and T. You, *Sensitivities of Prospective Future e+e- Colliders to Decoupled New Physics*, JHEP **03** (2016) 089, arXiv:1510.04561 [hep-ph].

[142] S.-F. Ge, H.-J. He, and R.-Q. Xiao, *Probing new physics scales from Higgs and electroweak observables at e^+ e^- Higgs factory*, JHEP **10** (2016) 007, arXiv:1603.03385 [hep-ph].

[143] S.-F. Ge, H.-J. He, and R.-Q. Xiao, *Testing Higgs coupling precision and new physics scales at lepton colliders*, Int. J. Mod. Phys. **A31** (2016) no. 33, 1644004, arXiv:1612.02718 [hep-ph]. [,55(2017)].

[144] G. Durieux, C. Grojean, J. Gu, and K. Wang, *The leptonic future of the Higgs*, JHEP **09** (2017) 014, arXiv:1704.02333 [hep-ph].

[145] W. H. Chiu, S. C. Leung, T. Liu, K.-F. Lyu, and L.-T. Wang, *Probing 6D Operators at Future e^-e^+ Colliders*, arXiv:1711.04046 [hep-ph].

[146] M. A. Fedderke, T. Lin, and L.-T. Wang, *Probing the fermionic Higgs portal at lepton colliders*, JHEP **04** (2016) 160, arXiv:1506.05465 [hep-ph].

[147] C. Cai, Z.-H. Yu, and H.-H. Zhang, *CEPC Precision of Electroweak Oblique Parameters and Weakly Interacting Dark Matter: the Fermionic Case*, Nucl. Phys. **B921** (2017) 181–210, arXiv:1611.02186 [hep-ph].

[148] N. Liu and L. Wu, *An indirect probe of the higgsino world at the CEPC*, Eur. Phys. J. **C77** (2017) no. 12, 868, arXiv:1705.02534 [hep-ph].

[149] C. Cai, Z.-H. Yu, and H.-H. Zhang, *CEPC Precision of Electroweak Oblique Parameters and Weakly Interacting Dark Matter: the Scalar Case*, Nucl. Phys. **B924** (2017) 128–152, arXiv:1705.07921 [hep-ph].

[150] Q.-F. Xiang, X.-J. Bi, P.-F. Yin, and Z.-H. Yu, *Exploring Fermionic Dark Matter via Higgs Precision Measurements at the Circular Electron Positron Collider*, arXiv:1707.03094 [hep-ph].

[151] J.-W. Wang, X.-J. Bi, Q.-F. Xiang, P.-F. Yin, and Z.-H. Yu, *Exploring Triplet-Quadruplet Fermionic Dark Matter at the LHC and Future Colliders*, arXiv:1711.05622 [hep-ph].

[152] PandaX-II Collaboration, X. Cui et al., *Dark Matter Results From 54-Ton-Day Exposure of PandaX-II Experiment*, Phys. Rev. Lett. **119** (2017) no. 18, 181302, arXiv:1708.06917 [astro-ph.CO].

[153] DARWIN Collaboration, J. Aalbers et al., *DARWIN: towards the ultimate dark matter detector*, JCAP **1611** (2016) 017, arXiv:1606.07001 [astro-ph.IM].

[154] R. J. Hill and M. P. Solon, *WIMP-nucleon scattering with heavy WIMP effective theory*, Phys. Rev. Lett. **112** (2014) 211602, arXiv:1309.4092 [hep-ph].

[155] M. Low and L.-T. Wang, *Neutralino dark matter at 14 TeV and 100 TeV*, JHEP **08** (2014) 161, arXiv:1404.0682 [hep-ph].

[156] J. Kawamura and Y. Omura, *Study of dark matter physics in non-universal gaugino mass scenario*, JHEP **08** (2017) 072, arXiv:1703.10379 [hep-ph].

[157] R. Krall and M. Reece, *Last Electroweak WIMP Standing: Pseudo-Dirac Higgsino Status and Compact Stars as Future Probes*, arXiv:1705.04843 [hep-ph].

[158] C. Cheung, L. J. Hall, D. Pinner, and J. T. Ruderman, *Prospects and Blind Spots for Neutralino Dark Matter*, JHEP **05** (2013) 100, arXiv:1211.4873 [hep-ph].

[159] P. Huang and C. E. M. Wagner, *Blind Spots for neutralino Dark Matter in the MSSM with an intermediate m_A*, Phys. Rev. **D90** (2014) no. 1, 015018, arXiv:1404.0392 [hep-ph].

[160] T. Han, F. Kling, S. Su, and Y. Wu, *Unblinding the dark matter blind spots*, JHEP **02** (2017) 057, arXiv:1612.02387 [hep-ph].

[161] R. Mahbubani and L. Senatore, *The Minimal model for dark matter and unification*, Phys. Rev. **D73** (2006) 043510, arXiv:hep-ph/0510064 [hep-ph].

[162] T. Cohen, J. Kearney, A. Pierce, and D. Tucker-Smith, *Singlet-Doublet Dark Matter*, Phys. Rev. **D85** (2012) 075003, arXiv:1109.2604 [hep-ph].

[163] A. Dedes and D. Karamitros, *Doublet-Triplet Fermionic Dark Matter*, Phys. Rev. **D89** (2014) no. 11, 115002, arXiv:1403.7744 [hep-ph].

[164] A. Basirnia, S. Macaluso, and D. Shih, *Dark Matter and the Higgs in Natural SUSY*, JHEP **03** (2017) 073, arXiv:1605.08442 [hep-ph].

[165] J. Elias-Miró, C. Grojean, R. S. Gupta, and D. Marzocca, *Scaling and tuning of EW and Higgs observables*, JHEP **05** (2014) 019, arXiv:1312.2928 [hep-ph].

[166] K. Harigaya, K. Ichikawa, A. Kundu, S. Matsumoto, and S. Shirai, *Indirect Probe of Electroweak-Interacting Particles at Future Lepton Colliders*, JHEP **09** (2015) 105, arXiv:1504.03402 [hep-ph].

[167] J. D. Wells and Z. Zhang, *Status and prospects of precision analyses with $e^+e^- \to W^+W^-$*, Phys. Rev. **D93** (2016) no. 3, 034001, arXiv:1507.01594 [hep-ph]. [Phys. Rev.D93,034001(2016)].

[168] M. Drees, K. Hagiwara, and A. Yamada, *Process independent radiative corrections in the minimal supersymmetric standard model*, Phys. Rev. **D45** (1992) 1725–1743.

[169] S. P. Martin, K. Tobe, and J. D. Wells, *Virtual effects of light gauginos and higgsinos: A Precision electroweak analysis of split supersymmetry*, Phys. Rev. **D71** (2005) 073014, arXiv:hep-ph/0412424 [hep-ph].

[170] A. Joglekar, P. Schwaller, and C. E. M. Wagner, *Dark Matter and Enhanced Higgs to Di-photon Rate from Vector-like Leptons*, JHEP **12** (2012) 064, arXiv:1207.4235 [hep-ph].

[171] N. Arkani-Hamed, K. Blum, R. T. D'Agnolo, and J. Fan, *2:1 for Naturalness at the LHC?*, JHEP **01** (2013) 149, arXiv:1207.4482 [hep-ph].

[172] C. Englert and M. McCullough, *Modified Higgs Sectors and NLO Associated Production*, JHEP **07** (2013) 168, arXiv:1303.1526 [hep-ph].

[173] R. K. Barman, G. Belanger, B. Bhattacherjee, R. Godbole, G. Mendiratta, and D. Sengupta, *Invisible decay of the Higgs boson in the context of a thermal and nonthermal relic in MSSM*, Phys. Rev. **D95** (2017) no. 9, 095018, arXiv:1703.03838 [hep-ph].

[174] LUX, LZ Collaboration, M. Szydagis, *The Present and Future of Searching for Dark Matter with LUX and LZ*, PoS **ICHEP2016** (2016) 220, arXiv:1611.05525 [astro-ph.CO].

[175] XENON Collaboration, E. Aprile et al., *Physics reach of the XENON1T dark matter experiment*, JCAP **1604** (2016) no. 04, 027, arXiv:1512.07501 [physics.ins-det].

[176] Z. Chacko, Y. Cui, and S. Hong, *Exploring a Dark Sector Through the Higgs Portal at a Lepton Collider*, Phys. Lett. **B732** (2014) 75–80, arXiv:1311.3306 [hep-ph].

[177] M. Karliner, M. Low, J. L. Rosner, and L.-T. Wang, *Radiative return capabilities of a high-energy, high-luminosity e^+e^- collider*, Phys. Rev. **D92** (2015) no. 3, 035010, arXiv:1503.07209 [hep-ph].

[178] D. Curtin, R. Essig, S. Gori, and J. Shelton, *Illuminating Dark Photons with High-Energy Colliders*, JHEP **02** (2015) 157, arXiv:1412.0018 [hep-ph].

[179] ILC Collaboration, G. Aarons et al., *International Linear Collider Reference Design Report Volume 2: Physics at the ILC*, arXiv:0709.1893 [hep-ph].

[180] L3 Collaboration, M. Acciarri et al., *Missing mass spectra in hadronic events from e+ e- collisions at s**(1/2) = 161-GeV - 172-GeV and limits on invisible Higgs decay*, Phys. Lett. **B418** (1998) 389–398.

[181] DELPHI Collaboration, P. Abreu et al., *A Search for invisible Higgs bosons produced in e+ e- interactions at LEP-2 energies*, Phys. Lett. **B459** (1999) 367–381.

[182] OPAL, DELPHI, LEP Higgs Working for Higgs boson searches, L3 CERN, ALEPH Collaboration, *Searches for invisible Higgs bosons: Preliminary combined results using LEP data collected at energies up to 209-GeV*, in *Lepton and photon interactions at high energies. Proceedings, 20th International Symposium, LP 2001, Rome, Italy, July 23-28, 2001*. 2001. arXiv:hep-ex/0107032 [hep-ex]. https://inspirehep.net/record/559835/files/arXiv:hep-ex_0107032.pdf.

[183] L.-B. Jia, *Study of WIMP annihilations into a pair of on-shell scalar mediators*, Phys. Rev. **D94** (2016) no. 9, 095028, arXiv:1607.00737 [hep-ph].

[184] B. Batell, N. Lange, D. McKeen, M. Pospelov, and A. Ritz, *Muon anomalous magnetic moment through the leptonic Higgs portal*, Phys. Rev. **D95** (2017) no. 7, 075003, arXiv:1606.04943 [hep-ph].

[185] T. Liu and C. T. Potter, *Exotic Higgs Decay $h \to a_1 a_1$ at the International Linear Collider: a Snowmass White Paper*, in *Proceedings, 2013 Community Summer Study on the Future of U.S. Particle Physics: Snowmass on the Mississippi (CSS2013): Minneapolis, MN, USA, July 29-August 6, 2013*. 2013. arXiv:1309.0021 [hep-ph]. https://inspirehep.net/record/1252062/files/arXiv:1309.0021.pdf.

[186] J. Kile, A. Kobach, and A. Soni, *Lepton-Flavored Dark Matter*, Phys. Lett. **B744** (2015) 330–338, arXiv:1411.1407 [hep-ph].

[187] J. Huang, T. Liu, L.-T. Wang, and F. Yu, *Supersymmetric Exotic Decays of the 125 GeV Higgs Boson*, Phys. Rev. Lett. **112** (2014) no. 22, 221803, arXiv:1309.6633 [hep-ph].

[188] E. Gabrielli, B. Mele, M. Raidal, and E. Venturini, *FCNC decays of standard model fermions into a dark photon*, Phys. Rev. **D94** (2016) no. 11, 115013, arXiv:1607.05928 [hep-ph].

[189] Q.-H. Cao, Y. Li, B. Yan, Y. Zhang, and Z. Zhang, *Probing dark particles indirectly at the CEPC*, Nucl. Phys. **B909** (2016) 197–217, arXiv:1604.07536 [hep-ph].

[190] P. Agrawal, S. Blanchet, Z. Chacko, and C. Kilic, *Flavored Dark Matter, and Its Implications for Direct Detection and Colliders*, Phys. Rev. **D86** (2012) 055002, arXiv:1109.3516 [hep-ph].

[191] P. Agrawal, Z. Chacko, E. C. F. S. Fortes, and C. Kilic, *Skew-Flavored Dark Matter*, Phys. Rev. **D93** (2016) no. 10, 103510, arXiv:1511.06293 [hep-ph].

[192] A. Birkedal, K. Matchev, and M. Perelstein, *Dark matter at colliders: A Model independent approach*, Phys. Rev. **D70** (2004) 077701, arXiv:hep-ph/0403004 [hep-ph].

[193] Y. J. Chae and M. Perelstein, *Dark Matter Search at a Linear Collider: Effective Operator Approach*, JHEP **05** (2013) 138, arXiv:1211.4008 [hep-ph].

[194] H. Dreiner, M. Huck, M. Krämer, D. Schmeier, and J. Tattersall, *Illuminating Dark Matter at the ILC*, Phys. Rev. **D87** (2013) no. 7, 075015, arXiv:1211.2254 [hep-ph].

[195] Z.-H. Yu, Q.-S. Yan, and P.-F. Yin, *Detecting interactions between dark matter and photons at high energy e^+e^- colliders*, Phys. Rev. **D88** (2013) no. 7, 075015, arXiv:1307.5740 [hep-ph].

[196] Z.-H. Yu, X.-J. Bi, Q.-S. Yan, and P.-F. Yin, *Dark matter searches in the mono-Z channel at high energy e^+e^- colliders*, Phys. Rev. **D90** (2014) no. 5, 055010, arXiv:1404.6990 [hep-ph].

[197] Y. Gao and M. Jin, *Z-pole test of effective dark matter diboson interactions at the CEPC*, arXiv:1712.02140 [hep-ph].

[198] SuperCDMS Collaboration, R. Agnese et al., *Search for Low-Mass Weakly Interacting Massive Particles with SuperCDMS*, Phys. Rev. Lett. **112** (2014) no. 24, 241302, arXiv:1402.7137 [hep-ex].

[199] CDEX Collaboration, H. Jiang et al., *Limits on Light Weakly Interacting Massive Particles from the First 102.8 kg $\times$ day Data of the CDEX-10 Experiment*, Phys. Rev. Lett. **120** (2018) no. 24, 241301, arXiv:1802.09016 [hep-ex].

[200] SuperCDMS Collaboration, R. Agnese et al., *New Results from the Search for Low-Mass Weakly Interacting Massive Particles with the CDMS Low Ionization Threshold Experiment*, Phys. Rev. Lett. **116** (2016) no. 7, 071301, arXiv:1509.02448 [astro-ph.CO].

[201] Fermi-LAT Collaboration, M. Ackermann et al., *Updated search for spectral lines from Galactic dark matter interactions with pass 8 data from the Fermi Large Area Telescope*, Phys. Rev. **D91** (2015) no. 12, 122002, arXiv:1506.00013 [astro-ph.HE].

[202] M. T. Frandsen, U. Haisch, F. Kahlhoefer, P. Mertsch, and K. Schmidt-Hoberg, *Loop-induced dark matter direct detection signals from gamma-ray lines*, JCAP **1210** (2012) 033, arXiv:1207.3971 [hep-ph].

[203] B. Batell and M. McCullough, *Neutrino Masses from Neutral Top Partners*, Phys. Rev. **D92** (2015) no. 7, 073018, arXiv:1504.04016 [hep-ph].

[204] P. S. B. Dev, R. N. Mohapatra, and Y. Zhang, *Lepton Flavor Violation Induced by a Neutral Scalar at Future Lepton Colliders*, arXiv:1711.08430 [hep-ph].

[205] LHC Higgs Cross Section Working Group Collaboration, J. R. Andersen et al., *Handbook of LHC Higgs Cross Sections: 3. Higgs Properties*, arXiv:1307.1347 [hep-ph].

[206] SNO Collaboration, Q. R. Ahmad et al., *Direct evidence for neutrino flavor transformation from neutral current interactions in the Sudbury Neutrino Observatory*, Phys. Rev. Lett. **89** (2002) 011301, arXiv:nucl-ex/0204008 [nucl-ex].

[207] Super-Kamiokande Collaboration, Y. Fukuda et al., *Evidence for oscillation of atmospheric neutrinos*, Phys. Rev. Lett. **81** (1998) 1562–1567, arXiv:hep-ex/9807003 [hep-ex].

[208] *NuFIT 3.2 (2018)*, HTTP://WWW.NU-FIT.ORG/.

[209] I. Esteban, M. C. Gonzalez-Garcia, M. Maltoni, I. Martinez-Soler, and T. Schwetz, *Updated fit to three neutrino mixing: exploring the accelerator-reactor complementarity*, JHEP **01** (2017) 087, arXiv:1611.01514 [hep-ph].

[210] M. Lattanzi and M. Gerbino, *Status of neutrino properties and future prospects - Cosmological and astrophysical constraints*, Front.in Phys. **5** (2018) 70, arXiv:1712.07109 [astro-ph.CO].

[211] E. Majorana, *Teoria simmetrica dell?elettrone e del positrone*, Nuovo Cim. **14** (1937) 171–184.

[212] Y. Cai, T. Han, T. Li, and R. Ruiz, *Lepton-Number Violation: Seesaw Models and Their Collider Tests*, arXiv:1711.02180 [hep-ph].

[213] K. N. Abazajian et al., *Light Sterile Neutrinos: A White Paper*, arXiv:1204.5379 [hep-ph].

[214] M. Drewes, *The Phenomenology of Right Handed Neutrinos*, Int. J. Mod. Phys. **E22** (2013) 1330019, arXiv:1303.6912 [hep-ph].

[215] E. Ma, *Pathways to naturally small neutrino masses*, Phys. Rev. Lett. **81** (1998) 1171–1174, arXiv:hep-ph/9805219 [hep-ph].

[216] S. L. Glashow, *The Future of Elementary Particle Physics*, NATO Sci. Ser. B **61** (1980) 687.

[217] M. Gell-Mann, P. Ramond, and R. Slansky, *Complex Spinors and Unified Theories*, Conf. Proc. **C790927** (1979) 315–321, arXiv:1306.4669 [hep-th].

[218] T. Yanagida, *Horizontal Symmetry and Masses of Neutrinos*, Prog. Theor. Phys. **64** (1980) 1103.

[219] J. Schechter and J. W. F. Valle, *Neutrino Masses in SU(2) x U(1) Theories*, Phys. Rev. **D22** (1980) 2227.

[220] M. Magg and C. Wetterich, *Neutrino Mass Problem and Gauge Hierarchy*, Phys. Lett. **94B** (1980) 61–64.

[221] T. P. Cheng and L.-F. Li, *Neutrino Masses, Mixings and Oscillations in SU(2) x U(1) Models of Electroweak Interactions*, Phys. Rev. **D22** (1980) 2860.

[222] G. Lazarides, Q. Shafi, and C. Wetterich, *Proton Lifetime and Fermion Masses in an SO(10) Model*, Nucl. Phys. **B181** (1981) 287–300.

[223] R. N. Mohapatra and G. Senjanovic, *Neutrino Masses and Mixings in Gauge Models with Spontaneous Parity Violation*, Phys. Rev. **D23** (1981) 165.

[224] R. Foot, H. Lew, X. G. He, and G. C. Joshi, *Seesaw Neutrino Masses Induced by a Triplet of Leptons*, Z. Phys. **C44** (1989) 441.

[225] C. D. Froggatt and H. B. Nielsen, *Hierarchy of Quark Masses, Cabibbo Angles and CP Violation*, Nucl. Phys. **B147** (1979) 277–298.

[226] A. Zee, *A Theory of Lepton Number Violation, Neutrino Majorana Mass, and Oscillation*, Phys. Lett. **93B** (1980) 389. [Erratum: Phys. Lett.95B,461(1980)].

[227] E. Witten, *Neutrino Masses in the Minimal O(10) Theory*, Phys. Lett. **91B** (1980) 81–84.

[228] A. Zee, *Quantum Numbers of Majorana Neutrino Masses*, Nucl. Phys. **B264** (1986) 99–110.

[229] K. S. Babu, *Model of 'Calculable' Majorana Neutrino Masses*, Phys. Lett. **B203** (1988) 132–136.

[230] E. Ma, *Verifiable radiative seesaw mechanism of neutrino mass and dark matter*, Phys. Rev. **D73** (2006) 077301, arXiv:hep-ph/0601225 [hep-ph].

[231] M. Shaposhnikov, *A Possible symmetry of the nuMSM*, Nucl. Phys. **B763** (2007) 49–59, arXiv:hep-ph/0605047 [hep-ph].

[232] J. Kersten and A. Yu. Smirnov, *Right-Handed Neutrinos at CERN LHC and the Mechanism of Neutrino Mass Generation*, Phys. Rev. **D76** (2007) 073005, arXiv:0705.3221 [hep-ph].

[233] K. Moffat, S. Pascoli, and C. Weiland, *Equivalence between massless neutrinos and lepton number conservation in fermionic singlet extensions of the Standard Model*, arXiv:1712.07611 [hep-ph].

[234] R. N. Mohapatra, *Mechanism for Understanding Small Neutrino Mass in Superstring Theories*, Phys. Rev. Lett. **56** (1986) 561–563.

[235] R. N. Mohapatra and J. W. F. Valle, *Neutrino Mass and Baryon Number Nonconservation in Superstring Models*, Phys. Rev. **D34** (1986) 1642.

[236] J. Bernabeu, A. Santamaria, J. Vidal, A. Mendez, and J. W. F. Valle, *Lepton Flavor Nonconservation at High-Energies in a Superstring Inspired Standard Model*, Phys. Lett. **B187** (1987) 303–308.

[237] E. K. Akhmedov, M. Lindner, E. Schnapka, and J. W. F. Valle, *Left-right symmetry breaking in NJL approach*, Phys. Lett. **B368** (1996) 270–280, arXiv:hep-ph/9507275 [hep-ph].

[238] E. K. Akhmedov, M. Lindner, E. Schnapka, and J. W. F. Valle, *Dynamical left-right symmetry breaking*, Phys. Rev. **D53** (1996) 2752–2780, arXiv:hep-ph/9509255 [hep-ph].

[239] T. Asaka, S. Blanchet, and M. Shaposhnikov, *The nuMSM, dark matter and neutrino masses*, Phys. Lett. **B631** (2005) 151–156, arXiv:hep-ph/0503065 [hep-ph].

[240] T. Asaka and M. Shaposhnikov, *The nuMSM, dark matter and baryon asymmetry of the universe*, Phys. Lett. **B620** (2005) 17–26, arXiv:hep-ph/0505013 [hep-ph].

[241] V. V. Khoze and G. Ro, *Leptogenesis and Neutrino Oscillations in the Classically Conformal Standard Model with the Higgs Portal*, JHEP **10** (2013) 075, arXiv:1307.3764 [hep-ph].

[242] B. Bajc and G. Senjanovic, *Seesaw at LHC*, JHEP **08** (2007) 014, arXiv:hep-ph/0612029 [hep-ph].

[243] B. Bajc, M. Nemevsek, and G. Senjanovic, *Probing seesaw at LHC*, Phys. Rev. **D76** (2007) 055011, arXiv:hep-ph/0703080 [hep-ph].

[244] F. del Aguila, J. A. Aguilar-Saavedra, A. Martinez de la Ossa, and D. Meloni, *Flavor and polarisation in heavy neutrino production at e+ e- colliders*, Phys. Lett. **B613** (2005) 170–180, arXiv:hep-ph/0502189 [hep-ph].

[245] T. Saito, M. Asano, K. Fujii, N. Haba, S. Matsumoto, T. Nabeshima, Y. Takubo, H. Yamamoto, and K. Yoshioka, *Extra dimensions and Seesaw Neutrinos at the International Linear Collider*, Phys. Rev. **D82** (2010) 093004, arXiv:1008.2257 [hep-ph].

[246] A. Das and N. Okada, *Inverse seesaw neutrino signatures at the LHC and ILC*, Phys. Rev. **D88** (2013) 113001, arXiv:1207.3734 [hep-ph].

[247] S. Banerjee, P. S. B. Dev, A. Ibarra, T. Mandal, and M. Mitra, *Prospects of Heavy Neutrino Searches at Future Lepton Colliders*, Phys. Rev. **D92** (2015) 075002, arXiv:1503.05491 [hep-ph].

[248] W. Liao and X.-H. Wu, *Signature of heavy sterile neutrinos at CEPC*, Phys. Rev. **D97** (2018) no. 5, 055005, arXiv:1710.09266 [hep-ph].

[249] T. G. Rizzo, *INVERSE NEUTRINOLESS DOUBLE BETA DECAY*, Phys. Lett. **116B** (1982) 23–28.

[250] T. Asaka and T. Tsuyuki, *Seesaw mechanism at electron-electron colliders*, Phys. Rev. **D92** (2015) no. 9, 094012, arXiv:1508.04937 [hep-ph].

[251] G. Anamiati, M. Hirsch, and E. Nardi, *Quasi-Dirac neutrinos at the LHC*, JHEP **10** (2016) 010, arXiv:1607.05641 [hep-ph].

[252] S. Antusch, E. Cazzato, and O. Fischer, *Heavy neutrino-antineutrino oscillations at colliders*, arXiv:1709.03797 [hep-ph].

[253] S. Antusch, E. Cazzato, M. Drewes, O. Fischer, B. Garbrecht, D. Gueter, and J. Klaric, *Probing Leptogenesis at Future Colliders*, arXiv:1710.03744 [hep-ph].

[254] E. J. Chun, K. Y. Lee, and S. C. Park, *Testing Higgs triplet model and neutrino mass patterns*, Phys. Lett. **B566** (2003) 142–151, arXiv:hep-ph/0304069 [hep-ph].

[255] J. Garayoa and T. Schwetz, *Neutrino mass hierarchy and Majorana CP phases within the Higgs triplet model at the LHC*, JHEP **03** (2008) 009, arXiv:0712.1453 [hep-ph].

[256] M. L. Swartz, *Limits on Doubly Charged Higgs Bosons and Lepton Flavor Violation*, Phys. Rev. **D40** (1989) 1521.

[257] P. Fileviez Perez, T. Han, G.-y. Huang, T. Li, and K. Wang, *Neutrino Masses and the CERN LHC: Testing Type II Seesaw*, Phys. Rev. **D78** (2008) 015018, arXiv:0805.3536 [hep-ph].

[258] A. Melfo, M. Nemevsek, F. Nesti, G. Senjanovic, and Y. Zhang, *Type II Seesaw at LHC: The Roadmap*, Phys. Rev. **D85** (2012) 055018, arXiv:1108.4416 [hep-ph].

[259] ATLAS Collaboration, M. Aaboud et al., *Search for doubly charged Higgs boson production in multi-lepton final states with the ATLAS detector using proton?proton collisions at* $\sqrt{s} = 13$ *TeV*, Eur. Phys. J. **C78** (2018) no. 3, 199, arXiv:1710.09748 [hep-ex].

[260] M. Mitra, S. Niyogi, and M. Spannowsky, *Type-II Seesaw Model and Multilepton Signatures at Hadron Colliders*, Phys. Rev. **D95** (2017) no. 3, 035042, arXiv:1611.09594 [hep-ph].

[261] S. Kanemura, M. Kikuchi, K. Yagyu, and H. Yokoya, *Bounds on the mass of doubly-charged Higgs bosons in the same-sign diboson decay scenario*, Phys. Rev. **D90** (2014) no. 11, 115018, arXiv:1407.6547 [hep-ph].

[262] M. Aoki, S. Kanemura, and K. Yagyu, *Testing the Higgs triplet model with the mass difference at the LHC*, Phys. Rev. **D85** (2012) 055007, arXiv:1110.4625 [hep-ph].

[263] Z.-L. Han, R. Ding, and Y. Liao, *LHC phenomenology of the type II seesaw mechanism: Observability of neutral scalars in the nondegenerate case*, Phys. Rev. **D92** (2015) no. 3, 033014, arXiv:1506.08996 [hep-ph].

[264] P. Agrawal, M. Mitra, S. Niyogi, S. Shil, and M. Spannowsky, *Probing the Type-II Seesaw Mechanism through the Production of Higgs Bosons at a Lepton Collider*, arXiv:1803.00677 [hep-ph].

[265] T. G. Rizzo, *Doubly Charged Higgs Bosons and Lepton Number Violating Processes*, Phys. Rev. **D25** (1982) 1355–1364. [Addendum: Phys. Rev.D27,657(1983)].

[266] M. Lusignoli and S. Petrarca, *EXOTIC HIGGS PRODUCTION AT E+ E- COLLIDERS*, Phys. Lett. **B226** (1989) 397–400.

[267] J. F. Gunion, J. Grifols, A. Mendez, B. Kayser, and F. I. Olness, *Higgs Bosons in Left-Right Symmetric Models*, Phys. Rev. **D40** (1989) 1546.

[268] S. Atag and K. O. Ozansoy, *Realistic constraints on the doubly charged bilepton couplings from Bhabha scattering with LEP data*, Phys. Rev. **D68** (2003) 093008, arXiv:hep-ph/0310046 [hep-ph].

[269] V. D. Barger, J. F. Beacom, K.-m. Cheung, and T. Han, *Production of weak bosons and Higgs bosons in e- e- collisions*, Phys. Rev. **D50** (1994) 6704–6712, arXiv:hep-ph/9404335 [hep-ph].

[270] W. Rodejohann and H. Zhang, *Higgs triplets at like-sign linear colliders and neutrino mixing*, Phys. Rev. **D83** (2011) 073005, arXiv:1011.3606 [hep-ph].

[271] J. C. Pati and A. Salam, *Lepton Number as the Fourth Color*, Phys. Rev. **D10** (1974) 275–289. [Erratum: Phys. Rev.D11,703(1975)].

[272] R. N. Mohapatra and J. C. Pati, *Left-Right Gauge Symmetry and an Isoconjugate Model of CP Violation*, Phys. Rev. **D11** (1975) 566–571.

[273] G. Senjanovic and R. N. Mohapatra, *Exact Left-Right Symmetry and Spontaneous Violation of Parity*, Phys. Rev. **D12** (1975) 1502.

[274] G. Senjanovic, *Spontaneous Breakdown of Parity in a Class of Gauge Theories*, Nucl. Phys. **B153** (1979) 334–364.

[275] A. Maiezza, M. Nemevsek, and F. Nesti, *Lepton Number Violation in Higgs Decay at LHC*, Phys. Rev. Lett. **115** (2015) 081802, arXiv:1503.06834 [hep-ph].

[276] M. Nemevsek, F. Nesti, and J. C. Vasquez, *Majorana Higgses at colliders*, JHEP **04** (2017) 114, arXiv:1612.06840 [hep-ph].

[277] F. del Aguila and J. A. Aguilar-Saavedra, *Distinguishing seesaw models at LHC with multi-lepton signals*, Nucl. Phys. **B813** (2009) 22–90, arXiv:0808.2468 [hep-ph].

[278] A. Abada, V. De Romeri, S. Monteil, J. Orloff, and A. M. Teixeira, *Indirect searches for sterile neutrinos at a high-luminosity Z-factory*, JHEP **04** (2015) 051, arXiv:1412.6322 [hep-ph].

[279] S. Antusch, E. Cazzato, and O. Fischer, *Sterile neutrino searches at future e^-e^+, pp, and e^-p colliders*, Int. J. Mod. Phys. **A32** (2017) no. 14, 1750078, arXiv:1612.02728 [hep-ph].

[280] S. Banerjee, B. Bhattacherjee, M. Mitra, and M. Spannowsky, *The Lepton Flavour Violating Higgs Decays at the HL-LHC and the ILC*, JHEP **07** (2016) 059, arXiv:1603.05952 [hep-ph].

[281] E. Arganda, M. J. Herrero, X. Marcano, and C. Weiland, *Imprints of massive inverse seesaw model neutrinos in lepton flavor violating Higgs boson decays*, Phys. Rev. **D91** (2015) no. 1, 015001, arXiv:1405.4300 [hep-ph].

[282] Q. Qin, Q. Li, C.-D. Lü, F.-S. Yu, and S.-H. Zhou, *Charged lepton flavor violating Higgs decays at the CEPC*, arXiv:1711.07243 [hep-ph].

[283] Particle Data Group Collaboration, C. Patrignani et al., *Review of Particle Physics*, Chin. Phys. **C40** (2016) no. 10, 100001.

[284] S. Antusch and O. Fischer, *Non-unitarity of the leptonic mixing matrix: Present bounds and future sensitivities*, JHEP **10** (2014) 094, arXiv:1407.6607 [hep-ph].

[285] J.-h. Park, *Lepton non-universality at LEP and charged Higgs*, JHEP **10** (2006) 077, arXiv:hep-ph/0607280 [hep-ph].

[286] S. Antusch, E. Cazzato, and O. Fischer, *Higgs production from sterile neutrinos at future lepton colliders*, JHEP **04** (2016) 189, arXiv:1512.06035 [hep-ph].

[287] S. Antusch, E. Cazzato, and O. Fischer, *Higgs production through sterile neutrinos*, Int. J. Mod. Phys. **A31** (2016) no. 33, 1644007. [,93(2017)].

[288] J. Baglio, S. Pascoli, and C. Weiland, W^+W^-H *Production at Lepton Colliders: A New Hope for Heavy Neutral Leptons*, arXiv:1712.07621 [hep-ph].

[289] I. Gogoladze, N. Okada, and Q. Shafi, *Higgs Boson Mass Bounds in the Standard Model with Type III and Type I Seesaw*, Phys. Lett. **B668** (2008) 121–125, arXiv:0805.2129 [hep-ph].

[290] B. He, N. Okada, and Q. Shafi, *125 GeV Higgs, type III seesaw and gauge?Higgs unification*, Phys. Lett. **B716** (2012) 197–202, arXiv:1205.4038 [hep-ph].

[291] C.-X. Yue, H.-L. Feng, and W. Ma, *Heavy charged leptons from type-III seesaw and pair production of the Higgs boson H at the International Linear e+ e- Collider*, Chin. Phys. Lett. **27** (2010) 011202.

[292] A. Maiezza, M. Nemevsek, and F. Nesti, *Perturbativity and mass scales in the minimal left-right symmetric model*, Phys. Rev. **D94** (2016) no. 3, 035008, arXiv:1603.00360 [hep-ph].

[293] S. Antusch and O. Fischer, *Testing sterile neutrino extensions of the Standard Model at future lepton colliders*, JHEP **05** (2015) 053, arXiv:1502.05915 [hep-ph].

[294] M. Drewes and B. Garbrecht, *Combining experimental and cosmological constraints on heavy neutrinos*, Nucl. Phys. **B921** (2017) 250–315, arXiv:1502.00477 [hep-ph].

[295] E. Accomando, L. Delle Rose, S. Moretti, E. Olaiya, and C. H. Shepherd-Themistocleous, *Extra Higgs boson and* Z' *as portals to signatures of*

heavy neutrinos at the LHC, JHEP **02** (2018) 109, arXiv:1708.03650 [hep-ph].

[296] F. F. Deppisch, W. Liu, and M. Mitra, *Long-lived Heavy Neutrinos from Higgs Decays*, arXiv:1804.04075 [hep-ph].

[297] A. G. Akeroyd and S. Moretti, *Enhancement of H to gamma gamma from doubly charged scalars in the Higgs Triplet Model*, Phys. Rev. **D86** (2012) 035015, arXiv:1206.0535 [hep-ph].

[298] P. S. Bhupal Dev, D. K. Ghosh, N. Okada, and I. Saha, *125 GeV Higgs Boson and the Type-II Seesaw Model*, JHEP **03** (2013) 150, arXiv:1301.3453 [hep-ph]. [Erratum: JHEP05,049(2013)].

[299] D. Das and A. Santamaria, *Updated scalar sector constraints in the Higgs triplet model*, Phys. Rev. **D94** (2016) no. 1, 015015, arXiv:1604.08099 [hep-ph].

[300] L. Basso, O. Fischer, and J. J. van der Bij, *A singlet-triplet extension for the Higgs search at LEP and LHC*, EPL **101** (2013) no. 5, 51004, arXiv:1212.5560 [hep-ph].

[301] J. Baglio and C. Weiland, *The triple Higgs coupling: A new probe of low-scale seesaw models*, JHEP **04** (2017) 038, arXiv:1612.06403 [hep-ph].

[302] A. Abada, C. Biggio, F. Bonnet, M. B. Gavela, and T. Hambye, *Low energy effects of neutrino masses*, JHEP **12** (2007) 061, arXiv:0707.4058 [hep-ph].

[303] R. Ruiz, *Lepton Number Violation at Colliders from Kinematically Inaccessible Gauge Bosons*, Eur. Phys. J. **C77** (2017) no. 6, 375, arXiv:1703.04669 [hep-ph].

[304] S. Antusch, C. Biggio, E. Fernandez-Martinez, M. B. Gavela, and J. Lopez-Pavon, *Unitarity of the Leptonic Mixing Matrix*, JHEP **10** (2006) 084, arXiv:hep-ph/0607020 [hep-ph].

[305] F. del Aguila, J. de Blas, and M. Perez-Victoria, *Effects of new leptons in Electroweak Precision Data*, Phys. Rev. **D78** (2008) 013010, arXiv:0803.4008 [hep-ph].

[306] S. Parke and M. Ross-Lonergan, *Unitarity and the three flavor neutrino mixing matrix*, Phys. Rev. **D93** (2016) no. 11, 113009, arXiv:1508.05095 [hep-ph].

[307] S. Antusch and O. Fischer, *Testing sterile neutrino extensions of the Standard Model at the Circular Electron Positron Collider*, Int. J. Mod. Phys. **A30** (2015) no. 23, 1544004.

[308] S. Antusch and O. Fischer, *Probing the nonunitarity of the leptonic mixing matrix at the CEPC*, Int. J. Mod. Phys. **A31** (2016) no. 33, 1644006, arXiv:1604.00208 [hep-ph]. [,83(2017)].

[309] A. Atre, T. Han, S. Pascoli, and B. Zhang, *The Search for Heavy Majorana Neutrinos*, JHEP **05** (2009) 030, arXiv:0901.3589 [hep-ph].

[310] A. de Gouvêa and A. Kobach, *Global Constraints on a Heavy Neutrino*, Phys. Rev. **D93** (2016) no. 3, 033005, arXiv:1511.00683 [hep-ph].

[311] E. Fernandez-Martinez, J. Hernandez-Garcia, and J. Lopez-Pavon, *Global constraints on heavy neutrino mixing*, JHEP **08** (2016) 033, arXiv:1605.08774 [hep-ph].

[312] F. J. Escrihuela, D. V. Forero, O. G. Miranda, M. Tortola, and J. W. F. Valle, *On the description of nonunitary neutrino mixing*, Phys. Rev. **D92** (2015) no. 5, 053009, arXiv:1503.08879 [hep-ph]. [Erratum: Phys. Rev.D93,no.11,119905(2016)].

[313] J. P. Chou, D. Curtin, and H. J. Lubatti, *New Detectors to Explore the Lifetime Frontier*, Phys. Lett. **B767** (2017) 29–36, arXiv:1606.06298 [hep-ph].

[314] F. Kling and S. Trojanowski, *Heavy Neutral Leptons at FASER*, arXiv:1801.08947 [hep-ph].

[315] S. Antusch, E. Cazzato, and O. Fischer, *Displaced vertex searches for sterile neutrinos at future lepton colliders*, JHEP **12** (2016) 007, arXiv:1604.02420 [hep-ph].

[316] Mathusla Collaboration, C. Alpigiani, *Ultra Long-Lived Particles with MATHUSLA*, PoS **EPS-HEP2017** (2017) 772.

[317] P. S. B. Dev, R. N. Mohapatra, and Y. Zhang, *Long Lived Light Scalars as Probe of Low Scale Seesaw Models*, Nucl. Phys. **B923** (2017) 179–221, arXiv:1703.02471 [hep-ph].

[318] P. Bhupal Dev, R. N. Mohapatra, and Y. Zhang, *Displaced photon signal from a possible light scalar in minimal left-right seesaw model*, Phys. Rev. **D95** (2017) no. 11, 115001, arXiv:1612.09587 [hep-ph].

[319] A. Freitas, *Weakly coupled neutral gauge bosons at future linear colliders*, Phys. Rev. **D70** (2004) 015008, arXiv:hep-ph/0403288 [hep-ph].

[320] S. Iso, N. Okada, and Y. Orikasa, *The minimal B-L model naturally realized at TeV scale*, Phys. Rev. **D80** (2009) 115007, arXiv:0909.0128 [hep-ph].

[321] L. Basso, A. Belyaev, S. Moretti, and G. M. Pruna, *Probing the Z-prime sector of the minimal B-L model at future Linear Colliders in the e+ e- —> mu+ mu- process*, JHEP **10** (2009) 006, arXiv:0903.4777 [hep-ph].

[322] S. Bertolini, A. Maiezza, and F. Nesti, *Present and Future K and B Meson Mixing Constraints on TeV Scale Left-Right Symmetry*, Phys. Rev. **D89** (2014) no. 9, 095028, arXiv:1403.7112 [hep-ph].

[323] A. Maiezza and M. Nemevsek, *Strong P invariance, neutron electric dipole moment, and minimal left-right parity at LHC*, Phys. Rev. **D90** (2014) no. 9, 095002, arXiv:1407.3678 [hep-ph].

[324] W.-Y. Keung and G. Senjanovic, *Majorana Neutrinos and the Production of the Right-handed Charged Gauge Boson*, Phys. Rev. Lett. **50** (1983) 1427.

[325] M. Nemevsek, F. Nesti, G. Senjanovic, and Y. Zhang, *First Limits on Left-Right Symmetry Scale from LHC Data*, Phys. Rev. **D83** (2011) 115014, arXiv:1103.1627 [hep-ph].

[326] A. Ferrari, J. Collot, M.-L. Andrieux, B. Belhorma, P. de Saintignon, J.-Y. Hostachy, P. Martin, and M. Wielers, *Sensitivity study for new gauge bosons and right-handed Majorana neutrinos in pp collisions at s = 14-TeV*, Phys. Rev. **D62** (2000) 013001.

[327] M. Mitra, R. Ruiz, D. J. Scott, and M. Spannowsky, *Neutrino Jets from High-Mass W_R Gauge Bosons in TeV-Scale Left-Right Symmetric Models*, Phys. Rev. **D94** (2016) no. 9, 095016, arXiv:1607.03504 [hep-ph].

[328] O. Mattelaer, M. Mitra, and R. Ruiz, *Automated Neutrino Jet and Top Jet Predictions at Next-to-Leading-Order with Parton Shower Matching in Effective Left-Right Symmetric Models*, arXiv:1610.08985 [hep-ph].

[329] G. Cottin, J. C. Helo, and M. Hirsch, *Searches for light sterile neutrinos with multitrack displaced vertices*, Phys. Rev. **D97** (2018) no. 5, 055025, arXiv:1801.02734 [hep-ph].

[330] M. Nemevsek, F. Nesti, and G. Popara, *Keung-Senjanović process at LHC: from LNV to displaced vertices to invisible decays*, arXiv:1801.05813 [hep-ph].

[331] N. D. Christensen and C. Duhr, *FeynRules - Feynman rules made easy*, Comput. Phys. Commun. **180** (2009) 1614–1641, arXiv:0806.4194 [hep-ph].

[332] A. Alloul, N. D. Christensen, C. Degrande, C. Duhr, and B. Fuks, *FeynRules 2.0 - A complete toolbox for tree-level phenomenology*, Comput. Phys. Commun. **185** (2014) 2250–2300, arXiv:1310.1921 [hep-ph].

[333] C. Degrande, *Automatic evaluation of UV and R2 terms for beyond the Standard Model Lagrangians: a proof-of-principle*, Comput. Phys. Commun. **197** (2015) 239–262, arXiv:1406.3030 [hep-ph].

[334] J. Bellm et al., *Herwig 7.0/Herwig++ 3.0 release note*, Eur. Phys. J. **C76** (2016) no. 4, 196, arXiv:1512.01178 [hep-ph].

[335] T. Gleisberg, S. Hoeche, F. Krauss, M. Schonherr, S. Schumann, F. Siegert, and J. Winter, *Event generation with SHERPA 1.1*, JHEP **02** (2009) 007, arXiv:0811.4622 [hep-ph].

[336] W. Kilian, T. Ohl, and J. Reuter, *WHIZARD: Simulating Multi-Particle Processes at LHC and ILC*, Eur. Phys. J. **C71** (2011) 1742, arXiv:0708.4233 [hep-ph].

[337] C. Degrande, C. Duhr, B. Fuks, D. Grellscheid, O. Mattelaer, and T. Reiter, *UFO - The Universal FeynRules Output*, Comput. Phys. Commun. **183** (2012) 1201–1214, arXiv:1108.2040 [hep-ph].

[338] C. Degrande, O. Mattelaer, R. Ruiz, and J. Turner, *Fully-Automated Precision Predictions for Heavy Neutrino Production Mechanisms at Hadron Colliders*, Phys. Rev. **D94** (2016) no. 5, 053002, arXiv:1602.06957 [hep-ph].

[339] L. Basso, A. Belyaev, S. Moretti, and C. H. Shepherd-Themistocleous, *Phenomenology of the minimal B-L extension of the Standard model: Z' and neutrinos*, Phys. Rev. **D80** (2009) 055030, arXiv:0812.4313 [hep-ph].

[340] L. Basso, S. Moretti, and G. M. Pruna, *Theoretical constraints on the couplings of non-exotic minimal Z' bosons*, JHEP **08** (2011) 122, arXiv:1106.4762 [hep-ph].

[341] A. Roitgrund, G. Eilam, and S. Bar-Shalom, *Implementation of the left-right symmetric model in FeynRules*, Comput. Phys. Commun. **203** (2016) 18–44, arXiv:1401.3345 [hep-ph].

[342] B. Fuks and R. Ruiz, *A comprehensive framework for studying W' and Z' bosons at hadron colliders with automated jet veto resummation*, JHEP **05** (2017) 032, arXiv:1701.05263 [hep-ph].

[343] F. del Aguila and M. Chala, *LHC bounds on Lepton Number Violation mediated by doubly and singly-charged scalars*, JHEP **03** (2014) 027, arXiv:1311.1510 [hep-ph].

[344] C. Degrande, K. Hartling, H. E. Logan, A. D. Peterson, and M. Zaro, *Automatic predictions in the Georgi-Machacek model at next-to-leading order accuracy*, Phys. Rev. **D93** (2016) no. 3, 035004, arXiv:1512.01243 [hep-ph].

[345] A. Maiezza, M. Nemevšek, F. Nesti, G. Popara, and J. C. Vasquez, *Left-Right Hep Tools*, *https://sites.google.com/site/leftrighthep/*, 2018. https://sites.google.com/site/leftrighthep/.

[346] C. Biggio and F. Bonnet, *Implementation of the Type III Seesaw Model in FeynRules/MadGraph and Prospects for Discovery with Early LHC Data*, Eur. Phys. J. **C72** (2012) 1899, arXiv:1107.3463 [hep-ph].

[347] A. Abada, C. Biggio, F. Bonnet, M. B. Gavela, and T. Hambye, *mu —> e gamma and tau —> l gamma decays in the fermion triplet seesaw model*, Phys. Rev. **D78** (2008) 033007, arXiv:0803.0481 [hep-ph].

[348] O. J. P. Eboli, J. Gonzalez-Fraile, and M. C. Gonzalez-Garcia, *Neutrino Masses at LHC: Minimal Lepton Flavour Violation in Type-III See-saw*, JHEP **12** (2011) 009, arXiv:1108.0661 [hep-ph].

[349] N. R. Agostinho, O. J. P. Eboli, and M. C. Gonzalez-Garcia, *LHC Run I Bounds on Minimal Lepton Flavour Violation in Type-III See-saw: A Case Study*, JHEP **11** (2017) 118, arXiv:1708.08456 [hep-ph].

[350] A. Sakharov, *Violation of CP Invariance, c Asymmetry, and Baryon Asymmetry of the Universe*, Pisma Zh.Eksp.Teor.Fiz. **5** (1967) 32–35.

[351] L. Canetti, M. Drewes, and M. Shaposhnikov, *Matter and Antimatter in the Universe*, New J. Phys. **14** (2012) 095012, arXiv:1204.4186 [hep-ph].

[352] M. Fukugita and T. Yanagida, *Baryogenesis Without Grand Unification*, Phys. Lett. **B174** (1986) 45–47.

[353] V. A. Kuzmin, V. A. Rubakov, and M. E. Shaposhnikov, *On the Anomalous Electroweak Baryon Number Nonconservation in the Early Universe*, Phys. Lett. **B155** (1985) 36.

[354] F. F. Deppisch, J. Harz, and M. Hirsch, *Falsifying High-Scale Leptogenesis at the LHC*, Phys. Rev. Lett. **112** (2014) 221601, arXiv:1312.4447 [hep-ph].

[355] F. F. Deppisch, J. Harz, M. Hirsch, W.-C. Huang, and H. Päs, *Falsifying High-Scale Baryogenesis with Neutrinoless Double Beta Decay and Lepton Flavor Violation*, Phys. Rev. **D92** (2015) no. 3, 036005, arXiv:1503.04825 [hep-ph].

[356] E. J. Chun et al., *Probing Leptogenesis*, Int. J. Mod. Phys. **A33** (2018) no. 05n06, 1842005, arXiv:1711.02865 [hep-ph].

[357] A. Pilaftsis and T. E. J. Underwood, *Resonant leptogenesis*, Nucl. Phys. **B692** (2004) 303–345, arXiv:hep-ph/0309342 [hep-ph].

[358] E. K. Akhmedov, V. A. Rubakov, and A. Yu. Smirnov, *Baryogenesis via neutrino oscillations*, Phys. Rev. Lett. **81** (1998) 1359–1362, arXiv:hep-ph/9803255 [hep-ph].

[359] T. Hambye and D. Teresi, *Higgs doublet decay as the origin of the baryon asymmetry*, Phys. Rev. Lett. **117** (2016) no. 9, 091801, arXiv:1606.00017 [hep-ph].

[360] M. Drewes et al., *A White Paper on keV Sterile Neutrino Dark Matter*, JCAP **1701** (2017) no. 01, 025, arXiv:1602.04816 [hep-ph].

[361] P. Hernández, M. Kekic, J. López-Pavón, J. Racker, and J. Salvado, *Testable Baryogenesis in Seesaw Models*, JHEP **08** (2016) 157, arXiv:1606.06719 [hep-ph].

[362] M. Drewes, B. Garbrecht, D. Gueter, and J. Klaric, *Testing the low scale seesaw and leptogenesis*, JHEP **08** (2017) 018, arXiv:1609.09069 [hep-ph].

[363] C. O. Dib, C. S. Kim, K. Wang, and J. Zhang, *Distinguishing Dirac/Majorana Sterile Neutrinos at the LHC*, Phys. Rev. **D94** (2016) no. 1, 013005, arXiv:1605.01123 [hep-ph].

[364] L. Canetti, M. Drewes, T. Frossard, and M. Shaposhnikov, *Dark Matter, Baryogenesis and Neutrino Oscillations from Right Handed Neutrinos*, Phys. Rev. **D87** (2013) 093006, arXiv:1208.4607 [hep-ph].

[365] L. Canetti, M. Drewes, and B. Garbrecht, *Probing leptogenesis with GeV-scale sterile neutrinos at LHCb and Belle II*, Phys. Rev. **D90** (2014) no. 12, 125005, arXiv:1404.7114 [hep-ph].

[366] DELPHI Collaboration, P. Abreu et al., *Searches for heavy neutrinos from Z decays*, Phys. Lett. **B274** (1992) 230–238.

[367] DELPHI Collaboration, P. Abreu et al., *Search for neutral heavy leptons produced in Z decays*, Z. Phys. **C74** (1997) 57–71. [Erratum: Z. Phys.C75,580(1997)].

[368] G. C. Branco, P. M. Ferreira, L. Lavoura, M. N. Rebelo, M. Sher, and J. P. Silva, *Theory and phenomenology of two-Higgs-doublet models*, Phys. Rept. **516** (2012) 1–102, arXiv:1106.0034 [hep-ph].

[369] ATLAS Collaboration, M. Aaboud et al., *Search for additional heavy neutral Higgs and gauge bosons in the ditau final state produced in 36 fb$^{?}$ of pp collisions at $\sqrt{s} = 13$ TeV with the ATLAS detector*, JHEP **01** (2018) 055, arXiv:1709.07242 [hep-ex].

[370] CMS Collaboration, C. Collaboration, *Search for additional neutral MSSM Higgs bosons in the di-tau final state in pp collisions at $\sqrt{s} = 13$ TeV*, .

[371] ATLAS Collaboration, M. Aaboud et al., *Search for heavy resonances decaying into WW in the $e\nu\mu\nu$ final state in pp collisions at $\sqrt{s} = 13$ TeV with the ATLAS detector*, Eur. Phys. J. **C78** (2018) no. 1, 24, arXiv:1710.01123 [hep-ex].

[372] ATLAS Collaboration, M. Aaboud et al., *Search for heavy ZZ resonances in the $\ell^+\ell^-\ell^+\ell^-$ and $\ell^+\ell^-\nu\bar{\nu}$ final states using proton proton collisions at $\sqrt{s} = 13$ TeV with the ATLAS detector*, arXiv:1712.06386 [hep-ex].

[373] CMS Collaboration, C. Collaboration, *Search for a new scalar resonance decaying to a pair of Z bosons in proton-proton collisions at $\sqrt{s} = 13$ TeV*, .

[374] ATLAS Collaboration, M. Aaboud et al., *Search for new phenomena in high-mass diphoton final states using 37 fb^{-1} of proton–proton collisions collected at $\sqrt{s} = 13$ TeV with the ATLAS detector*, Phys. Lett. **B775** (2017) 105–125, arXiv:1707.04147 [hep-ex].

[375] ATLAS Collaboration, M. Aaboud et al., *Search for heavy resonances decaying into a W or Z boson and a Higgs boson in final states with leptons and b-jets in 36 fb^{-1} of $\sqrt{s} = 13$ TeV pp collisions with the ATLAS detector*, arXiv:1712.06518 [hep-ex].

[376] ATLAS Collaboration, T. A. collaboration, *Search for charged Higgs bosons in the $H^{\pm} \to tb$ decay channel in pp collisions at $\sqrt{s} = 13$ TeV using the ATLAS detector*, .

[377] ATLAS Collaboration, T. A. collaboration, *Search for charged Higgs bosons in the ÏĎ+jets final state using 14.7 fbâĹŠ1 of pp collision data recorded at sâĹŽ=13 TeV with the ATLAS experiment*, .

[378] *Beyond Standard Model Higgs boson searches at a High-Luminosity LHC with ATLAS*, ATL-PHYS-PUB-2013-016, CERN, Geneva, Oct, 2013. http://cds.cern.ch/record/1611190.

[379] CMS Collaboration, C. Collaboration, *2HDM Neutral Higgs Future Analysis Studies*, .

[380] M. Carena, I. Low, N. R. Shah, and C. E. M. Wagner, *Impersonating the Standard Model Higgs Boson: Alignment without Decoupling*, JHEP **04** (2014) 015, arXiv:1310.2248 [hep-ph].

[381] P. S. Bhupal Dev and A. Pilaftsis, *Maximally Symmetric Two Higgs Doublet Model with Natural Standard Model Alignment*, JHEP **12** (2014) 024, arXiv:1408.3405 [hep-ph]. [Erratum: JHEP11,147(2015)].

[382] G. P. Lepage, P. B. Mackenzie, and M. E. Peskin, *Expected Precision of Higgs Boson Partial Widths within the Standard Model*, arXiv:1404.0319 [hep-ph].

[383] M. Baak et al., *Working Group Report: Precision Study of Electroweak Interactions*, in *Proceedings, 2013 Community Summer Study on the Future of U.S. Particle Physics: Snowmass on the Mississippi (CSS2013): Minneapolis, MN, USA, July 29-August 6, 2013*. 2013. arXiv:1310.6708 [hep-ph]. http://www.slac.stanford.edu/econf/C1307292/docs/EnergyFrontier/Electroweak-19.pdf.

[384] Gfitter Group Collaboration, M. Baak, J. CÃžth, J. Haller, A. Hoecker, R. Kogler, K. MÃűnig, M. Schott, and J. Stelzer, *The global electroweak fit at NNLO and prospects for the LHC and ILC*, Eur. Phys. J. **C74** (2014) 3046, arXiv:1407.3792 [hep-ph].

[385] Z. Liang, *Z and W Physics at CEPC*, http://indico.ihep.ac.cn/getFile.py/access?contribId=32&sessionId=2&resId=1&materialId=slides&confId=4338.

[386] J. Bernon, J. F. Gunion, H. E. Haber, Y. Jiang, and S. Kraml, *Scrutinizing the alignment limit in two-Higgs-doublet models: m_h=125 GeV*, Phys. Rev. **D92** (2015) no. 7, 075004, arXiv:1507.00933 [hep-ph].

[387] B. Coleppa, F. Kling, and S. Su, *Constraining Type II 2HDM in Light of LHC Higgs Searches*, JHEP **01** (2014) 161, arXiv:1305.0002 [hep-ph].

[388] V. Barger, L. L. Everett, H. E. Logan, and G. Shaughnessy, *Scrutinizing the 125 GeV Higgs boson in two Higgs doublet models at the LHC, ILC, and Muon Collider*, Phys. Rev. **D88** (2013) no. 11, 115003, arXiv:1308.0052 [hep-ph].

[389] G. Belanger, B. Dumont, U. Ellwanger, J. F. Gunion, and S. Kraml, *Global fit to Higgs signal strengths and couplings and implications for extended Higgs sectors*, Phys. Rev. **D88** (2013) 075008, arXiv:1306.2941 [hep-ph].

[390] P. M. Ferreira, J. F. Gunion, H. E. Haber, and R. Santos, *Probing wrong-sign Yukawa couplings at the LHC and a future linear collider*, Phys. Rev. **D89** (2014) no. 11, 115003, arXiv:1403.4736 [hep-ph].

[391] X.-F. Han and L. Wang, *Wrong sign Yukawa coupling of 2HDM with a scalar dark matter confronted with dark matter and Higgs data*, arXiv:1708.06882 [hep-ph].

[392] S. Kanemura, M. Kikuchi, and K. Yagyu, *Fingerprinting the extended Higgs sector using one-loop corrected Higgs boson couplings and future precision measurements*, Nucl. Phys. **B896** (2015) 80–137, arXiv:1502.07716 [hep-ph].

[393] S. Kanemura, M. Kikuchi, and K. Yagyu, *Radiative corrections to the Yukawa coupling constants in two Higgs doublet models*, Phys. Lett. **B731** (2014) 27–35, arXiv:1401.0515 [hep-ph].

[394] S. Kanemura, Y. Okada, E. Senaha, and C. P. Yuan, *Higgs coupling constants as a probe of new physics*, Phys. Rev. **D70** (2004) 115002, arXiv:hep-ph/0408364 [hep-ph].

[395] N. Chen, T. Han, S. Su, W. Su, and Y. Wu, *Type-II 2HDM under the Precision Measurements at the Z-pole and a Higgs Factory*, In preparation.

[396] JADE Collaboration, S. Bethke, S. Kluth, C. Pahl, and J. Schieck, *Determination of the Strong Coupling alpha(s) from hadronic Event Shapes with O(alpha**3(s)) and resummed QCD predictions using JADE Data*, Eur. Phys. J. **C64** (2009) 351–360, arXiv:0810.1389 [hep-ex].

[397] G. Dissertori, A. Gehrmann-De Ridder, T. Gehrmann, E. W. N. Glover, G. Heinrich, G. Luisoni, and H. Stenzel, *Determination of the strong coupling constant using matched NNLO+NLLA predictions for hadronic event shapes in e+e- annihilations*, JHEP **08** (2009) 036, arXiv:0906.3436 [hep-ph].

[398] G. Dissertori, A. Gehrmann-De Ridder, T. Gehrmann, E. W. N. Glover, G. Heinrich, and H. Stenzel, *Precise determination of the strong coupling constant at NNLO in QCD from the three-jet rate in electron–positron annihilation at LEP*, Phys. Rev. Lett. **104** (2010) 072002, arXiv:0910.4283 [hep-ph].

[399] OPAL Collaboration, G. Abbiendi et al., *Determination of $alpha_s$ using OPAL hadronic event shapes at $\sqrt{s} = 91$ - 209 GeV and resummed NNLO calculations*, Eur. Phys. J. **C71** (2011) 1733, arXiv:1101.1470 [hep-ex].

[400] JADE Collaboration, J. Schieck, S. Bethke, S. Kluth, C. Pahl, and Z. Trocsanyi, *Measurement of the strong coupling $alpha_S$ from the three-jet rate in e+e- - annihilation using JADE data*, Eur. Phys. J. **C73** (2013) no. 3, 2332, arXiv:1205.3714 [hep-ex].

[401] R. A. Davison and B. R. Webber, *Non-Perturbative Contribution to the Thrust Distribution in e+ e- Annihilation*, Eur. Phys. J. **C59** (2009) 13–25, arXiv:0809.3326 [hep-ph].

[402] R. Abbate, M. Fickinger, A. H. Hoang, V. Mateu, and I. W. Stewart, *Precision Thrust Cumulant Moments at N^3LL*, Phys. Rev. **D86** (2012) 094002, arXiv:1204.5746 [hep-ph].

[403] T. Gehrmann, G. Luisoni, and P. F. Monni, *Power corrections in the dispersive model for a determination of the strong coupling constant from the thrust distribution*, Eur. Phys. J. **C73** (2013) no. 1, 2265, arXiv:1210.6945 [hep-ph].

[404] A. H. Hoang, D. W. Kolodrubetz, V. Mateu, and I. W. Stewart, *C-parameter distribution at N^{3}LLâĂš including power corrections*, Phys. Rev. **D91** (2015) no. 9, 094017, arXiv:1411.6633 [hep-ph].

[405] A. H. Hoang, D. W. Kolodrubetz, V. Mateu, and I. W. Stewart, *Precise determination of α_s from the C-parameter distribution*, Phys. Rev. **D91** (2015) no. 9, 094018, arXiv:1501.04111 [hep-ph].

[406] T. Becher and M. D. Schwartz, *A precise determination of α_s from LEP thrust data using effective field theory*, JHEP **07** (2008) 034, arXiv:0803.0342 [hep-ph].

[407] Y.-T. Chien, R. Kelley, M. D. Schwartz, and H. X. Zhu, *Resummation of Jet Mass at Hadron Colliders*, Phys. Rev. **D87** (2013) no. 1, 014010, arXiv:1208.0010 [hep-ph].

[408] A. Kardos, S. Kluth, G. Somogyi, Z. TulipÃąnt, and A. Verbytskyi, *Precise determination of $\alpha_S(M_Z)$ from a global fit of energy-energy correlation to NNLO+NNLL predictions*, arXiv:1804.09146 [hep-ph].

[409] I. Moult and H. X. Zhu, *Simplicity from Recoil: The Three-Loop Soft Function and Factorization for the Energy-Energy Correlation*, arXiv:1801.02627 [hep-ph].

[410] Z. Nagy and Z. Trocsanyi, *Next-to-leading order calculation of four jet observables in electron positron annihilation*, Phys. Rev. **D59** (1999) 014020, arXiv:hep-ph/9806317 [hep-ph]. [Erratum: Phys. Rev.D62,099902(2000)].

[411] OPAL Collaboration, G. Abbiendi et al., *Determination of alpha(s) using jet rates at LEP with the OPAL detector*, Eur. Phys. J. **C45** (2006) 547–568, arXiv:hep-ex/0507047 [hep-ex].

[412] A. Gehrmann-De Ridder, T. Gehrmann, E. W. N. Glover, and G. Heinrich, *Second-order QCD corrections to the thrust distribution*, Phys. Rev. Lett. **99** (2007) 132002, arXiv:0707.1285 [hep-ph].

[413] A. Gehrmann-De Ridder, T. Gehrmann, E. W. N. Glover, and G. Heinrich, *NNLO corrections to event shapes in e+ e- annihilation*, JHEP **12** (2007) 094, arXiv:0711.4711 [hep-ph].

[414] S. Weinzierl, *NNLO corrections to 3-jet observables in electron-positron annihilation*, Phys. Rev. Lett. **101** (2008) 162001, arXiv:0807.3241 [hep-ph].

[415] V. Del Duca, C. Duhr, A. Kardos, G. Somogyi, and Z. TrÃşcsÃąnyi, *Three-Jet Production in Electron-Positron Collisions at Next-to-Next-to-Leading Order Accuracy*, Phys. Rev. Lett. **117** (2016) no. 15, 152004, arXiv:1603.08927 [hep-ph].

[416] V. Del Duca, C. Duhr, A. Kardos, G. Somogyi, Z. SzÅŚr, Z. TrÃşcsÃąnyi, and Z. TulipÃąnt, *Jet production in the CoLoRFulNNLO method: event shapes in electron-positron collisions*, Phys. Rev. **D94** (2016) no. 7, 074019, arXiv:1606.03453 [hep-ph].

[417] S. Badger, C. BrÃÿnnum-Hansen, H. B. Hartanto, and T. Peraro, *First look at two-loop five-gluon scattering in QCD*, Phys. Rev. Lett. **120** (2018) no. 9, 092001, arXiv:1712.02229 [hep-ph].

[418] S. Abreu, F. Febres Cordero, H. Ita, B. Page, and M. Zeng, *Planar Two-Loop Five-Gluon Amplitudes from Numerical Unitarity*, arXiv:1712.03946 [hep-ph].

[419] T. Gehrmann, J. M. Henn, and N. A. Lo Presti, *Analytic form of the two-loop planar five-gluon all-plus-helicity amplitude in QCD*, Phys. Rev. Lett. **116** (2016) no. 6, 062001, arXiv:1511.05409 [hep-ph]. [Erratum: Phys. Rev. Lett.116,no.18,189903(2016)].

[420] C. G. Papadopoulos, D. Tommasini, and C. Wever, *The Pentabox Master Integrals with the Simplified Differential Equations approach*, JHEP **04** (2016) 078, arXiv:1511.09404 [hep-ph].

[421] A. Banfi, H. McAslan, P. F. Monni, and G. Zanderighi, *The two-jet rate in e^+e^- at next-to-next-to-leading-logarithmic order*, Phys. Rev. Lett. **117** (2016) no. 17, 172001, arXiv:1607.03111 [hep-ph].

[422] M. Dasgupta and G. P. Salam, *Accounting for coherence in interjet E(t) flow: A Case study*, JHEP **03** (2002) 017, arXiv:hep-ph/0203009 [hep-ph].

[423] A. Banfi, G. Marchesini, and G. Smye, *Away from jet energy flow*, JHEP **08** (2002) 006, arXiv:hep-ph/0206076 [hep-ph].

[424] R. B. Appleby and M. H. Seymour, *Nonglobal logarithms in interjet energy flow with kt clustering requirement*, JHEP **12** (2002) 063, arXiv:hep-ph/0211426 [hep-ph].

[425] M. Rubin, *Non-Global Logarithms in Filtered Jet Algorithms*, JHEP **05** (2010) 005, arXiv:1002.4557 [hep-ph].

[426] A. Banfi, M. Dasgupta, K. Khelifa-Kerfa, and S. Marzani, *Non-global logarithms and jet algorithms in high-pT jet shapes*, JHEP **08** (2010) 064, arXiv:1004.3483 [hep-ph].

[427] R. Kelley, M. D. Schwartz, and H. X. Zhu, *Resummation of jet mass with and without a jet veto*, arXiv:1102.0561 [hep-ph].

[428] A. Hornig, C. Lee, I. W. Stewart, J. R. Walsh, and S. Zuberi, *Non-global Structure of the $O(\alpha_s^2)$ Dijet Soft Function*, JHEP **08** (2011) 054, arXiv:1105.4628 [hep-ph]. [Erratum: JHEP10,101(2017)].

[429] A. J. Larkoski and I. Moult, *Nonglobal correlations in collider physics*, Phys. Rev. **D93** (2016) no. 1, 014012, arXiv:1510.05657 [hep-ph].

[430] H. Weigert, *Nonglobal jet evolution at finite N(c)*, Nucl. Phys. **B685** (2004) 321–350, arXiv:hep-ph/0312050 [hep-ph].

[431] Y. Hatta and T. Ueda, *Resummation of non-global logarithms at finite N_c*, Nucl. Phys. **B874** (2013) 808–820, arXiv:1304.6930 [hep-ph].

[432] Y. Hagiwara, Y. Hatta, and T. Ueda, *Hemisphere jet mass distribution at finite N_c*, Phys. Lett. **B756** (2016) 254–258, arXiv:1507.07641 [hep-ph].

[433] M. D. Schwartz and H. X. Zhu, *Nonglobal logarithms at three loops, four loops, five loops, and beyond*, Phys. Rev. **D90** (2014) no. 6, 065004, arXiv:1403.4949 [hep-ph].

[434] K. Khelifa-Kerfa and Y. Delenda, *Non-global logarithms at finite N_c beyond leading order*, JHEP **03** (2015) 094, arXiv:1501.00475 [hep-ph].

[435] S. Caron-Huot, *Resummation of non-global logarithms and the BFKL equation*, JHEP **03** (2018) 036, arXiv:1501.03754 [hep-ph].

[436] A. J. Larkoski, I. Moult, and D. Neill, *Non-Global Logarithms, Factorization, and the Soft Substructure of Jets*, JHEP **09** (2015) 143, arXiv:1501.04596 [hep-ph].

[437] T. Becher, M. Neubert, L. Rothen, and D. Y. Shao, *Effective Field Theory for Jet Processes*, Phys. Rev. Lett. **116** (2016) no. 19, 192001, arXiv:1508.06645 [hep-ph].

[438] D. Neill, *The Edge of Jets and Subleading Non-Global Logs*, arXiv:1508.07568 [hep-ph].

[439] T. Becher, M. Neubert, L. Rothen, and D. Y. Shao, *Factorization and Resummation for Jet Processes*, JHEP **11** (2016) 019, arXiv:1605.02737 [hep-ph]. [Erratum: JHEP05,154(2017)].

[440] A. J. Larkoski, I. Moult, and D. Neill, *The Analytic Structure of Non-Global Logarithms: Convergence of the Dressed Gluon Expansion*, JHEP **11** (2016) 089, arXiv:1609.04011 [hep-ph].

[441] T. Becher, B. D. Pecjak, and D. Y. Shao, *Factorization for the light-jet mass and hemisphere soft function*, JHEP **12** (2016) 018, arXiv:1610.01608 [hep-ph].

[442] D. Neill, *The Asymptotic Form of Non-Global Logarithms, Black Disc Saturation, and Gluonic Deserts*, JHEP **01** (2017) 109, arXiv:1610.02031 [hep-ph].

[443] T. Becher, R. Rahn, and D. Y. Shao, *Non-global and rapidity logarithms in narrow jet broadening*, JHEP **10** (2017) 030, arXiv:1708.04516 [hep-ph].

[444] J. Gao, *Probing light-quark Yukawa couplings via hadronic event shapes at lepton colliders*, arXiv:1608.01746 [hep-ph].